University of Alberta
Department of Civil &
Environmental Engineering

Structural Engineering Report

Properties of Concretes and Wood Composites Using A Phosphate-Based Binder

by

Luong T. Hong

and

Adam S. Lubell

May, 2013

PROPERTIES OF CONCRETES AND WOOD COMPOSITES USING A PHOSPHATE-BASED BINDER

by

Luong T. Hong

and

Adam S. Lubell

Structural Engineering Report

Department of Civil and Environmental Engineering

University of Alberta, Edmonton, Alberta

May 2013

ABSTRACT

Magnesium potassium phosphate ceramics are from the family of phosphate-based cements which can be used as alternatives to Portland cements. In this study, concretes and wood composites were produced using magnesium potassium phosphate ceramic binders and supplementary materials including fly ash, sand, silica fume and sawdust. Bentonite, Delvo Stabilizer and baking soda were used as additives to increase the workability and the setting time of the fresh mixutres and decrease the density of the hardened products. The materials were then reinforced with chopped glass-fibers or textile glass-fabrics to increase their hardened properties. At 50% fly ash by total mass of the binder, the concretes had compressive strength and density of 33 MPa and 2170 kg/m^3, respectively, after 90 days of simple curing. At 20% fly ash by total mass of the binder, the wood composites had compressive strength and density of 13 MPa and 1320 kg/m^3, respectively, after 90 days. The flexural strengths were about 10% to 47% of the corresponding cylinder compressive strengths for these mixes. Increases in both compressive and flexural strengths for these mixes were observed with the addition of chopped glass-fibers or textile glass-fabrics.

ACKNOWLEDGEMENTS

This report is based on the thesis of the first author.

Financial support for this project was provided by the Mekong 1000 Project of Vietnam, the Natural Sciences and Engineering Research Council of Canada and C-Bond Technology Ltd. Donation of materials by Lafarge North America, Elkon, CANTRIM, Nippon Electric Glass America, BASF, and St. Gobain Technical Fabrics are also gratefully acknowledged.

Technical assistance was provided by Mr. Rizaldy Mariano at the Concrete Laboratory and Mr. Greg Miller at the Morrison Structures Laboratory. Special thanks are also due to Mr. Samson Tassew, Mr. Sadegh Kazemi and other graduate students that provided assistance.

TABLE OF CONTENTS

List of Figures

List of Tables

Notations

A_{cube} = cube area based on the loaded size of the specimen (mm^2)

A_{cyl} = cross-sectional area of cylinder; calculated based on averaging two measurements of diameter taken at right angles to each other at mid-height of the cylinder (mm^2)

b = average width of prism or panel (mm)

d = average depth of prism (notch accounted) or of panel (mm)

d_i = average value of three vertical displacements recorded by LVDTs (mm)

E = modulus of elasticity (MPa)

σ_2 = stress corresponding to 40% of ultimate strength (MPa)

σ_1 = stress corresponding to a longitudinal strain of $5x10^{-5}$ mm/mm (MPa)

ε_c = strain corresponding to f_c (mm/mm)

ε_c' = strain corresponding to f_c' (mm/mm)

ε_2 = longitudinal strain at σ_2 (mm/mm)

f_{cu} = cube compressive strength (MPa)

f_{cu7} = cube compressive strength at 7 days after casting (MPa)

f_{cu28} = cube compressive strength at 28 days after casting (MPa)

f_c = compressive stress of cylinder (MPa)

f_c' = peak compressive stress of cylinder (MPa)

f_{b-pr} = flexural strength of prism specimen (MPa)

f_{b-pa} = flexural strength of panel specimen (MPa)

f_{r-pr} = modulus of rupture of prism specimen (MPa)

f_{r-pa} = modulus of rupture of panel specimen (MPa)

γ = density of MPPC concrete/wood composites (kg/m^3)

γ_{ave} = average density of MPPC concrete/wood composites (kg/m^3)

L = span length of prism or panel (mm)

L_g = gauge length between the top and bottom collar which is 100mm for cylinder test

P = maximum load (N)

P_i = corresponding load (N)

Acronyms

CBC = chemically bonded ceramic

CBPC = chemically bonded phosphate cement/ceramic

MPC = magnesium phosphate cement/ceramic

MPPC = magnesium potassium phosphate cement/ceramic

SF = silica fume

FA = fly ash

COV = coefficient of variation

w/b = water-to-binder mass ratio

b/s = binder-to-sand mass ratio

b/sdt = binder-to-sawdust mass ratio

Chapter 1 # INTRODUCTION

1.1 Research statement

Portland cement is a common construction material with an annual global production reaching 2.8 billion metric tons (U.S. Geological Survey, 2010). However, its manufacture causes high environmental impacts at all stages of the process. These include emissions of airborne pollution in the form of dust and carbon dioxide (CO_2) gases; the consumption of large quantities of resources and energy during the manufacture process; and the release of CO_2 from the raw material during the process. In the production of one ton of Portland cement, about 1.5 tons of raw materials are needed while, at the same time, about one ton of carbon dioxide (CO_2) is released into the environment (Li et al. 2004). Additional CO_2 may come from the energy source. In addition, concrete made with Portland cement has several disadvantages including high permeability, high self-weight, slow curing and rate of strength gain, and it is susceptible to the severe environment (Li et al. 2004). Thus, to sustain the development of our modern society, alternative cementitious materials have been developed.

Phosphate-based cementitious materials have been suggested as alternatives to Portland cements in recent years. Phosphate-based cements are also known as chemically bonded phosphate ceramics (CBPC) (Wagh et al., 1997; Wagh et al., 1998; Wagh, 2004). Wagh and his colleagues showed that CBPCs can be formulated to have quick setting times, high early age strength gain, very good durability including chemical attack resistance, deicer scaling resistance and permeation resistance. They also developed (Wagh et al., 1998) magnesium potassium phosphate ceramic (MPPC) which exhibits superior properties among CBPC materials.

In recent years, the properties of CBPC binders have been studied by some researchers (Quiao et al., 2009; Ding and Li, 2005; Quiao et al., 2010). Quiao et al. (2009) found that the fineness of magnesium oxide particle influenced the

setting time of CBPCs. Ding and Li (2005) found that when fly ash was incorporated at 30% to 50% by total mass of the binder, sand mortars using CBPC binders exhibited the highest compressive strengths. They also reported that the increase in water/binder ratio decreased the compressive strength and modulus of elasticity of sand mortars using CBPC binders. The compressive strength of sand mortars using CBPC binders also decreased when the mass fraction of aggregates increased (Ding and Li, 2005; Quiao et al., 2010).

Furthermore, CBPCs based on a magnesium potassium phosphate binder can also be formulated to incorporate large quantities of nontoxic industrial waste, including fly ash and waste fibers. Fly ash is a by-product from coal-fired thermal power plants which can be added to CBPCs to improve the bonding and compressive strength of CBPCs, even at very early ages (Wagh, 2004). The CBPC matrix can also incorporate a wide range of fibers including natural fibers (such as wood, cellulose, and cotton) and artificial fibers (such as nylon) (Wagh, 2004).

Li et al. (2004) reported that wood waste can be bonded with CBPC to produce lightweight particleboard having flexural strengths of 2.1 MPa to 10.4 MPa. Donahue and Aro (2009) also reported that waste pulp and paper mill residues can be added to MPPCs to produce board specimens having flexural strength of 3.3 MPa. The influence of chopped glass fibers on the properties of CBPC matrix has been examined by several researchers (Jeong and Wagh, 2003; Tassew et al., 2010). Jeong and Wagh (2003) reported an increase in flexural strength when fibers were used. Tassew et al. (2010) also reported an increase in compressive strength and maximum load capacity for flexural strength when fibers were added.

Traditional concretes have used silica fume as an admixture to increase their performance. Silica fume is formed from the condensed gas escaping from electric arc furnaces from the production of elemental silicon or alloys containing silicon (ACI 116R-90). ACI 116R-90 indicates that silica fume can be used to enhance the compressive strength, the strength development rate and the

durability of concrete. Moreover, silica fume was reported to influence the properties of fresh concrete including: water demand, workability, bleeding and plastic shrinkage (ACI 116R-90). However, no prior research has been reported which examines the influence of silica fume on the properties of CBPC.

Besides silica fume, bentonite is also used as an admixture to increase the performance of Portland cement concrete (IMA-NA, 2009). Bentonite is a clay consisting mostly of montmorillonite. It significantly increases in volume when coming in contact with water and becomes a gelatinous and viscous fluid. Thus, bentonite can be added to Portland cement and mortars to increase their viscosity and plasticity (IMA-NA, 2009). However, no prior research has been conducted to find the effect of bentonite on the properties of CBPC materials.

High self-weight is one of the disadvantages of traditional concretes. Addition of foaming agents during the mixing procedure can create cellular concretes which are much lighter than traditional concretes (Dattel, 2002). These cellular concretes can sustain suitable compressive strengths at very low densities. Several foaming agents have been used to facilitate the formation of foam which is then blended into the cement paste. With the unique chemistry of CBPCs compared to Portland cements, alternative foaming mechanisms are possible. Sodium bicarbonate (i.e. baking soda) releases carbonic air bubbles when in contact with some acids. The viability to use baking soda as a foaming agent during the mixing procedure has not been previously examined. Evaluation of effect of baking soda on the properties of CBPCs was also an objective of this research.

1.2 Research significance

Traditional concretes incorporating Portland cement are widely used in construction. However, these traditional concretes have several disadvantages and their production has very high impacts on the environment. Thus, chemically bonded phosphate ceramics (CBPC) become an excellent candidate for the replacement of Portland cement concretes. Many studies have been conducted to

determine the properties of CBPCs but there is still lack of knowledge in this area, especially for magnesium potassium phosphate ceramics (MPPCs). More research is required to improve the performance of MPPCs as well as to reduce the cost of the products, making them a viable and widespread alternative for Portland cement concretes.

This research extends the knowledge base of MPPC materials by evaluating the viability of incorporating silica fume, bentonite, baking soda, sawdust, sand, and glass-fibers in MPPC matrix. These compositions were believed to alter the rheological and mechanical properties of MPPC products. In addition, competitive MPPC-based products with lower density and lower cost can be produced which make them more production of the concrete market.

1.3 Objective and scope

Magnesium potassium phosphate ceramic (MPPC) concretes and MPPC wood composites were produced using MPPC binder and other compositions including: fly ash, silica fume, sawdust, bentonite, baking soda and sand. MPPC concretes/wood composites were also produced that contained chopped glass-fibers and textile glass-fabrics.

The main objective of this research was to determine the basic characteristics of MPPC concretes/wood composites and MPPC concretes/wood composites reinforced with glass-fibers. A laboratory program was conducted to characterize the properties of the MPPC concretes/wood composites in the following categories:

- Properties of fresh mixtures of MPPC concretes/wood composites.
- Mechanical properties of the hardened MPPC concretes/wood composites.

Trial mixes were first examined using the MPPC binder and other compositions as listed above. Six candidate mixes were selected among trial mixes for further study based on their reasonable workability and good compressive strength. Fresh property, working time, compression and flexure

properties of these six mixtures were evaluated. Finally, these mixtures were reinforced with chopped glass-fibers or textile glass-fabrics and the evaluation of the above properties were conducted and compared with the plain mixes.

1.4 Organization

This report is composed of seven chapters. In addition to this introductory chapter, Chapter 2 presents the fundamental knowledge based on previous literature on chemically bonded phosphate ceramics (CBPCs) and Portland cements. Information on magnesium potassium phosphate ceramics (MPPCs) and other materials required for the research program is introduced.

Chapter 3 reports the development of the MPPC concretes/wood composites using MPPC binder. Characterizations and sources of each material, the mixing and casting procedures, sample preparation, and the testing methods are reported in this chapter.

Chapter 4 reports the trial mix program in which MPPC binder was incorporated with other ingredients including: fly ash, silica fume, sawdust, bentonite, baking soda and sand. For each composition, compressive strength was evaluated using cube specimens. Workability of fresh mixture of each composition is also presented in this chapter. Based on the results obtained from this chapter, six mixtures were selected for further study.

Chapter 5 reports the further experimental program for the six mixtures selected in chapter 4. Workability as obtained from a slump flow test and the setting time obtained from needle penetration tests are presented in this chapter. Compression and flexure properties were evaluated using cube and cylinder specimens, as well as prism and panel specimens, respectively.

In chapter 6, the six mixtures discussed in chapter 5 were modified by reinforcement with either chopped glass-fibers or textile glass-fabrics. Workability, compression and flexure properties for these mixes were evaluated.

Chapter 7 summarizes the major findings and gives recommendations for future research.

Chapter 2 LITERATURE REVIEW

2.1 Magnesium Potassium Phosphate Ceramic/Cement

2.1.1 Traditional ceramics and hydraulic cements

Traditional ceramics and hydraulic cements are two families of man-made materials that are inorganic, nonmetallic solids and common in use (Glasser, 1990). Traditional ceramics are formed by heating and cooling the powders at temperatures ranging from 700 to 2000^{o}C (Wagh, 2004). Bricks, pottery and high temperature superconductors are examples of traditional ceramics. Hydraulic cements are made by adding water to their powders and letting them set and cure at room temperature. Porland cement (PC) is an example of a hydraulic cement.

Traditional ceramics are highly crystalline while hydraulic cements are non-crystalline. The bonds of hydraulic cement particles produced by the chemical reaction between water and the powder are typically controlled by Van der Waals forces (Wagh, 2004). The bonds of traditional ceramic particles, meanwhile, are ionic or covalent bonding which are produced by the fusion and consolidation of material particles at very high temperature (Wagh, 2004). According to Wagh (2004), the ionic and covalent bonds are stronger than Van der Waals forces so traditional ceramics can have higher strengths than hydraulic cements.

For common applications, ceramic materials have a denser structure than hydraulic cement based materials. Porosity for the best ceramics is <1% by volume while it is often about 15-20% by volume for cements (Wagh, 2004). Ceramic products can withstand very high temperatures and are durable in environments having relative high or low pH. Meanwhile, high temperatures and acidic environments can damage hydraulic cements. Although ceramics are better than hydraulic cements in many aspects, they are more expensive and less

commonly used in structural applications (Wagh, 2004). Their production process may also limit the potential applications.

2.1.2 Chemically bonded phosphate ceramics/cements (CBPCs)

There are intermediate products that exhibit both the characteristics of traditional ceramic materials and hydraulic cement materials. Some of those products are produced by first partially sintering the materials at high temperature like traditional ceramics and then letting them set like hydraulic cements. Other products are made by reactions at room temperature like cements but have crystalline structure like traditional ceramics. Roy (1987) and Roy et al. (1986, 1991) named these intermediate products as Chemically Bonded Ceramics (CBCs). Wagh (2004) used this term for all inorganic solids produced by chemical reactions instead of using heat treatment as in the conventional production process of traditional ceramics. CBCs are also called as acid-base cements because they are products of a chemical reaction between an acid and a base. The reaction between the acidic and alkaline components occurs rapidly and the resulting mixture sets quickly into a hard mass with neutral pH (Wagh, 2004).

CBCs exhibit properties of both cements and ceramics. The particles in CBCs are mostly crystalline as in traditional ceramics. The bonding between particles, however, is provided by a paste formed by chemical reactions as in hydraulic cements. CBCs are stronger than hydraulic cements but weaker than traditional ceramics. CBCs inherit very good characteristics for resistance to chemical attack from traditional ceramics but they are also easily damaged by erosion like hydraulic cements.

When phosphates are used to produce CBCs, they are called chemically bonded phosphate ceramics/cements (CBPCs). In the 19^{th} century, CBPCs were first developed as dental cements (Wagh, 2004). Since 1970, magnesium phosphate ceramics (MPCs) have been developed for structural applications based in part on the experimental programs conducted at Brookhaven National Laboratory (Wagh, 2004). In the 1990s, CBPCs based on magnesium phosphate

ceramics were extensively developed for radioactive and hazardous waste management applications at Argonne National Laboratory. These ceramics have also found application in structural materials (Wagh, 2004).

Chemically bonded phosphate ceramics are inorganic and nontoxic materials which are formed by reaction of metal cations with phosphate anions; so-called acid-base cements. While Portland cements are formed in an alkaline solution and have cured products with high pH, cured CBPCs have relatively neutral pH. Thus, they are stable in environments having a wide range of pH. The compressive strengths of these acid-base cements can be several times higher than the corresponding strengths of conventional cements such as Porland cement. However, they are also brittle materials due to their very low fracture toughness (Wagh, 2004). They are self-bonding, so a second layer could bond to the first layer of the same material (Wagh, 2004).

When magnesium oxide or equivalent is used as the alkaline source to produce CBPCs, the product is called magnesium phosphate ceramic/cement (MPC). The earliest reported research on MPC was by Prosen (1939, 1941) and Earnshaw (1960). Some magnesium phosphate-based ceramics set very fast and they are also soluble which make them unpractical for structural applications (Finch & Sharp, 1989). The solubility of these ceramics can be reduced by an additional cation provided as a soluble phosphate. The necessary additional cation can be provided by salts such as ammonium monohydrogen phosphate, ammonium dihydrogen phosphate, ammonium polyphosphate (Sugama & Kukacka, 1983), aluminum hydrophosphate (Ando et al., 1974), sodium polyphosphate (Demotakis et al., 1992), or potassium dihydrogen phosphate (Wagh et al., 2001; Wagh, 2004).

One example of MPCs is magnesium ammonium phosphate ceramic grout which is used for rapid repair of structures in cold climates, and for repair of industrial floors and airport runways (El-Jazairi, 1982). Magnesium potassium phosphate is also among the magnesium-phosphate-based ceramics which is used

for stabilization and solidification of low-level radioactive and hazardous wastes (Wagh et al., 2001).

MPC mortars also exhibit double the abrasion resistance when compared with slab-on-grade floor concrete and to be nearly equal to that of pavement concrete (Yoshizake et al., 1989; Seehra et al., 1994).

In cold climates, concrete can be damaged by frost action. The use of deicer chemicals amplifies the problem. Experiments were conducted by Yoshizake et al. (1989) and Yang et al. (2002) to find the deicer-frost resistance of MPC. They used the cooling rate of about 0.5°C/min. for 4 hours to -20±2°C and then thawed the material for 4 hrs to 20±5°C. A 3% NaCl solution was used as the deicer solution. The results showed that MPC has very high deicer-frost resistance. The surface of MPC can resist 40 freeze-thaw cycles before scaling occurred. The freezing-thawing resistance of MPC was, in general, equal to that of air-entrained PC concrete (Yoshizake et al., 1989; Yang et al., 2002).

When reinforced with steel, MPC forms an iron phosphate film at the surface of the steel which prevents the corrosion of the steel (Li et al., 2004). The permeability of hardened MPC mortars can be one half that of PC concrete (Yoshizake et al., 1989). These characteristics result in higher resistance to the onset of steel corrosion when compared with PC concrete.

2.1.3 Magnesium potassium phosphate ceramics (Ceramicrete)

In an effort to develop a new material suitable for radioactive and harzadous waste management applications, Wagh and his colleagues (Wagh et al., 1997; Wagh et al.,1998; Wagh & Jeong, 2003) developed a magnesium potassium phosphate ceramic (MPPC) by the reaction between calcined magnesium oxide (MgO) and monopotassium phosphate (KH_2PO_4) in an aqueous solution as follows:

$$MgO + KH_2PO_4 + 5.H_2O = MgKPO_4 \cdot 6H_2O \qquad (2\text{-}1)$$

The product, which was named Ceramicrete, sets at room temperature like concrete and has a highly crystalline structure (Wagh, 2004). “In a small scale (a little size), the slurry is mixed for ≈ 25 minutes till it forms a thick but pourable paste. It is then allowed to set. The setting time is approximately one hour. In larger scale, this mixing time is reduced significantly” (Wagh, 2004). In addition to high strength, Wagh (2004) also indicated that Eqn. 2-1 is less exothermic than other magnesium phosphate-based ceramics and its reaction rate is slow enough to allow for large castings.

To further control the reaction rate during the production of magnesium-phosphate-based ceramics, the pretreatment of MgO or the use of chemicals to decrease the MgO dissolution rate can be used. In the pretreatment of MgO, the material is calcined at high temperature to reduce the porosity of individual grains, increase the particle size and recrystallize the amorphous coatings on individual grains (Eubank, 1951). Thus, the solubility of MgO in the acidic solution is reduced and the reaction rate is retarded.

Chemicals can also be used to retard the reaction rate of magnesium-phosphate-based ceramics. Several retardants, including boric acid and borates are used to delay the setting time for magnesium-potassium and magnesium-ammonium phosphate ceramics (Sarkar, 1991; Wagh & Jeong, 2003). According to Sarkar (1991), boric acid can retard the reaction between MgO and ammonium phosphate by developing a polymeric coating on MgO grains and thus reduce the solubility of MgO. The mixing and setting time of the slurry of MgO and potassium phosphate (KH_2PO_4) can be increased from 1.5h to 4.5h when only 1% boric acid is added (Wagh, 2004).

The properties of MPPCs are mainly influenced by the reactivity of magnesia, the molar ratio of magnesium to phosphate, and the water usage (Quiao et al., 2010; Quiao et al., 2009). Mixing time has influence on compressive strength of MPPCs as studied by Tassew and Lubell (2013). They found that as the mixing time increased, the compressive strength of hardened MPPCs and the uniformity of fresh mixture of MPPCs increased (Tassew & Lubell, 2013). They

reported that the mixing time of 7.5 minutes gave good results in terms of compressive strengths and workability (Tassew & Lubell, 2013). The effect of varying the water to binder (*w/b*) mass ratio on compressive strength of MPPCs was also examined by Tassew and Lubell (2013). The results showed that when the fly ash loading was at 40% to 60% by total mass of the binder, the specimens had the highest compressive strength for the *w/b* ratio of 0.20 (Tassew & Lubell, 2013).

2.2 Chemically bonded phosphate ceramic (CBPC) matrix composites

CBPC matrix composites can be produced by mixing a CBPC binder with a second-phase material and water. Properties of the product can be altered by changing the mass ratio or characteristics of additives. According to Wagh (2004), the inclusion of fly ash in the mixture can enhance the compressive strength of the product by about two fold. He also indicated that the thermal insulation property of the product can be increased by adding insulating particles such as ash, sawdust or hollow microspheres of silica. "The ability of CBPCs to bind a range of materials ("extender") and to form composites makes them promising for niche applications that cannot be fulfilled by conventional cement" (Wagh, 2004).

When binders containing Mg, Fe, Zn, and Ca are used to produce CBPC composites, these composites have similar physical properties to conventional Portland cement but suitable extenders can be added to enhance them at very high loading (Wagh, 2004). Meanwhile, Portland cement can only incorporate extenders at lower loading than CBPCs. This difference is explained by the acid-base reaction to produce CBPCs, while it is an alkaline system for Portland cement. Since acidic, neutral or alkaline components can be added in an acid-base reaction, this makes CBPCs capable of incorporating higher loading of extenders compared with conventional cement, which only accepts neutral and alkaline components at a small load factor (Wagh, 2004).

Furthermore, CBPC matrix composites can incorporate a high volume of industrial wastes including: fly ash, iron tailings, red mud, machining swarfs, and wood wastes such as sawdust and wood chips (Wagh, 2004). Li et al. (2004) stated that "MPC can bind a lot of non-toxic industrial wastes to useful construction materials. If the wastes were toxic, MPC can solidify and stabilize them". By incorporating these industrial waste products, these CBPC composites can be produced with a lower unit cost compared to a pure MPPC matrix.

2.2.1 Chemically bonded phosphate ceramics incorporating fly ash

Wagh (2004) stated that fly ash is not only miscible in a CBPC slurry, but it can reduce the viscosity and make the slurry smooth, for easier pumping and pouring. According to Wagh (2004), CBPC matrix composites can incorporate 50-70 wt% fly ash which is significantly higher than the typical maximum loading of 25 wt% for Portland cement. This higher loading of fly ash helps to reduce the effective cost of CBPC products which is much higher than that of Portland cement.

The inclusion of Class F fly ash could increase the compressive strength of CBPC matrix composites by 75% compared to Portland cement (Wagh, 2004). When Class C fly ash is used, the compressive strength could be increased by three fold compared with Portland cement (Wagh, 2004). The compressive strength of ash-based CBPC matrix composite could reach the maximum with a fly ash loading of 50-60% (Wagh, 2004). Tassew and Lubell (2013) also conducted experiments to examine the influence of Class C fly ash loading on the compressive strength of MPPC binders and sand mortars using the MPPC binders. The results showed that the highest compressive strength was achieved when the fly ash content was 50% of the total binder mass and the *w/b* ratio was 0.20.

Ding et al. (2005) explained the increase in compressive strength of MPC binders when fly ash is included by two factors: physical factor and chemical factor. "A physical effect may occur in which the fly ash particles fill the voids in the MPC matrix and densify the overall structure of the MPC binder. A chemical

effect may also occur where by interaction happens at the interface of the fly ash grains and the phosphate gel" (Ding et al., 2005).

Li et al. (2004) examined the strength development of MPC mortars using different hard burnt magnesia (containing 89.6% and 71.6% magnesium oxide) and a Class F fly ash. The results showed that, for both types of magnesia, the MPC mortars with 30-50% fly ash by weight exhibited higher strengths than the samples without fly ash. The highest strength occurred for the samples with 40% fly ash. The research also showed an increase in the elastic modulus of MPC mortars when fly ash was included. For MPC mortars with 89.6%-magnesium-oxide-containing magnesia, the elastic modulus increased from 27.47 to 31.85 GPa when the content of fly ash increased from 0% to 40%, respectively (Li et al., 2004). Li et al. (2004) also found that mixes containing fly ash developed strength much faster than mixes without fly ash. "The test results show that FA has the effect of reinforcement to strength, even if MPC mortar were cured under very low temperatures" (Li et al., 2004).

CBPC products using Class C fly ash have shorter setting times than products using Class F fly ash (Wagh, 2004). Wagh (2004) explained this by the level of CaO contained in Class C fly ash which is much higher than that in Class F fly ash. Since CaO dissolves rapidly in the acidic solution, Class C fly ash is more reactive than Class F fly ash (Wagh, 2004). However, Class C fly ash should be used in combination with Class F fly ash in large-size ceramics because the reaction between CaO and the acid solution generates considerable heat during the setting time of the products (Wagh, 2004).

Tassew and Lubell (2013) also examined the influence of Class C fly ash loading on density of the hardened MPPCs. They used a control MgO:MKP:FA mass ratio of 1:3.4:4.4 and the water to binder ratio of 0.22. They found that when the fly ash content increased, the density of MPPCs decreased accordingly. Since the unit weight of fly ash is lower than that of the MPPC binder, adding more fly ash resulted in decrease in overall density of the product (Tassew & Lubell, 2013). When the fly ash content varied from 40% to 80% of the total mass of

binder, the average densities measured were from 1820 kg/m^3 to 1553 kg/m^3 (Tassew & Lubell, 2013).

2.2.2 CBPC mortars produced using sand aggregates

Quiao et al. (2010) and Ding et al. (2005) found that the elastic modulus and compressive strength of MPC mortars decreased when the sand to binder ratio or the water to binder ratio increased. Tassew and Lubell (2013) confirmed this by conducting experiments on sand ceramic mortars (SCM) using MPC binders. The experiments used the MgO:MKP:FA mass ratio of 1:3.4:4.4, a *w/b* mass ratio of 0.20 and two different types of sand. The results showed that the compressive strength of both SCMs increased by 28.7% as the binder to sand (*b/s*) ratio increased from 1.0 to 3.0. However, with the MgO:MKP:FA mass ratio as 1:3.4:10.3, the compressive strength of both SCMs showed negligible difference as the *b/s* ratio increased from 1.0 to 3.0. This was explained by the overall weaker binder matrix from the binder with MgO:MKP:FA ratio of 1:3.4:10.3 compared to the binder with the ratio of 1:3.4:4.4.

Tassew and Lubell (2013) also examined the rate of compressive strength development of SCMs. The results showed that SCMs with MgO:MKP:FA mass ratio of 1:3.4:4.4 reached 18.3%, 51.5% and 75.9% of 28-day compressive strengths at 2 hrs, 7 hrs and 24 hrs after casting, respectively. At the age of 3 days and 7 days, these mixes exhibited 84.0% and 93.8% of the 28-day compressive strength, respectively. The strength development also varied with the fly ash content and adding more fly ash resulted in lower strength gain (Tassew & Lubell, 2013).

For the elastic modulus of SCMs, Tassew and Lubell (2013) showed that with different types of sand used, SCMs exhibited similar stress-strain responses with only minor non-linearity up to the peak stress. For three types of sand examined, the modulus of elasticity of SCMs with the MgO:MKP:FA mass ratio of 1:3.4:4.4 ranged from 21.3 to 24.1 GPa at 28-day age (Tassew & Lubell, 2013).

Flexural strength of SCMs was also determined in the study by Tassew and Lubell (2013). For three types of sand examined, the moduli of rupture of SCMs with the MgO:MKP:FA mass ratio of 1:3.4:4.4 were from 5.8% to 6.7% of the corresponding compressive strength at 28 days (Tassew & Lubell, 2013). They found that the mixture with the coarsest aggregate grading exhibited the highest compressive strength, modulus of elasticity and modulus of rupture.

2.2.3 Chemically bond phosphate ceramics reinforced with glass fibers

Bentur and Mindes (1990) and Banthia and Sheng (1996) studied the use of discontinuous short fibers randomly distributed within concrete. They showed that the fibers can increase flexural strength, post-cracking capacity, impact resistance, and energy absorption capacity.

Jeong and Wagh (2003) examined the effect of glass fibers in ash-containing MPPC. Chopped glass fibers of length 0.25 in (0.6 cm) and 0.5 in (1.3 cm) were added to the ash powder blend and MPPC at 1-3% by total weight of the mixture. They found no agglomeration of fibers occurred during the mixing. The flexural strength increased as more fibers were added (Jeong & Wagh, 2003). Higher flexural strengths were obtained for mixes containing longer fibers (Jeong & Wagh, 2003). They also found that the glass fibers increased the fracture toughness for these mixes. Jeong & Wagh (2003) reported that the fiber surface is not damaged by corrosion because the hardened MPPC matrix is a neutral pH whereas in the highly alkaline matrix of conventional cement, the glass fibers are damaged (Jeong & Wagh, 2003).

The influence of the glass fiber mass content on the bending response, density and compressive strength of ceramic concrete under quasi-static loading was evaluated by Tassew et al. (2010). The researchers used ceramic concretes which combined MPPC binders with lightweight expanded clay aggregate and chopped glass fibers of length 13 mm. The results showed that an increase in the fiber content had a negligible influence on the concrete density. The compressive strength increased by 26.7% when the fiber content increased from 0% to 2% by

mass of the total mix (Tassew et al., 2010). For flexural strength under the 4-point bending with quasi-static loading, Tassew et al. (2010) reported that fibers had negligible influence on the initial stiffness. However, the maximum load capacity increased with an increase in the fiber content. An increase by 176% was achieved when the fiber content was 2% by total mass of the mix compared to a similar mix without fibers (Tassew et al., 2010). An increase in the fiber dosage from 0% to 2% by total mass of the mix also resulted in an increase in the modulus of rupture from 8.6 to 12.6% of the compression strength (Tassew et al., 2010). For fiber contents above 1% by total mass of the mix, the increase in fiber content also increased the toughness of the specimens (Tassew et al., 2010).

Textile reinforcement has been proposed for application within structural members since it provides advantages compared to conventional steel reinforcement. Glass textile reinforcement is lightweight and has excellent resistance to corrosion, can match almost any geometric shape, and offers easier handling and rapid placement (Tassew & Lubell, 2010).

A study by Tassew and Lubell (2010) examined a layered system of ceramic composites with textile reinforcement. Two types of glass-fiber textiles were used to reinforce structural panels cast with either sand concrete or lightweight concrete containing expanded clay aggregate. MPPC binders were used to produce the concretes. Full-depth panels and partial-depth precast panels were examined in this study. The results showed that the specimen height, the number of layers of textile reinforcement and the construction type all influenced the peak load sustained by the panels (Tassew & Lubell, 2010). The post peak response was also reported to be influenced by the type of fiber, the stiffness of fiber and the type of construction (Tassew & Lubell, 2010).

2.2.4 Chemically bonded phosphate ceramics reinforced with natural fibers

Since the hardened CBPC matrix is a neutral pH and it is formed at room temperature, a wide range of fibers can be added in the matrix such as natural fibers (wood, cellulose, cotton…) and artificial fibers (such as nylon) (Wagh,

2004). Among those, wood composites have the greatest potential because bonding can be developed between the natural fiber surface and the CBPC matrix (Wagh, 2004). This bonding helps to produce the superior fiber-reinforced composites (Wagh, 2004).

Li et al. (2004) examined particleboards produced with MPC binder and wood waste that was described as 1 to 5 mm long, 1 mm thick and 2 to 3 mm wide. After mixing and casting, a pressure of 18.3 MPa was applied to the fresh mixture of wood waste and MPPC binder for 30 to 90 minutes. They reported that with the composition of 50wt% of wood and 50wt% of binder, the particleboards exhibited approximately 10.4 MPa in flexural strength (Li et al., 2004). When 60wt% and 70wt% of wood were used, the flexural strength of the specimens reduced significantly to 2.8 and 2.1 MPa, respectively (Li et al., 2004).

A study conducted by Donahue and Aro (2009) showed that waste pulp and paper mill residues can be added to MPPCs to create durable building materials. They examined board specimens produced with MPPC binder, waste residue, fly ash and other additives. These boards were cold-pressed during setting. Four waste residue:MPPC mass fractions from 0.63 to 1.1 and four FA:binder mass ratios from 0.25 to 1.0 were used. The results showed that the densities of these boards were from 1112 to 1177 kg/m^3 and they decreased as the waste residue:MPPC mass ratio increased. Water absorptions and volume swelling of the boards after a 24 hour water soak were from 25.2 to 31.4% and from 1.2 to 2.6%, respectively, with the higher values associated with higher waste residue:MPPC mass ratios. The highest modulus of rupture (3.3 MPa) was obtained for a board which had the waste residue:MPPC mass ratio of 0.79 and the FA:binder ratio of 0.43. Donahue and Aro (2009) suggested using a FA mass fraction at 0.40-0.45 of the total mass of FA + MPPC binder because it may be best for increasing the modulus of rupture.

Other properties of these boards were also examined by Donahue and Aro (2009) including thickness swell, screw withdrawal and internal bond strength. They reported that the particleboards met or exceeded the minimum requirement

for all properties of LD-1 grade particleboard except MOR (Donahue & Aro, 2009).

2.3 Prior studies on Portland cement concrete

Although MPPC materials have been used in structural applications in recent years, the knowledge base in this area is still limited. In contrast, Portland cement has been a popular construction material for a long time. Thus more literature is available for studies using Portland cement than for MPPC-based materials. Supplementary materials including silica fume, bentonite and Delvo Stabilizer have all been proposed for Portland cement concretes to increase their performance. However, there is no literature available for use of those materials with MPPCs. This section presents the results from prior research on the use of silica fume, bentonite and Delvo Stabilizer in Portland cement concretes. Based on the knowledge obtained from this section, silica fume, bentonite and Delvo Stabilizer were trialed to examine their effect on MPPC binders.

There is also no reference available about use of baking soda in Portland cement concrete or MPPCs. However, the idea of using a foaming agent to create a light weight concrete is not new in Portland cement concrete. Since baking soda is also a foaming agent, the influence of foaming agents on the properties of concrete is discussed in this section.

2.3.1 Incorporation of silica fume in Portland cement concrete

Silica fume (SF) was defined by ACI 116R-90 as "very fine noncrystalline silica produced in electric arc furnaces as a by-product of the production of elemental silicon or alloys containing silicon". It contains mostly of amorphous silicon dioxide in spherical particles with the typical diameter from 0.1 to 0.2 μm (ACI 234R-06).

Silica fume was first considered for use in concrete to improve the properties of fresh mortar (Sharp, 1946) and to partially replace the cement (ACI 234R-06). However, SF is currently used in the production of high-performance

concrete mainly because it can enhance the compressive strength and durability of concrete (ACI 234R-06).

Silica fume has several influences on the properties of fresh concrete including: water demand, workability, bleeding and plastic shrinkage.

The addition of SF increases the cohesion of fresh concrete and makes it less prone to segregation than concrete without SF (ACI 234R-06). Silica fume has very high surface area (13,000 – 30,000 m^2/kg) which leads to an increase in water demand of concrete as SF is added (Scali et al., 1987). Also, the high surface area of SF to be wetted reduces the free water in the mixture and thus significantly reduces the bleeding of fresh concrete (Grutzeck et al., 1982). However, this reduction in bleeding increases the potential for plastic-shrinkage cracking which occurs when water evaporates from the concrete surface faster than bleeding water appears at the surface, or when water is lost into the subgrade (ACI 234R-06). Thus, rapid moisture loss at early ages should be prevented by protecting the surface of freshly placed concrete containing SF (Jahren, 1983).

Based on experiments conducted by many researchers, ACI 234R-06 shows that the modulus of elasticity, Poisson's ratio, creep, total shrinkage, flexural and splitting tensile strengths of hardened Portland cement concrete containing SF are similar to those of Portland cement concrete without SF.

Silica fume, however, influences the compressive strength of Portland cement concrete. Under normal curing temperature, SF can improve the strength development of concrete at early ages up to 28 days (ACI 234R-06). When SF is added to the mixture of Portland cement and fly ash, it significantly increases the compressive strength of the mixture at the age of 1 day (ACI 234R-06). ACI 234R-06 also indicates that the compressive strength at 28 days of concrete containing SF is always higher, significantly in some cases, than that of the concrete without SF.

Several studies have been conducted to determine the influence of curing temperature on the compressive strength of SF concrete. When concrete was

cured at 50°F (10°C), the addition of SF did not significantly influence the compressive strength of concrete at 7 days but it did at both 28 days and 91 days (Yamato et al., 1986). However, when the curing temperature was increased to 68, 86, or 149°F (20, 30 or 65°C), the 7-day compressive strength and strengths after longer curing periods were increased significantly with the presence of SF (Yamato et al., 1986).

According to ACI 234R-06, the strength development of SF concrete is faster than that of concrete without SF at ages up to 91 days regardless of the curing conditions. After 91 days, the strength gain of concrete containing SF is generally lower than that of the concrete without SF (ACI 234R-06).

Although silica fume has been widely used in Portland cement concrete, no prior study on use of silica fume in MPPCs can be found.

2.3.2 Use of Delvo Stabilizer in Portland cement concrete

Delvo Stabilizer was first developed in 1986 to help concrete producers deal with the disposal of returned plastic concrete and concrete wash-water from truck drums (Glauberman, 2011). Moreover, it can be used to extend setting time of conventional concrete and preserve fresh concrete during job delays/truck breakdowns (Glauberman, 2011).

The influence of Delvo Stabilizer on properties of Portland cement concrete was examined by the California Department of Transportation (Poole, 1990). The results showed that the stabilizing agent had insignificant influence on the flexural strength, modulus of elasticity and abrasion resistance for concrete specimens. Slightly higher drying shrinkage values were observed for the specimens from the stabilized mix compared to those from a control mix during the first 21 days but the difference was negligible after six months (Poole, 1990).

The effect of the stabilizing agent on the properties of mortars was also examined by Borger et al. (1994). They reported that the workability was not

affected by Delvo Stabilizer. Specimens from the stabilized mix had equal or higher strength than those from the control mix (Borger et al., 1994).

Although Delvo Stabilizer has been used to control the setting time of Portland cement concrete, no prior literature on its influence on the setting time of MPPCs can be found.

2.3.3 Use of bentonite in Portland cement concrete

Bentonite is a clay typically produced from the alteration of volcanic ash which contains mainly smectite minerals, usually montmorillonite (IMA-NA, 2009). Bentonite exhibits strong colloidal properties and when coming into contact with water it increases several times in volume, creating a gelatinous and viscous fluid (IMA-NA, 2009). Moreover, it also has some special properties including hydration, swelling, water absorption, viscosity, and thixotropic which make it a valuable material for many applications (IMA-NA, 2009).

Bentonite can be used in civil engineering applications as a thixotropic, supporting and lubricating material in the construction of diaphragm walls, foundations, tunneling, drilling and pipe jacking (IMA-NA, 2009). Since bentonite enhances viscosity and plasticity, it is also used in Portland cement and mortars (IMA-NA, 2009).

Dolen and Benavidez (1998) examined the influence of bentonite on the mechanical properties and workability properties of low-strength concrete. Bentonite was used at zero (control mix), 10, 15 and 20% by mass of cement plus bentonite. The results showed that bentonite reduced the compressive strength of low-strength concrete at 3, 7, 14, 28, and 90 days after casting and the decrease in strength increased when higher bentonite fractions were used (Dolen & Benavidez, 1998). The modulus of elasticity also reduced when bentonite was added (Dolen & Benavidez, 1998). The study found that the design water content required to maintain a constant slump increased with the increase in bentonite content. Due to higher design water content, when the bentonite content increased

from zero to 10, 15 and 20%, the density of fresh concrete decreased by 3.1, 4.1 and 5.5%, respectively (Dolen & Benavidez, 1998).

Although bentonite has been used previously in Portland cement concrete, no prior literature on the use of bentonite in MPPCs can be found.

2.3.4 Use of baking soda in Portland cement concrete

Lightweight foamed or cellular concretes are typically produced by adding a foam to a cement slurry. Cellular concretes have much lower densities than typical concrete due to the air bubbles of the foam entrained within the concrete (Dattel, 2002). According to Dattel (2002), although cellular concretes have significantly lower density compared with normal concretes, they can sustain impressive compressive forces. This makes cellular concrete ideal for use in roofs, flooring materials, and in cases where normal concretes can create soil settling problems (Dattel, 2002).

Baking soda (i.e. sodium bicarbonate) releases carbonic air bubbles when coming in contact with an acidic solution. It was hypothesized that baking soda could be used as a foaming agent in MPPCs because they are produced by an acid-based reaction. Meanwhile, baking soda will not work as a foaming agent with Portland cement which is an alkaline system. No prior research on the use of baking soda to create foam in MPPCs can be found.

Chapter 3

MIX DEVELOPMENT

3.1 Introduction

According to Wagh and his colleagues (Wagh et al., 1997; Wagh et al., 1998; Wagh & Jeong, 2003), MPPC can be produced by the reaction between calcined magnesium oxide (MgO) and monopotassium phosphate (KH_2PO_4) (i.e. MKP) in an aqueous solution as follows:

(3-1)

The reaction rate and properties of the product obtained from Eqn. 3-1 depend on the molar ratios between MgO and MKP or the addition of fly ash and other compounds (Wagh et al., 1997; Wagh et al., 1998; Wagh & Jeong, 2003).

This chapter reports the development of MPPC concretes/wood composites using the MPPC binder described in Eqn. 3-1.

In this research, MPPC concretes/wood composites were produced with the desired properties including: light weight, moderate strength, suitable workability and low cost. Several additives and aggregates were examined including: fly ash, silica fume, sand, sawdust, bentonite, baking soda, and Delvo stabilizer. The effect of chopped glass-fibers and textile glass-fibers on the properties of MPPC concretes/wood composites was also examined. Characterization of materials, development of mixing and casting procedures, and testing methods are reported in this chapter.

3.2 Materials

3.2.1 Magnesium oxide

The calcined magnesium oxide (MgO) used in this study was obtained from Martin Marietta Magnesia Specialties, LLC and had the product name MagChem10CR. The manufacturer reported material properties are 97% MgO by

weight with a specific surface area of 0.3m^2/g and a minimum 95% of particles passing the 200 mesh size.

3.2.2 Mono-potassium phosphate

The fertilizer grade mono-potassium phosphate [MKP] (KH_2PO_4) was produced by Rotem Amfert Negev Ltd. The chemical composition of MKP is 51.5% P_2O_5 and 34.0% K_2O.

3.2.3 Fly ash

Class C fly ash obtained from a local coal-fired thermal power plant was examined in this research. The fly ash source was the same as used in earlier studies by Tassew and Lubell (2012) so that the chemical composition was relatively consistent. The chemical composition as reported by Tassew and Lubell (2012) is provided in Table 3-1.

Table 3-1: Chemical Composition of Class C Fly Ash (Tassew & Lubell, 2012)

Mass fraction (%)						
MgO	CaO	SiO_2	Fe_2O_3	Al_2O_3	SO_3	Na_2O
1.22	10.97	55.53	3.62	23.24	0.24	2.83

3.2.4 Aggregates

Angular quartz sand in four different particle size gradations was examined in this study. The particle size distributions were given by Sil Industrial Minerals and shown in Figure 3-1. The fineness modulus of sand types 1, 2, 3 and 4 were 1.0, 2.4, 3.4 and 4.0, respectively. All sand had the specific gravity of 2.65 g/cm^3 and moisture content of <0.1%.

3.2.5 Sawdust

The sawdust used in this study was waste MDF (medium density fiberboard) dust supplied by Canadian MDF Products Company (CANTRIM). The particle size distribution of the sawdust was obtained from sieve analysis according to ASTM C136-06 and is shown in Figure 3-1. The moisture content of

the sawdust of 5.1% by mass was obtained using the moisture content test procedures specified by the Alberta Ministry of Transportation (ATT-15/96). The sawdust had loose and compact unit weights of 178 kg/m^3 and 230 kg/m^3, respectively, based on ASTM C29/C29M-09.

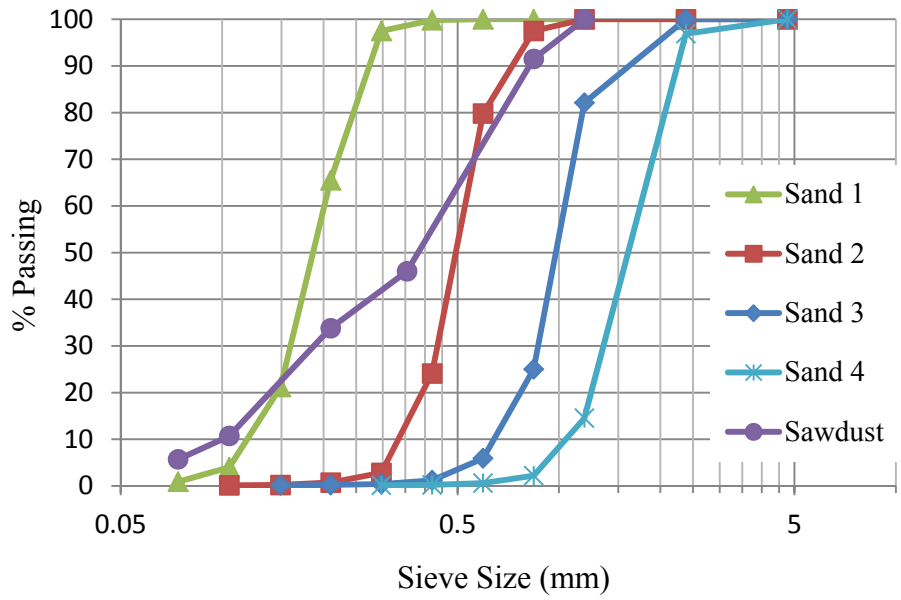

Figure 3-1: Particle size distribution of sand and sawdust

3.2.6 Silica fume

Silica fume is a by-product collected in electric arc furnaces from the production of elemental silicon or alloys containing silicon (ACI 116R-90). Silica fume can be used to enhance the mechanical property and fresh property of concrete. The undensified silica fume examined in this study was obtained from Elkon Products Inc. From the supplier, the material is reported to have a specific gravity of 2.2 g/cm^3, with 2.95% of particles retained on the No.325 Sieve (i.e. 45 μm). The chemical composition as reported by the supplier is given in Table 3-2:

Table 3-2: Chemical composition of Silica Fume

Mass fraction (%)						
SiO_2	SO_3	Cl^-	K_2O	Na_2O	Moisture Content	Loss on Ignition
95.57	0.3	0.06	0.51	0.17	0.61	1.93

3.2.7 Baking Soda

Baking soda (i.e. Sodium Bicarbonate) was used in this study as a foaming agent. During the mixing procedure, baking soda reacts with the acid part of the mixtures to release CO_2 in the form of bubbles. These bubbles help reduce the density of the cement paste. The foaming action also provides a lubrication effect for the materials to allow improved mixing, thereby increasing the quality of the mix. The food grade baking soda examined in this study is a product of ARM & HAMMER.

3.2.8 Bentonite

Aquagel viscosifier grade Bentonite was obtained from Baroid. From the manufacturer, Bentonite provides viscosity and reduces fluid loss for the mix. Also, Bentonite swells significantly in water and can fill the voids of the concrete (Kosmatka, 2002). This helps decrease the permeability of concrete. The chemical composition of Aquagel as reported by the manufacturer is shown in Table 3-3.

Table 3-3: Chemical composition of Bentonite

Substances	**Percentage (%)**
Bentonite	92-100
Crystalline silica, cristobalite	0-1
Crystalline silica, tridymite	0-1
Crystalline silica, quartz	1-6

3.2.9 Retarder

In prior studies, borax or lignosulphonate were used to retard the setting time of MPPCs (Wagh, 2004; Tassew & Lubell, 2012; Tassew & Lubell, 2013) but no study has examined the influence of Delvo Stabilizer on the setting time of MPPCs. In this research, the additive Delvo Stabilizer was examined to control the reaction rate between the MgO and MKP and retard the setting time. Delvo Stabilizer is a product of BASF Canada Inc. and is reported to contain 1-5% Phosphonic acid.

3.2.10 Glass-fibers and textile glass-fabrics

Alkali resistant (AR) glass-fibers used in this study were obtained from Nippon Electric Glass America, Inc. From the supplier, the diameter, length and tensile strength of the individual fibers were 0.0134 mm, 13 mm and 0.44 kN, respectively (Figure 3-2). The fibers are in bundles as cut roving and their density was 2723 kg/m^3. AR-glass fibers were added in mixes for cube, prism and cylinder specimens.

A commercially available glass-fiber textile fabric used to reinforce some panel specimens was supplied by St. Gobain Technical Fabrics (Figure 3-2). The mesh spacing and breaking strength of the textile were 8.33 mm in both directions and 200 kN/m, respectively. The textile was flexible and could be rolled for ease of transportation.

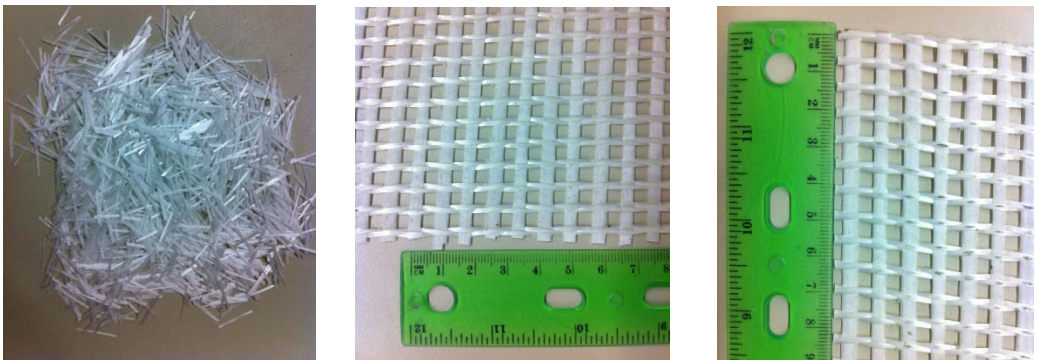

Figure 3-2: Glass-fibers and textile glass-fibers

3.2.11 Water

Municipal tap water from Edmonton, Alberta was used for all mixes in this research.

3.3 Mixing procedures and specimen preparation

The dry ingredients of the MPPC binders were prepared at the mass ratio of MgO:MKP=1:3 which is similar to the molar ratios in Eqn 3-1. The fly ash content was used at 50% by weight of the total binder. Prior research by Ding and Li (2005) and Tassew and Lubell (2013) showed that when FA is added with the content of 40-50%, the MPPC binders exhibit superior properties.

For mixes using sawdust, prior study by Donahue and Aro (2009) suggests using a FA mass fraction at 40 to 45% of the total mass of FA + MPPC binder because it may be best for increasing modulus of rupture. In this study, the FA content was varied from 20% to 50% by weight of the total binder to examine the effect of FA content on the compressive strength of the MPPC wood composites.

The water to binder (*w*/*b*) ratio was varied for each mix to find the influence of *w*/*b* ratio on the strength of the product. The mixing water quantity must also be sufficient to ensure an acceptable workability for the fresh mixtures. In this study, flowable mixes that were easy to cast and to compact were desired.

3.3.1 Trial mixes using bentonite, silica fume, sand, baking soda and sawdust

For different types of aggregates and fillers examined in this study, seven groups of mixes were prepared with the mix compositions as shown in Table 3-4, 3-5 and 3-6. Two groups of MPPCs named as TB and TS were produced using viscosifier Bentonite and filler Silica Fume. Two groups of sand mortars named as TSS and TBaS were made by combining sand with Silica Fume or Baking soda. The last three groups were MPPCs wood composites which were named as TSa, TSaS and TSaBaS. These MPPC wood composites were produced by mixing sawdust, sand and baking soda.

For convenience of recording and managing the data, all mixes in this study were given a coded mix identifier. For trial mixes that consisted of only MPPC binders (control mixes), the mix ID naming convention had the form: T(x); where T denoted a trial mix and x represented the age of the specimen at the time of testing. For example: T(3) was the trial mix of only MPPC binder and the specimens were tested at the age of 3 days after casting.

For MPPC concretes, the nomenclature to identify the mix design is illustrated in Fig. 3-3. Depending on the compositions and ingredients of each mix, the naming convention had several components as shown in the figure: the first letters indicated the inclusion of Bentonite, SF or baking soda in the mix; the following number indicated the content by mass percent of those ingredients; the

next two components indicated the sand type and sand content; two values in the parentheses showed the age of the specimen at the time of testing and the *w/b* mass ratio, respectively.

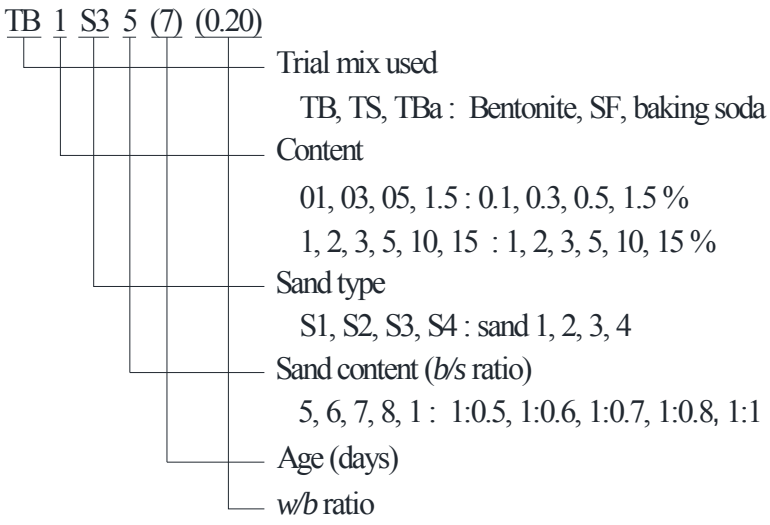

Figure 3-3: Specimen identification for MPPC concretes

For MPPC wood composites, the nomenclature used to identify the mix design is illustrated in Fig. 3-4. The naming convention had several components as shown in the figure: the first letters indicated the trial mix incorporating sawdust; the following number indicated the FA content by percent of the total mass of MgO, MKP and FA; the next two components indicated the baking soda content by percent of the total mass of the mix and sand type; two values in the parentheses showed the age of the specimen at the time of testing and the *w/b* mass ratio, respectively.

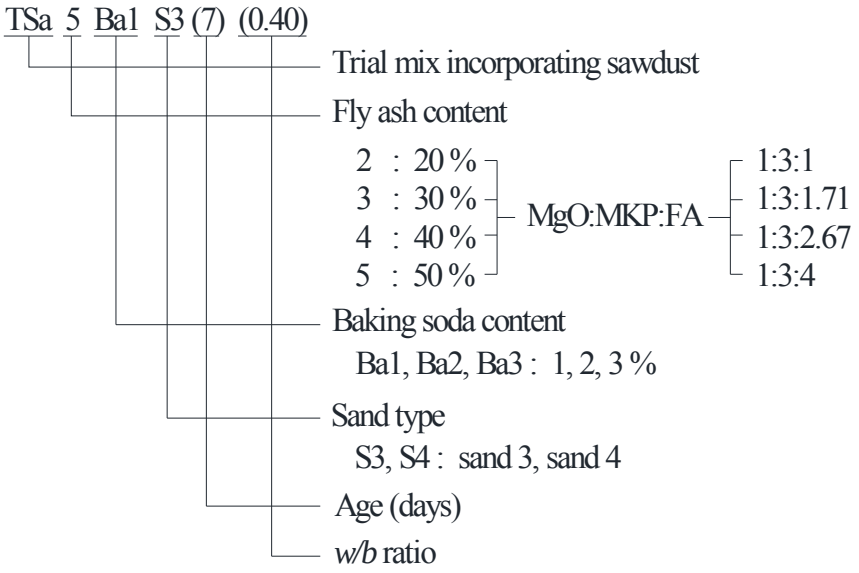

Figure 3-4: Specimen identification for MPPC wood composites

Table 3-4: Mix compositions of MPPCs and sand mortars

Group	Series	MgO:MKP:FA	Bentonite*	SF*	binder/sand ratio			w/b ratio
					Sand 1	Sand 2	Sand 3	
T	T	1:3:4	-	-	-	-	-	0.20
TB	TB1	1:3:4	1.0	-	-	-	-	0.16-0.28
	TB1.5	1:3:4	1.5	-	-	-	-	0.16-0.26
	TB3	1:3:4	3.0	-	-	-	-	0.18-0.28
TS	TS5	1:3:4	-	5	-	-	-	0.20
	TS10	1:3:4	-	10	-	-	-	0.20
	TS15	1:3:4	-	15	-	-	-	0.20
TSS	TS5S1	1:3:4	-	5	1:1	-	-	0.20
	TS5S2	1:3:4	-	5	-	1:1	-	0.20
	TS5S3	1:3:4	-	5	-	-	1:1	0.20
	TS10S1	1:3:4	-	10	1:1	-	-	0.20
	TS10S2	1:3:4	-	10	-	1:1	-	0.20
	TS10S3	1:3:4	-	10	-	-	1:1	0.20
	TS15S1	1:3:4	-	15	1:1	-	-	0.20
	TS15S2	1:3:4	-	15	-	1:1	-	0.20
	TS15S3	1:3:4	-	15	-	-	1:1	0.20

* *Bentonite and SF content by mass percent of the binder*

Table 3-5: Mix compositions of sand mortars and MPPC wood composites

Group	Series	MgO:MKP:FA	Baking soda*	binder/sand ratio		w/b ratio
				Sand 3	Sand 4	
TBaS	TBa01S45	1:3:4	0.1	-	1:0.5	0.20
	TBa03S45	1:3:4	0.3	-	1:0.5	0.20
	TBa05S45	1:3:4	0.5	-	1:0.5	0.20
	TBa1S31	1:3:4	1.0	1:1	-	0.20-0.26
	TBa1S45	1:3:4	1.0	-	1:0.5	0.20
	TBa1S46	1:3:4	1.0	-	1:0.6	0.20
	TBa1S47	1:3:4	1.0	-	1:0.7	0.20
	TBa1S48	1:3:4	1.0	-	1:0.8	0.20
	TBa2S45	1:3:4	2.0	-	1:0.5	0.20

* *baking soda content by percent of the total mass of dry ingredients;*

Table 3-6: Mix compositions of sand mortars and MPPC wood composites

Group	Series	MgO:MKP:FA	Baking soda*	b/sdt**	binder/sand ratio		w/b ratio
					Sand 3	Sand 4	
TSa	TSa5	1:3:4	-	1:0.2	-	-	0.32-0.50
TSaS	TSa2S4	1:3:1	-	1:0.2	-	1:0.5	0.36
	TSa3S4	1:3:1.71	-	1:0.2	-	1:0.5	0.36
	TSa4S4	1:3:2.67	-	1:0.2	-	1:0.5	0.36
TSaBaS	TSa2Ba1S3	1:3:1	1.0	1:0.2	1:0.5	-	0.36
	TSa2Ba2S3	1:3:1	2.0	1:0.2	1:0.5	-	0.36
	TSa2Ba3S3	1:3:1	3.0	1:0.2	1:0.5	-	0.36

* *baking soda content by percent of the total mass of dry ingredients;* ** *b/sdt: binder-to-sawdust mass ratio*

The influence of different water-to-binder (*w/b)* ratios on the fresh properties of mixes and the mechanical properties of hardened products was examined. Different amounts of Bentonite, Silica Fume, baking soda, sand and sawdust were examined to find the optimum amount of each material for each product. The specimens were tested at 1, 3, 7, 14, 28, 56 days after casting to determine the increase in strength with time for each product.

For the mixing operation, a 20 liter capacity portable mixer was used. The mixing speed was 60 rpm. To prepare each mix, the dry ingredients (MgO, MKP, FA, SF, sand, bentonite and baking soda) were first blended for 5 minutes. The retarder Delvo Stabilizer was separately added to the mixing water of all mixes at 2% by total mass of the binder (MgO + MKP) and mixed for 60 seconds. All dry-mixed ingredients were then gradually added to the water mixture using a scoop and mixed for an additional 5 minutes. The resulting mixture was then placed into plastic molds (50x50x50 mm cubes) using the scoop. A vibrating table was used to consolidate the mixture for 45 seconds. The top plane surface of the specimens was made flush with the top of the mold by using a trowel.

For mixes using sawdust, the dry ingredients (MgO, FA, sand and baking soda) were first mixed for 5 minutes and set aside. MKP and Delvo Stabilizer were then added to the water of all mixes at 2% by total mass of the binder (MgO + MKP) and mixed for 3 minutes to make an acidic solution. Sawdust was then added to the solution and mixed for an additional 7 minutes. According to Donahue and Aro (2009), MKP can act as a dispersant and disentangle the wood fibers. In addition, it may penetrate the fiber network which increases the fiber surface availability for bonding (Giri et al., 1998). Finally, the dry-mixed ingredients were gradually added to the wet sawdust mixture by using a scoop and mixed for 5 minutes. The resulting mixture was then placed into plastic molds (50x50x50 mm cubes, Figure 3-5) using the scoop. The resulting fresh mixture was placed to two-third the height of the mold and tamped 15 times on the surface using a tamper for consolidation. The mold was filled and tamped again with the

same number of strokes as for the first layer. A trowel was used to make the top plane surface flush with the top of the mold.

Evaporation of water can cause cracks on the surface. To prevent this moisture loss, plastic sheets were used to cover the top surface of the specimens. The specimens were removed from the molds 1 day after casting. Curing was conducted under the ambient laboratory temperature (23±2^{o}C) and relative humidity (50±5%) until testing.

Test results for trial mixes are presented in chapter 4. Detailed test data for each sample can be found in Appendix A.

3.3.2 Magnesium potassium phosphate ceramic concretes/wood composites using silica fume, sand, baking soda and sawdust

In this stage of the research, six different mixes were further studied to determine the mechanical properties and fresh properties of the product. The mix compositions are shown in Table 3-7. Two mixes named S5 and S10 added 5% and 10% SF by mass of the binder, respectively. The other two mixes named SS5 and SS10 also used 5% and 10% SF by mass of the binder but included sand. The last two mixes, named Sa and SaB, used saw dust and baking soda.

Table 3-7: Mix compositions of MPPC concretes/wood composites for further studies

Mix ID	MgO:MKP:FA ratio	Binder-to-sand ratio (*b/s*)	Binder-to-sawdust ratio (*b/sdt*)	Silica fume (%)	Baking soda (%)
S5	1:3:4	-	-	5	-
S10	1:3:4	-	-	10	-
SS5	1:3:4	1:1.0	-	5	-
SS10	1:3:4	1:1.0	-	10	-
Sa	1:3:1	1:0.5	1:0.2	-	-
SaB	1:3:1	1:0.5	1:0.2	-	2

The water to binder (*w*/*b*) mass ratios were kept at 0.2 for all mixes without sawdust and 0.36 for mixes with sawdust in this stage. The retarder Delvo

Stabilizer was separately added to the mixing water of all mixes at 2% by total mass of the binder (MgO + MKP) as described in Section 3.3.1. All products were tested at 90 days after casting to find the compressive strength and flexural strength.

The 20 liter capacity portable mixer was used for the mixing. The mixing operation was similar to that of trial mixes described in Section 3.3.1. Four types of specimen were cast: 50x50x50 mm cubes, 50x50x200 mm prisms, 100 mm-diameter x 200 mm-high cylinders, and 20x150x600 mm panels (Figure 3-5).

Cube

Prism

Cylinders

Panel

Figure 3-5: Four types of specimens

For mixes using sawdust, the resulting fresh mixtures were tamped until consolidated (the number of strokes depending on the horizontal dimension of the specimens and the size of the tamper). A pressure of 1.5 kPa was applied on the top of the panel specimens after the casting. The specimens were cured in a

similar manner to the trial mixes in Section 3.3.1. Because of some expansion of the panel specimens during the setting time, those specimens were de-molded at 2 hours after casting. The 1.5kPa load was also removed at the age of one day.

Test results for these mixes are presented in chapter 5. Detailed test data for each sample can be found in Appendix B.

3.3.3 Magnesium potassium phosphate ceramic concretes/wood composites reinforced with chopped glass-fibers and textile glass-fabrics

In the final phase of this research project, chopped glass-fibers and textile glass-fabrics were utilized to improve the performance of the material. The six mixes described in Section 3.2.2 were employed again in this stage as the matrices.

The water to binder (*w*/*b*) mass ratios were kept at 0.2 for all mixes without sawdust and 0.36 for mixes with sawdust in this stage. The retarder Delvo Stabilizer was separately added to the mixing water of all mixes at 2% by total mass of the binder (MgO + MKP) as described in Section 3.3.1. The chopped glass-fibers were added at 1% by total mass of the mix to the cube, cylinder and prism specimens. The textile glass-fibers were added to the panel specimen. All products were tested at 90 days after casting to find the compressive strength and flexural strength.

The mixing operation and specimen preparation were similar to those of mixes in Section 3.2.2. The chopped glass-fibers were dry-mixed at the same time with the other dry ingredients in the mixing sequence.

The small-scale prototype panel specimens were constructed in the configuration shown in Figure 3-6. The nominal panel thickness was 20 mm. Two layers of textile glass-fibers were positioned at 5 mm from the bottom and the top of the specimens. These panels were cast by placing a 6-7 mm thick MPPC layer in the bottom of the mold prior to placement of the first fabric. The fabric was then pressed gently into the MPPC layer and a second layer of MPPC material

was used to fill the mold to the total depth of 16-17 mm. The top fabric was then placed on the second MPPC layer and pressed gently. Finally, additional MPPC was added to fill the mold to the depth of 20 mm. The curing procedure was the same to that described in Section 3.2.2.

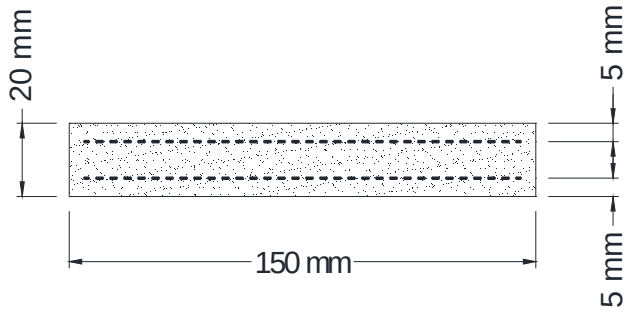

Figure 3-6: Panel cross-section

3.4 Test methods

3.4.1 Fresh property tests

The flow property of the fresh materials was determined using the Flow Table Test Method (ASTM C1437-07). A flow table and a cone as described in ASTM C230/C230 M (2008) were used to perform the test (Figure 3-7). The cone has the dimensions of 50 mm height, 100 mm bottom diameter and 70 mm top diameter. To perform the test, the cone was placed at the center of the flow table. The fresh mixture was poured into the cone to the height of 25 mm and tamped 20 times with the tamper. Then the cone was filled and tamped another 20 times. A trowel was used to make the top plane surface flush with the top of the cone. The cone was lifted away from the mortar within 1 minute after completing the mixing. The initial average spread diameter was measured and recorded. Then, the flow table was dropped 25 times in 15 seconds. The average spread was measured again. The flow is defined here as the percentage increase in average base diameter of the mortar mass after the flow table was dropped.

Figure 3-7: Flow test

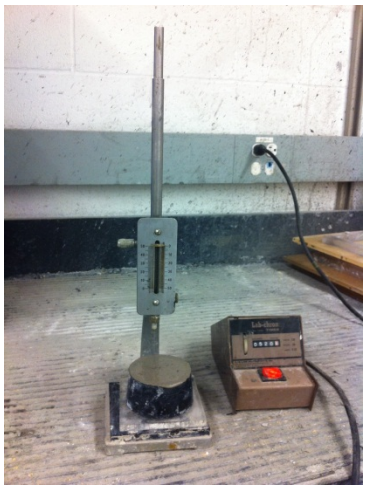

Figure 3-8: Setting time test

The setting time of the fresh mortar was determined using a Vicat Needle (ASTM C191-08) (Figure 3-8). The initial setting time was measured from the time the dry ingredients contacted with the water to the time when the penetration of Vicat Needle into the paste was measured to be 25 mm. The final setting time was measured from the time the dry ingredients contacted with the water to the time when there was no penetration of Vicat Needle into the paste.

3.4.2 Compression tests

The compressive strength of the hardened material was determined by testing the 50x50x50 mm cube specimens. A Forney machine with compression capacity of 3100 kN was used for the test. The loading rate was 250 kPa/s (ASTM C39/C39M-09) (Fig. 3-9a). The averages of three tests are reported unless noted otherwise.

The uniaxial compression stress-strain response for the material, including the post-peak response, was determined by testing the cylinders in a MTS 2600 universal testing machine with a compressive capacity of 2600 kN. The cylinders have the dimensions of 100 mm diameter and 200 mm height. The cylinder ends were ground in accordance with the requirements of ASTM C617-10. The loading was displacement controlled at a rate of 1.25 mm/min (ASTM C469-02). Figure 3-9b shows the test arrangement for the cylinders with a collar system and three high precision LVDTs separated by 120^{o} that were used to determine the axial

deformation of the cylinders during the loading. The initial gauge length of the LVDTs was 100 mm. The averages of three tests are reported unless noted otherwise.

(a) Cube test *(b) Cylinder test*

Figure 3-9: Compression tests

3.4.3 Flexure tests

The flexural strength versus mid-span deflection response, including the post-peak response, of the 50x50x200 mm prisms was determined by using a 4-point bending configuration. The bottom face of each specimen was saw-cut to make a 5 mm deep notch at the mid-span. MTS 1000 universal testing machine with the capacity of 1000 kN was used for all tests (Figure 3-10a and Figure 3-11a). The loading was displacement controlled at a rate of 0.1 mm/sec. The mid-span deflection of the prism during the test was measured as the average displacement of two LVDTs at mid-span. The averages of three tests are reported unless noted otherwise.

For the flexural response of panels, a 3-point bending test configuration was used. All flexural tests were conducted according to ASTM C78-10. A Lloyd testing machine with 30 kN capacity was used for all tests. The loading was displacement controlled at a rate of 0.1 mm/sec (Figure 3-10b and Figure 3-11b). The mid-span deflection of the panel during the test was measured as the average

displacement of two LVDTs at mid-span. The averages of three tests are reported unless noted otherwise.

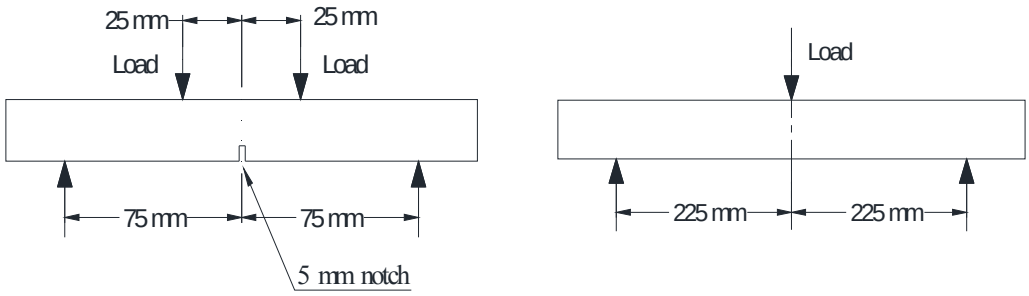

(a) Four-point bending test (b) Three-point bending test

Figure 3-10: Loading arrangements

(a) Prim test *(b) Panel test*

Figure 3-11: Flexure tests

Chapter 4

TRIAL MIX PROGRAM

4.1 Introduction

This chapter presents the test results for trial mixes that were prepared with different compositions and ingredients. The mix compositions were described in Section 3.3.1. The aim of this phase of the study was to find the influence of bentonite, baking soda, silica fume and fly ash additions on the compression and workability properties of MPPC concretes/wood composites. Mixes that meet the requirements for suitable compressive strength, low density and low cost were desired. In terms of workability, flowable mixes that were easy to cast and to compact were desired. Detailed results of all mixes are presented in Appendix A.

4.2 Properties of MPPC concretes and MPPC wood composites

The workability of the trial mixes was examined by observation during the mixing and casting procedures. The compressive strengths of MPPC concretes from the trial mixes were evaluated by testing 50x50x50 mm cube specimens. The maximum loading value indicated by the testing machine was recorded and the compressive strength was calculated as follows:

$$f_{cu} = \frac{P}{A_{cube}} \qquad (4\text{-}1)$$

where f_{cu} : cube compressive strength (MPa)

P : maximum load (N)

A_{cube} : area based on the loaded side of the specimen (mm^2)

Detailed values of f_{cu} for each individual specimen, the average and the coefficient of variation for each mix series are presented in Appendix A.

Values of compressive strength of three cube specimens of the same batch and tested at the same age were averaged and reported to the nearest 0.1 MPa.

According to ASTM C109/C109M-12, the compressive strength of each specimen should not differ by more than 8.7% of the average value of three cubes. Since this trial mix program was established to understand basic trends, when the compressive strengths exceeded 8.7% the average value of three cubes, the most deviated result was discarded and the remaining two specimens was checked again. The compressive strength of each of two remaining specimens should not differ by more than 7.6% the average value of two cubes.

4.2.1 MPPC binders and sand mortars

4.2.1.1 Strength development of MPPC binders

Six trial mixes (control mixes) named T(1), T(3), T(7), T(14), T(28) and T(56) were prepared. All mixes had a MgO:MKP:FA mass ratio of 1:3:4 and a *w/b* ratio of 0.20. Specimens were tested at several ages of up to 56 days as shown in Fig. 4-1. A summary of the experimental data is provided in Table 4-1.

It can be observed from Fig. 4-1 that MPPC binders had a rapid strength gain in the first 7 days in which more than 70% of the corresponding 56-day strength was reached. The rate of strength development was significantly lower between 7 and 28 days, with the strength increasing by 23% of the corresponding 56-day strength for a period of 21 days. The strength gain was very low after 28 days with only a 5% gain of the corresponding 56-day strength for a period of 28 days. This trend of rapid strength gain at early ages is consistent with the results of prior research on MPPC binders (e.g. Wagh, 2004) and it is suitable for some concrete applications that need short construction duration.

Figure 4-2 shows the variation in density of MPPC binders at ages of up to 56 days. It can be observed that the density decreased slightly over time. The density at 56-day age was 97% of the corresponding 1-day density.

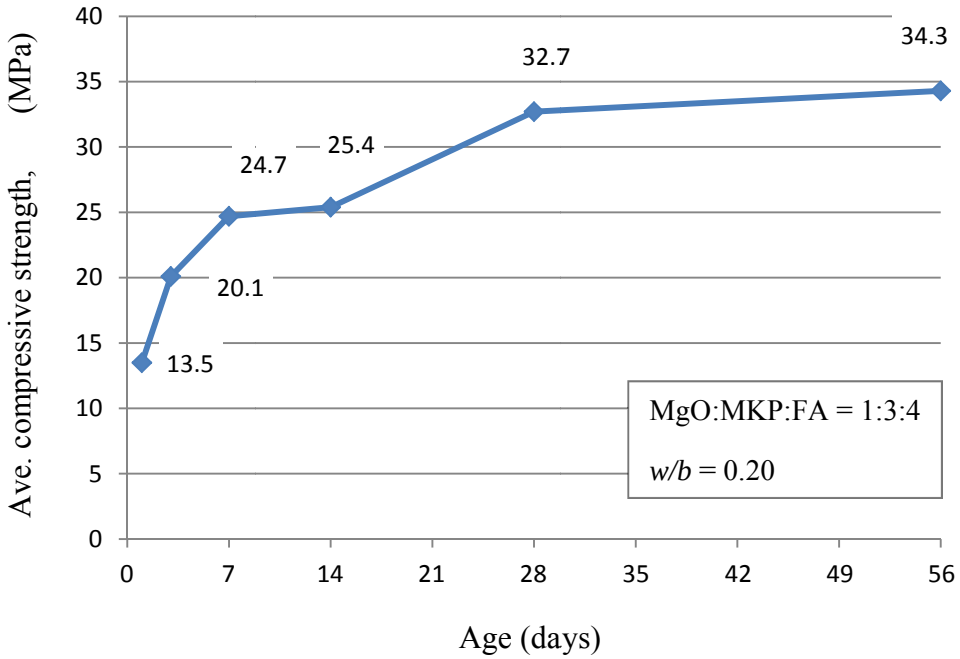

Figure 4-1: Strength development of MPPC binders in T–series

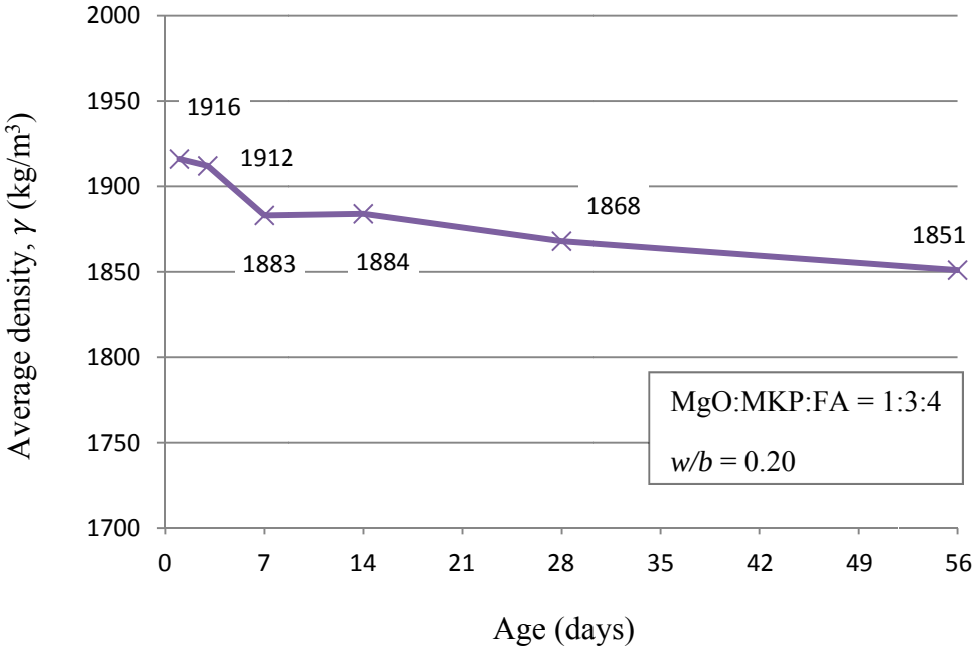

Figure 4-2: Density vs. age of MPPC binders in T–series

Table 4-1: Strength development of MPPC binders (w/b=0.2)

Mix ID	Age (days)	Average compressive strength, f_{cu} (MPa)	COV	Average density, γ (kg/m^3)	COV
T(1)	1	13.5	0.068	1916	0.010
T(3)	3	20.1	0.064	1912	0.003
T(7)	7	24.7	0.097	1883	0.013
T(14)	14	25.4	0.091	1884	0.013
T(28)	28	32.7	0.095	1868	0.006
T(56)	56	34.3	0.057	1851	0.006

4.2.1.2 Effect of bentonite on compressive strength of MPPC binders

The influence on strength of including bentonite was studied by preparing a group of trial mixes named TB. These mixes used the MgO:MKP:FA mass ratio of 1:3:4. The compressive strengths from the cube tests were obtained at 7 and 28 days after casting. Test results are summarized in Table 4-2 and 4-3.

Table 4-2: 7-day age test result for mixes containing bentonite

Series	Mix ID	Bentonite (%)	w/b mass ratio	Average compressive strength, f_{cu} (MPa)	COV	Average density, γ (kg/m^3)	COV
TB1	TB1(7)(0.16)	1.0	0.16	41.2	0.128	1948	0.001
	TB1(7)(0.18)		0.18	53.0	0.056	1923	0.011
	TB1(7)(0.20)		0.20	43.7	0.042	1911	0.008
	TB1(7)(0.22)		0.22	36.0	0.105	1871	0.008
	TB1(7)(0.24)		0.24	26.1	0.063	1837	0.006
	TB1(7)(0.26)		0.26	12.4	0.062	1747	0.008
	TB1(7)(0.28)		0.28	19.6	0.074	1705	0.005
TB1.5	TB1.5(7)(0.16)	1.5	0.16	42.2	0.078	1934	0.009
	TB1.5(7)(0.18)		0.18	42.4	0.031	1921	0.001
	TB1.5(7)(0.20)		0.20	45.7	0.051	1912	0.007
	TB1.5(7)(0.22)		0.22	38.8	0.042	1859	0.009
	TB1.5(7)(0.24)		0.24	30.9	0.048	1833	0.021
	TB1.5(7)(0.26)		0.26	18.6	0.034	1791	0.009
TB3	TB3(7)(0.18)	3.0	0.18	49.6	0.009	1909	0.010
	TB3(7)(0.20)		0.20	35.8	0.008	1924	0.003
	TB3(7)(0.22)		0.22	39.4	0.056	1876	0.006
	TB3(7)(0.24)		0.24	36.5	0.073	1857	0.007
	TB3(7)(0.26)		0.26	11.2	0.062	1781	0.001
	TB3(7)(0.28)		0.28	16.4	0.067	1746	0.011

Bentonite content is by mass percent of the binder

Table 4-3: 28-day age test result for mixes containing bentonite

Series	Mix ID	Bentonite (%)	w/b mass ratio	Average compressive strength, f_{cu} (MPa)	COV	Average density, γ (kg/m^3)	COV
TB1	TB1(28)(0.16)	1.0	0.16	59.9	0.054	1935	0.012
	TB1(28)(0.18)		0.18	54.9	0.157	1933	0.012
	TB1(28)(0.20)		0.20	54.2	0.040	1899	0.002
	TB1(28)(0.22)		0.22	47.2	0.094	1858	0.012
	TB1(28)(0.24)		0.24	32.9	0.066	1814	0.002
	TB1(28)(0.26)		0.26	29.9	0.097	1713	0.003
	TB1(28)(0.28)		0.28	21.3	0.062	1655	0.008
TB1.5	TB1.5(28)(0.16)	1.5	0.16	57.9	0.018	1935	0.008
	TB1.5(28)(0.18)		0.18	45.9	0.106	1936	0.003
	TB1.5(28)(0.20)		0.20	56.9	0.041	1893	0.006
	TB1.5(28)(0.22)		0.22	49.2	0.009	1852	0.007
	TB1.5(28)(0.24)		0.24	41.5	0.107	1800	0.003
	TB1.5(28)(0.26)		0.26	27.3	0.044	1741	0.006
TB3	TB3(28)(0.18)	3.0	0.18	53.1	0.099	1910	0.003
	TB3(28)(0.20)		0.20	59.4	0.011	1901	0.012
	TB3(28)(0.22)		0.22	45.4	0.049	1864	0.003
	TB3(28)(0.24)		0.24	46.7	0.026	1835	0.006
	TB3(28)(0.26)		0.26	16.1	0.127	1761	0.010
	TB3(28)(0.28)		0.28	17.6	0.008	1724	0.005

Bentonite content is by mass percent of the binder

The relationship between f_{cu} and bentonite content is illustrated in Fig. 4-3. It can be observed that the cube compressive strength increased when bentonite was added to the mix. At 1% by mass of the binder, bentonite increased the strength by 76% and 66% at 7 and 28 days, respectively, when compared with mixes without bentonite. However, adding more than 1% bentonite by mass of the binder did not give significant further increases in strength. Regardless of the amount of bentonite used, the compressive strength of all specimens increased with age as shown in Fig. 4-3 and Table 4-4.

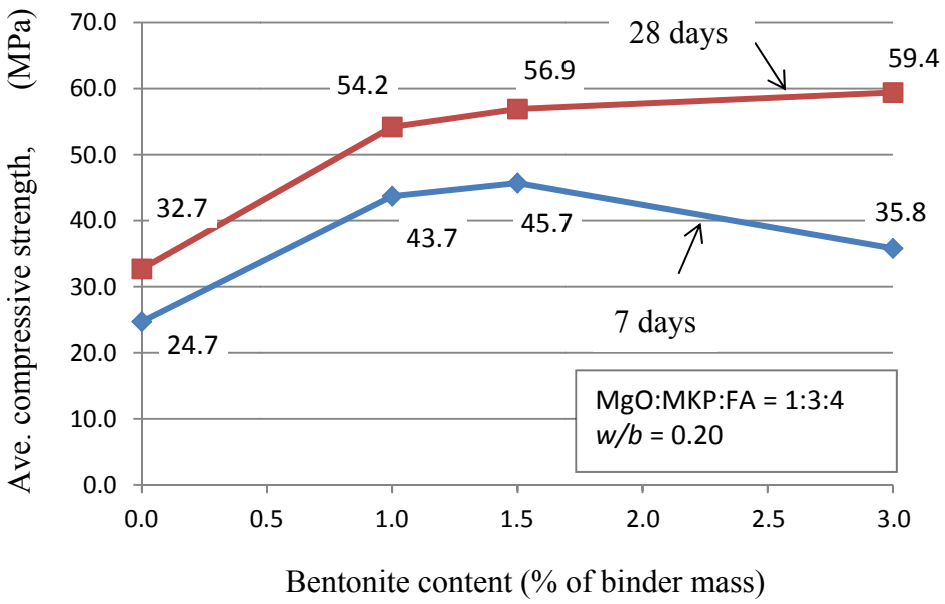

Figure 4-3: Compressive strength vs. bentonite content in TB-series

Effect of varied *w/b* mass ratios on the compressive strength of MPPC binders containing bentonite is shown in Fig. 4-4 and Fig. 4-5 in which bentonite was used at 1.0, 1.5 and 3% by mass of the binder. It is observed that at both 7 and 28 days, the strength decreased when the *w/b* ratio increased regardless of bentonite content.

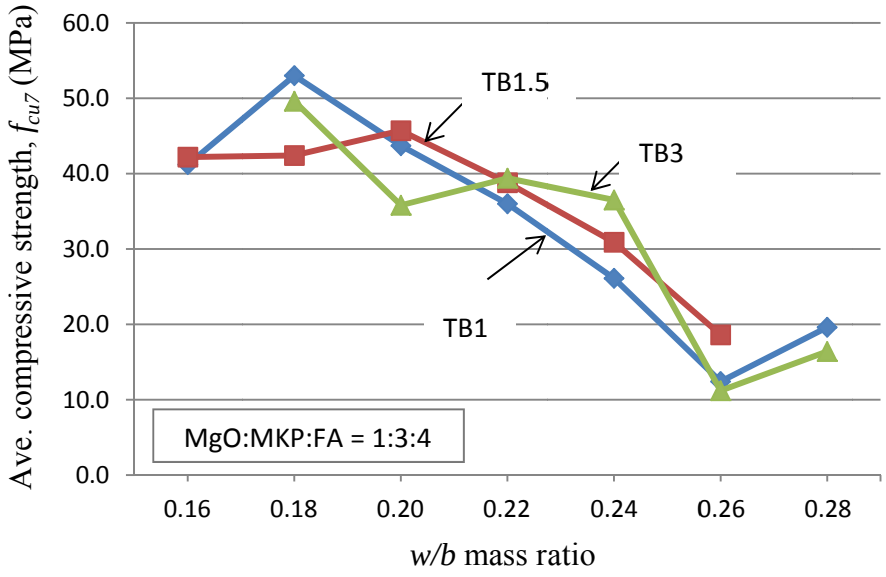

Figure 4-4: 7-day cube compressive strength vs. w/b ratio for TB-series

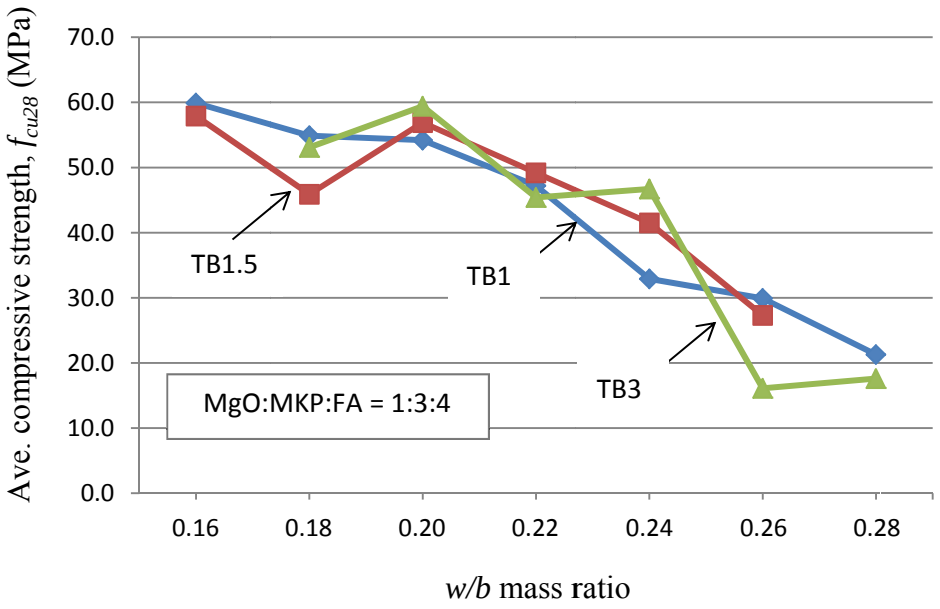

Figure 4-5: 28-day cube compressive strength vs. w/b ratio for TB-seires

Table 4-4: Cube compressive strength of MPPC binders containing bentonite

w/b	**Average cube compressive strength, f_{cu} (MPa)**					
	1% bentonite		1.5% bentonite		3% bentonite	
	7-day age	28-day age	7-day age	28-day age	7-day age	28-day age
0.16	41.2	59.9	42.2	57.9	-	-
0.18	53.0	54.9	42.4	45.9	49.6	53.1
0.20	43.7	54.2	45.7	56.9	35.8	59.4
0.22	36.0	47.2	38.8	49.2	39.4	45.4
0.24	26.1	32.9	30.9	41.5	36.5	46.7
0.26	12.4	29.9	18.6	27.3	11.2	16.1
0.28	19.6	21.3	-	-	16.4	17.6

bentonite content is by mass percent of the binder

In terms of workability of the fresh mixture, it was found easier to perform the mixing and casting procedures for mixes with higher *w/b* ratios. However, no change in workability can be qualitatively recognized with changes in bentonite content.

Densities of mixes using different bentonite contents tested at 7-day and 28-day ages are shown in Fig. 4-6 and 4-7. In general, the densities reduced when

the *w/b* mass ratio increased. Changes in bentonite content had negligible effect on the densities of all mixes.

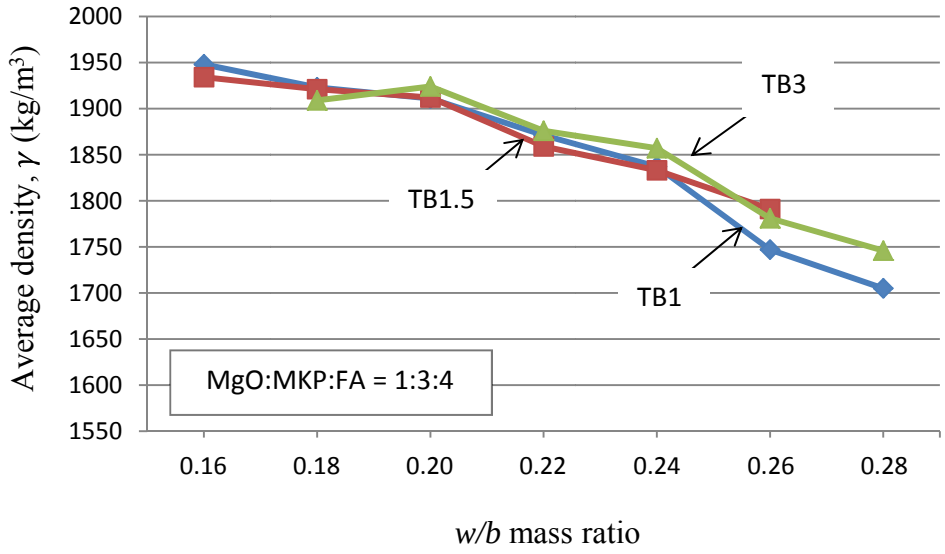

Figure 4-6: 7-day density vs. w/b ratio for TB-series

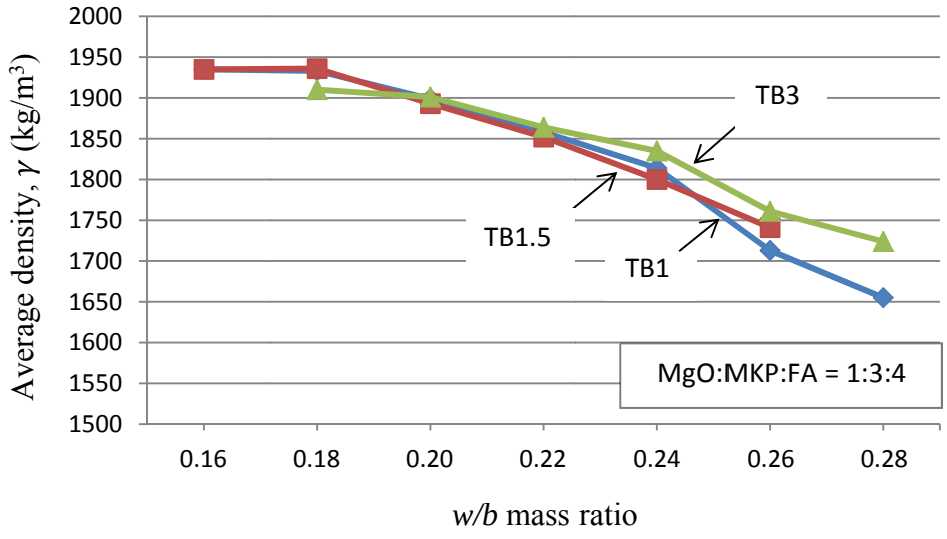

Figure 4-7: 28-day density vs. w/b mass ratio for TB-seires

4.2.1.3 Effect of silica fume on compressive strength of MPPC binders

To study the effect of SF on the compressive strength of MPPC binders, several trial mixes named TS were prepared with MgO:MKP:FA mass ratio = 1:3:4 and *w/b* = 0.20. Silica fume was added at 5, 10 and 15% by mass of the

binder. The compressive strength was determined by testing the cubes at different ages of up to 56 days after casting. Test results are summarized in Table 4-5.

Table 4-5: Test results of mixes containing SF (w/b = 0.20)

Mix ID	Silica fume (%)	Age (days)	Average compressive strength, f_{cu} (MPa)	COV	Average density, γ (kg/m^3)	COV
TS5(1)	5	1	14.8	0.078	1956	0.005
TS5(3)		3	44.8	0.061	1918	0.006
TS5(7)		7	46.4	0.000	1899	0.010
TS5(14)		14	49.0	0.078	1905	0.004
TS5(28)		28	42.7	0.135	1901	0.005
TS5(56)		56	49.2	0.132	1910	0.003
TS10(1)	10	1	15.8	0.075	1944	0.007
TS10(3)		3	47.1	0.086	1930	0.002
TS10(7)		7	53.5	0.085	1907	0.005
TS10(14)		14	54.5	0.055	1920	0.007
TS10(28)		28	57.9	0.072	1919	0.003
TS10(56)		56	65.6	0.048	1913	0.011
TS15(1)	15	1	17.7	0.085	1921	0.004
TS15(3)		3	48.2	0.087	1940	0.009
TS15(7)		7	53.1	0.007	1916	0.004
TS15(14)		14	48.4	0.021	1930	0.003
TS15(28)		28	63.4	0.058	1923	0.008
TS15(56)		56	64.6	0.058	1907	0.007

Figure 4-8 shows that at one day after casting, the strengths of all mixes were approximately 15 MPa. At 3 days, the strengths of mixes containing SF had increased significantly, by approximately 190% of the corresponding 1-day strength. Meanwhile, the 3-day strength of the mix without SF (control mix) increased by only 50% of the corresponding 1-day strength. For the period between 3 and 28 days, steady strength increases can be observed for all mixes. Strength increases were negligible for all mixes in the TB-series after 28 days.

The results show that the addition of SF can effectively increase the compressive strength of MPPC binders and enhance the strength development rate

at early ages. When more SF was added, the strength increased accordingly. There appeared to be negligible benefit if more than 10% SF is added to the mix.

Regarding the workability property, it was qualitatively observed that adding SF increased the viscosity and reduced the setting time of the fresh mixture.

Densities at several ages for mixes containing different SF contents are shown in Fig. 4-9. In general, the densities reduced rapidly between 1 and 7 days and then slowly reduced after 7 days. The densities at 56 days were 97, 98 and 99% of the corresponding 1-day densities for mixes containing 5, 10 and 15%, respectively. It is also noticed that the changes in SF content had little influence on the density of mixes.

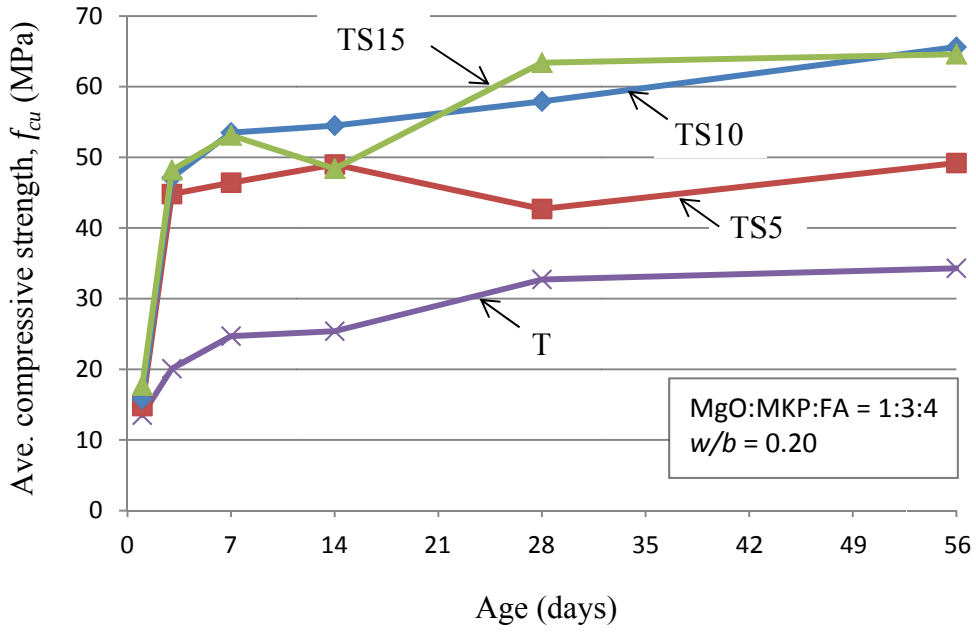

Figure 4-8: Compressive strength vs. age of mixes containing silica fume

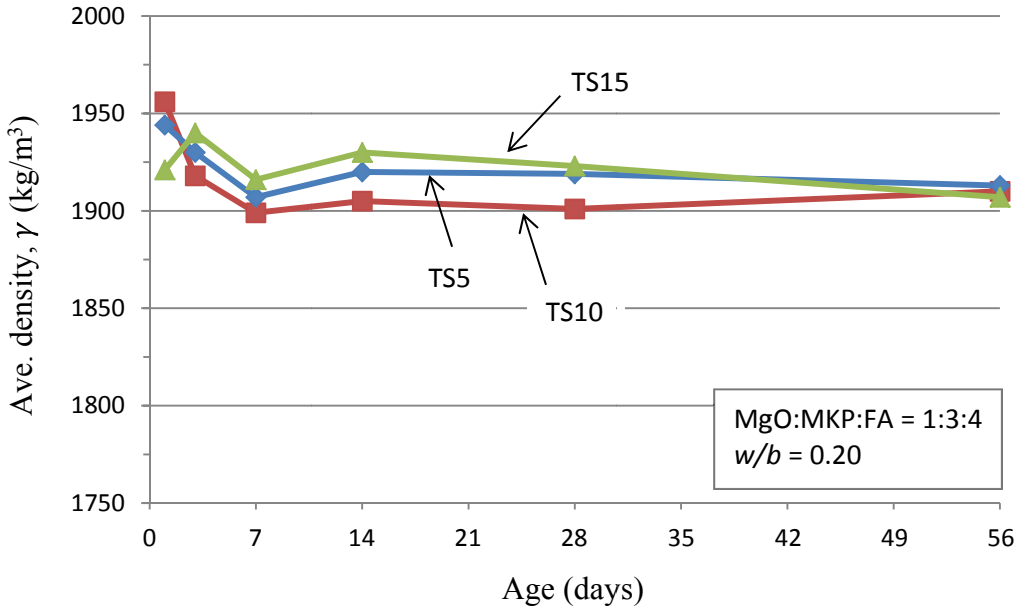

Figure 4-9: Density vs. age of mixes containing silica fume

4.2.1.4 Effect of silica fume on compressive strength of sand mortars

Several trial mixes named TSS were conducted to study the influence of SF on the cube compressive strength of sand mortars using MPPC binders. Sand mortars containing sand 1, sand 2 and sand 3 were examined. These mixes used MgO:MKP:FA mass ratio of 1:3:4, *w/b* mass ratio of 0.20 and were tested at different ages of up to 56 days after casting. According to Tassew and Lubell (2013), the compressive strength of sand mortars using MPPC binders increased by approximately 28% when the binder-to-sand (*b/s*) mass ratio increased from 1.0 to 3.0. Since the unit cost of sand is lower than the binder, a lower *b/s* ratio will result in a lower unit cost for the mortar. Thus, a *b/s* ratio of 1.0 was chosen for all mixes in this section even though it would not produce the highest possible strength. Test results are summarized in Table 4-6, 4-7 and 4-8.

Table 4-6: Test results for sand-1 mortars (w/b = 0.20)

Mix ID	Silica fume (%)	Age (days)	Average compressive strength, f_{cu} (MPa)	COV	Average density, γ (kg/m^3)	COV
TS5S1(1)	5	1	27.7	0.081	2151	0.010
TS5S1(3)		3	30.4	0.019	2153	0.007
TS5S1(7)		7	35.6	0.025	2125	0.010
TS5S1(14)		14	36.8	0.087	2126	0.007
TS5S1(28)		28	44.0	0.071	2124	0.008
TS10S1(1)	10	1	30.7	0.016	2178	0.008
TS10S1(3)		3	34.5	0.032	2180	0.004
TS10S1(7)		7	35.0	0.044	2136	0.011
TS10S1(14)		14	43.1	0.029	2154	0.008
TS10S1(28)		28	39.1	0.122	2127	0.003
TS15S1(1)	15	1	33.5	0.069	2197	0.006
TS15S1(3)		3	37.8	0.038	2204	0.007
TS15S1(7)		7	37.7	0.076	2180	0.004
TS15S1(14)		14	40.8	0.080	2174	0.011
TS15S1(28)		28	46.0	0.065	2168	0.009

Silica fume content is by mass percent of the binder

Table 4-7: Test results for sand-2 mortars (w/b = 0.20)

Mix ID	Silica fume (%)	Age (days)	Average compressive strength, f_{cu} (MPa)	COV	Average density, γ (kg/m^3)	COV
TS5S2(1)	5	1	21.8	0.022	2101	0.013
TS5S2(3)		3	25.7	0.016	2098	0.003
TS5S2(7)		7	25.9	0.118	2088	0.008
TS5S2(14)		14	31.4	0.093	2097	0.012
TS5S2(28)		28	36.7	0.093	2077	0.012
TS5S2(56)		56	44.8	0.036	2099	0.001
TS10S2(1)	10	1	27.9	0.007	2212	0.009
TS10S2(3)		3	34.3	0.080	2199	0.011
TS10S2(7)		7	34.6	0.085	2174	0.011
TS10S2(14)		14	37.1	0.039	2180	0.007
TS10S2(28)		28	44.2	0.088	2184	0.007
TS10S2(56)		56	49.4	0.069	2183	0.014
TS15S2(1)	15	1	34.3	0.094	2227	0.004
TS15S2(3)		3	40.9	0.009	2216	0.007
TS15S2(7)		7	35.5	0.025	2214	0.005
TS15S2(14)		14	41.5	0.068	2178	0.007
TS15S2(28)		28	47.9	0.057	2199	0.007
TS15S2(56)		56	50.7	0.052	2185	0.009

Silica fume content is by mass percent of the binder

Table 4-8: Test results for sand-3 mortars (w/b = 0.20)

Mix ID	Silica fume (%)	Age (days)	Average compressive strength, f_{cu} (MPa)	COV	Average density, γ (kg/m^3)	COV
TS5S3(1)	5	1	22.7	0.044	2223	0.011
TS5S3(3)		3	27.4	0.008	2181	0.007
TS5S3(7)		7	30.2	0.054	2161	0.007
TS5S3(14)		14	29.7	0.042	2151	0.008
TS5S3(28)		28	38.4	0.006	2147	0.011
TS5S3(56)		56	40.3	0.090	2157	0.005
TS10S3(1)	10	1	26.8	0.056	2229	0.009
TS10S3(3)		3	31.3	0.087	2209	0.011
TS10S3(7)		7	35.1	0.053	2207	0.008
TS10S3(14)		14	38.0	0.074	2196	0.011
TS10S3(28)		28	43.1	0.041	2225	0.012
TS10S3(56)		56	46.5	0.047	2190	0.013
TS15S3(1)	15	1	29.6	0.037	2234	0.008
TS15S3(3)		3	35.7	0.038	2220	0.007
TS15S3(7)		7	39.8	0.034	2214	0.011
TS15S3(14)		14	41.1	0.038	2162	0.009
TS15S3(28)		28	46.8	0.029	2207	0.008
TS15S3(56)		56	52.4	0.053	2178	0.008

Silica fume content is by mass percent of the binder

It can be seen in Fig. 4-10 that when 5% SF by mass of binder was added to the binder (i.e. mix TS5), the strength of the cubes increased significantly from 20.1 MPa to 44.8 MPa at the age of 3 days compared to the control mix without SF (i.e. mix T). When sand was included, however, the strengths of mixes at the same age dropped to 30.4, 27.4 and 25.7 MPa for sand 1, sand 3 and sand 2, respectively (TS5S1, TS5S2, TS5S3). It is also noticeable that at the age of one day, all cubes using sand had higher strengths than the specimens without sand. Past the age of 3 days, the strength development trends of all mixes are similar in which the rate of strength gain gradually decreased after 7 days and strength gain was very small after 28 days. Note that test results for mixes using sand type 1 were not available after 28 days.

Trial mixes were also prepared using 10% and 15% SF by mass of binder as shown in Fig. 4-11 and Fig. 4-12. The strength development trends for these mixes were similar to the 5% SF mixes in Fig. 4-10. By comparing Fig. 4-10 through Fig. 4-12, it is observed that the sand type had more influence on the

strengths of sand mortars containing 5% SF than the strengths of sand mortars containing 10 or 15% SF.

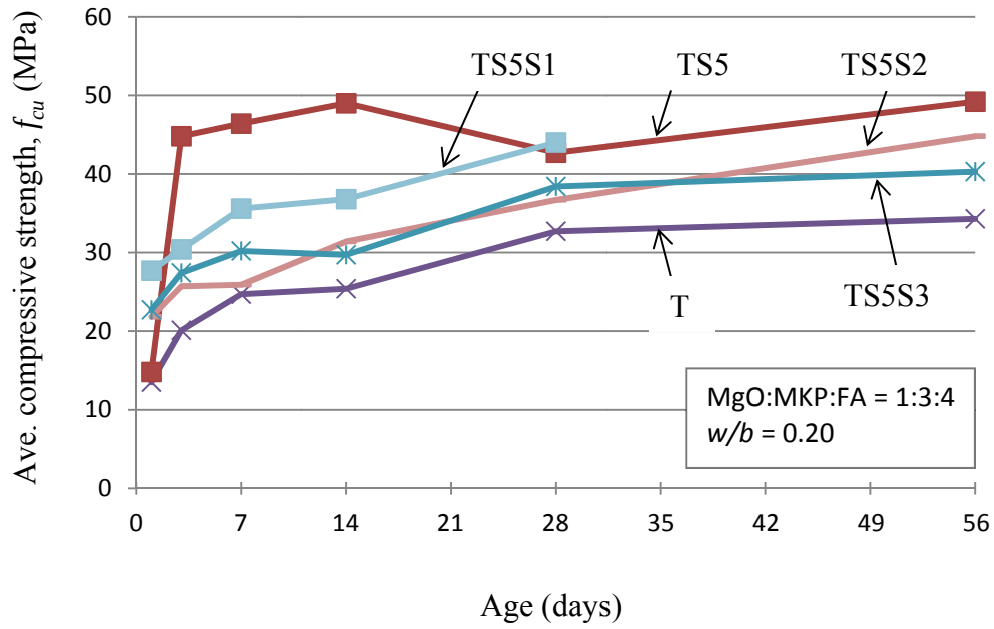

Figure 4-10: Compressive strength of sand mortars with 5% silica fume

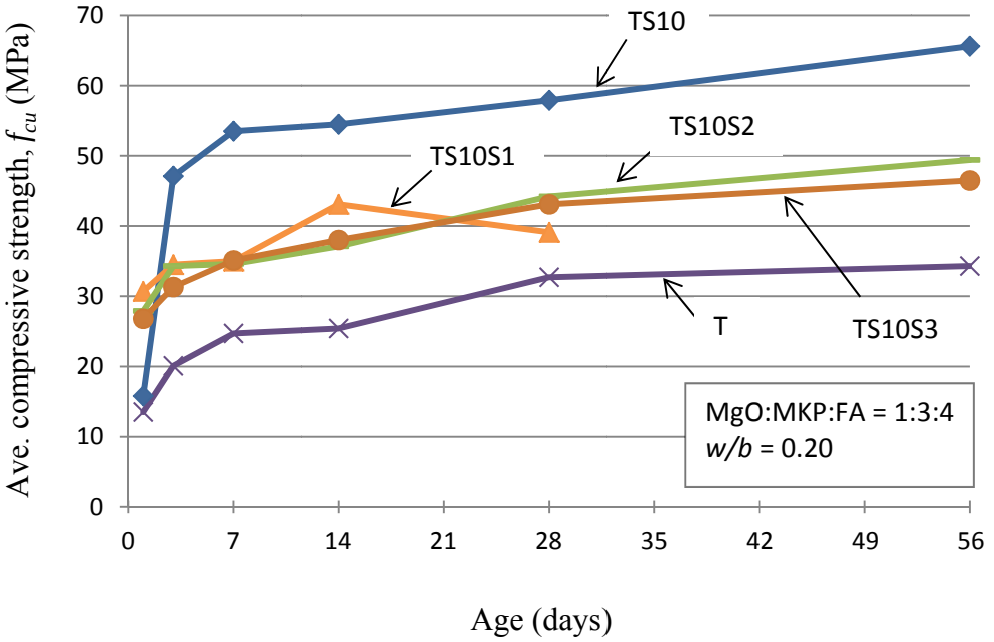

Figure 4-11: Compressive strength of sand mortars with 10% silica fume

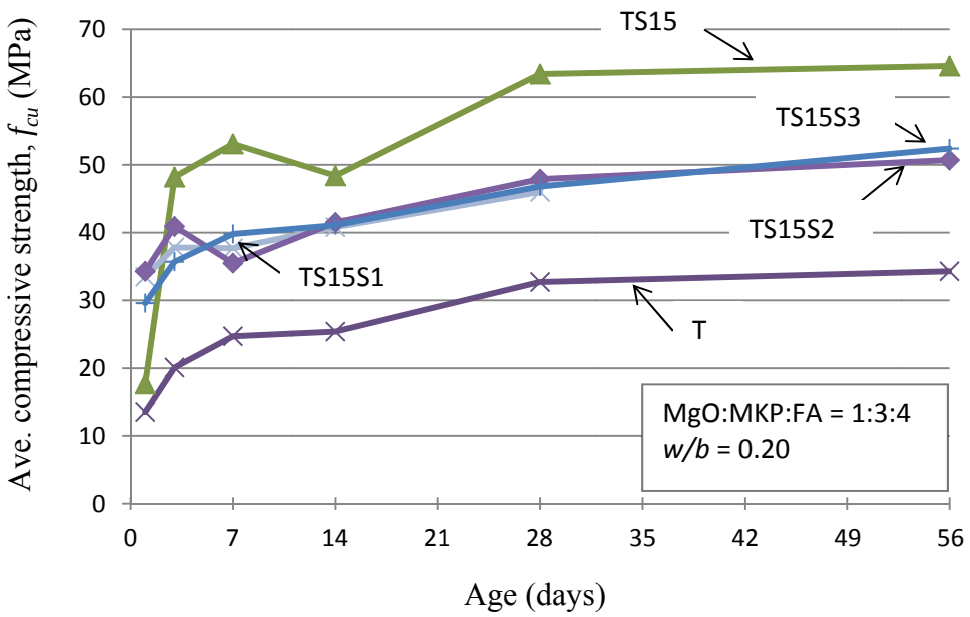

Figure 4-12: Compressive strength of sand mortars with 15% silica fume

The influence of different SF contents on the compressive strength of sand mortars using MPPC binders was plotted in Fig. 4-13 to Fig. 4-15. The figures show that the compressive strengths of the samples increased when SF content increased. The strength development trends of sand-3 mortars in Fig. 4-15 have less fluctuation than sand-1 and sand-2 mortars in Fig. 4-13 and Fig. 4-14, respectively. This is explained by the different particle size grading curves for the three sands (see Fig. 3-1, section 3.1.5) which affect the uniformity of the samples in the same batch and so affect the strengths of the samples.

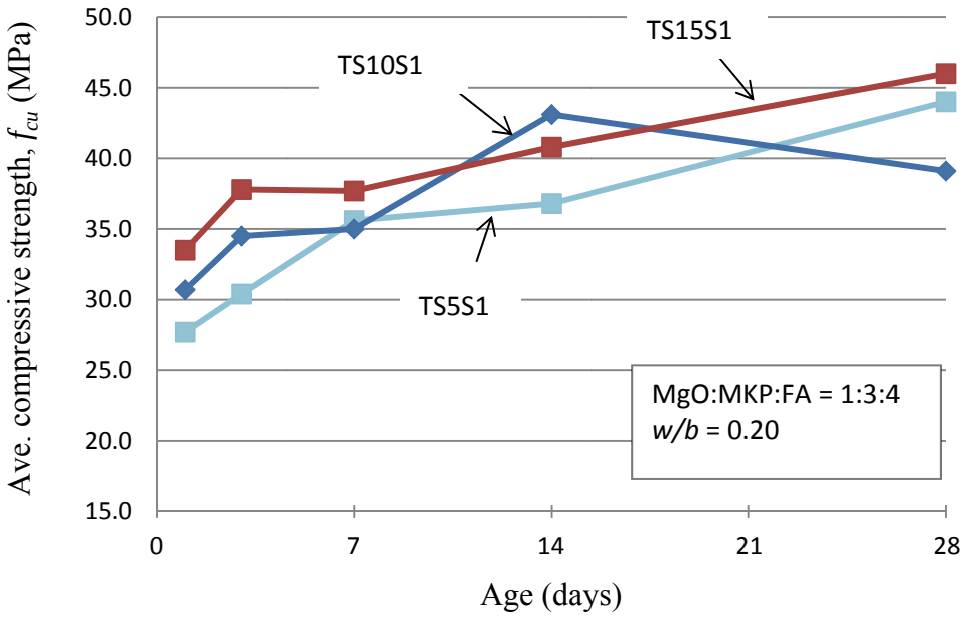

Figure 4-13: Effect of SF content on sand-1 mortars

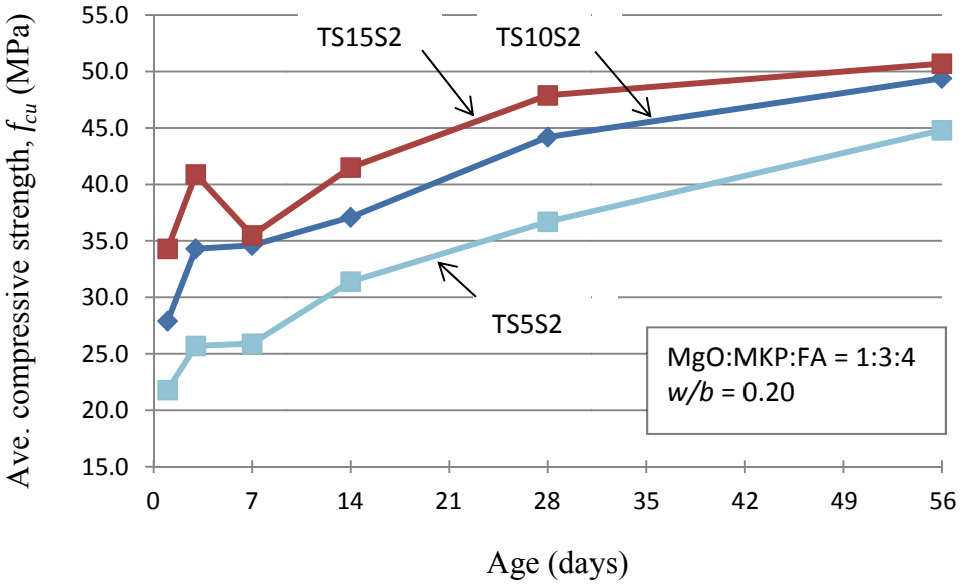

Figure 4-14: Effect of SF content on sand-2 mortars

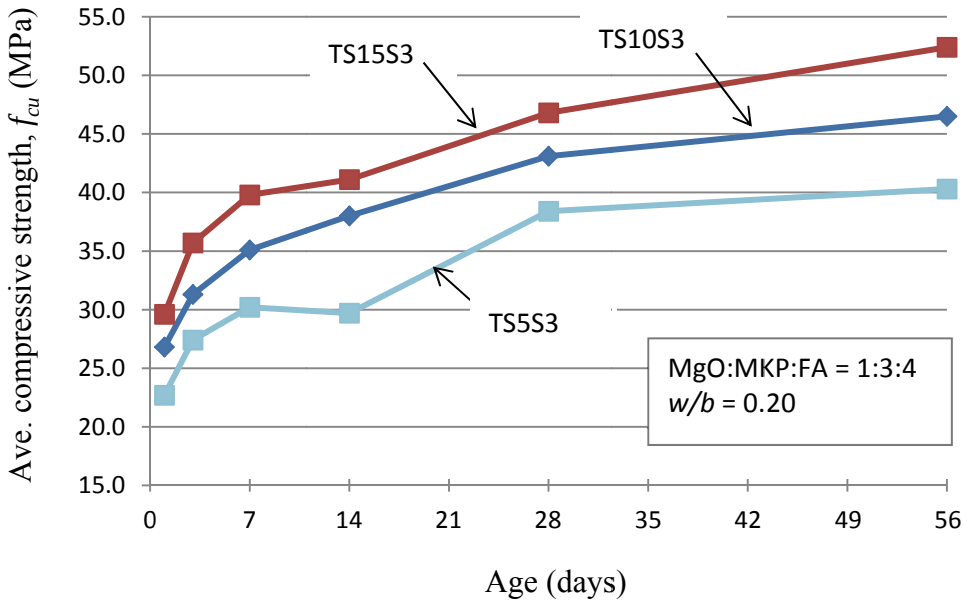

Figure 4-15: Effect of SF content on sand-3 mortars

In terms of workability, the addition of SF visibly increased the viscosity and decreased the setting time of the fresh mixtures. For sand mortars using 15% SF, for example, the fresh mixtures started to set right after the mixing finished and so there was only about 5 minutes to complete the casting before the pastes hardened.

Since Section 4.2.1.3 showed that different SF contents had little influence on the density of MPPC binders containing SF, in this section the comparison was only made for densities of mixes using different sand types. Fig. 4-16 shows the average densities of mixes using sand 1, sand 2 or sand 3. Each value in Fig. 4-16 was obtained by averaging the densities of mixes containing 5, 10 and 15% SF for each sand type. It is observed that the densities reduced as the age increased for all sand types used. Fig. 4-16 also shows that mixes with sand 3 had higher density than mixes with sand 1 or sand 2. This can be explained by different sand size gradations for the three sand types (see Fig. 3-1, section 3.1.5). The densities at 56-day age for sand-2 and sand-3 mortars were 2067 and 2096 kg/m^3. For sand-1 mortars, the density was 2060 kg/m^{3}at 28-day age.

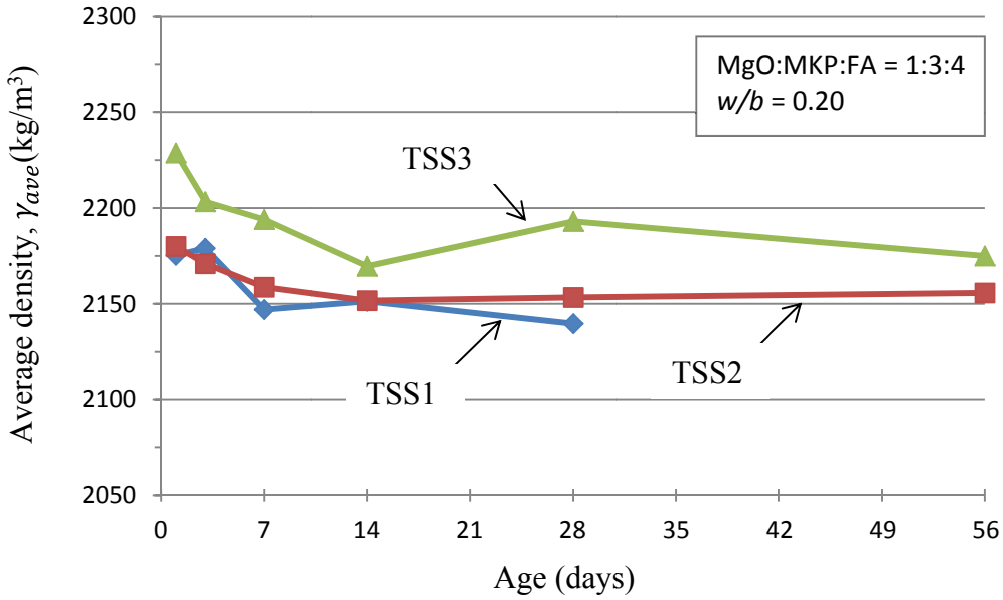

Figure 4-16: Average densities of sand mortars containing silica fume

4.2.1.5 Effect of baking soda on compressive strength of sand mortars

The influence on strength of sand mortars by the addition of baking soda was studied through trial mixes named TBaS. At first, these mixes used sand 4 with a binder-to-sand mass ratio (*b/s*) of 1:0.5. As shown in Fig. 4-17, the compressive strength of sand mortars reduced when more baking soda was added in the mix. When 2% baking soda by the total mass of dry ingredients was added, the samples had the lowest compressive strength (19.1 MPa) which was only 55% of the corresponding strength at 1% baking soda (34.3 MPa). This is explained by the increase in the amount of small voids in the samples when baking soda was added due to off-gassing in the reaction between the baking soda and the other binder components. Table 4-9 shows that adding more baking soda resulted in a decrease in the density from these voids.

Table 4-9: Average compressive strength and density of sand mortars containing baking soda from cube tests at 3 days (w/b = 0.20, b/s = 1:0.5)

Mix ID	Baking soda (%)	Average compressive strength, f_{cu} (MPa)	COV	Average density, (kg/m^3)	COV
TBa01S45(3)(0.20)	0.1	38.8	0.062	2146	0.012
TBa03S45(3)(0.20)	0.3	38.5	0.050	2142	0.010
TBa05S45(3)(0.20)	0.5	34.7	0.042	2073	0.013
TBa1S45(3)(0.20)	1.0	34.3	0.051	2107	0.008
TBa2S45(3)(0.20)	2.0	19.1	0.042	1934	0.024

Baking soda content is by mass percent of the dry mix

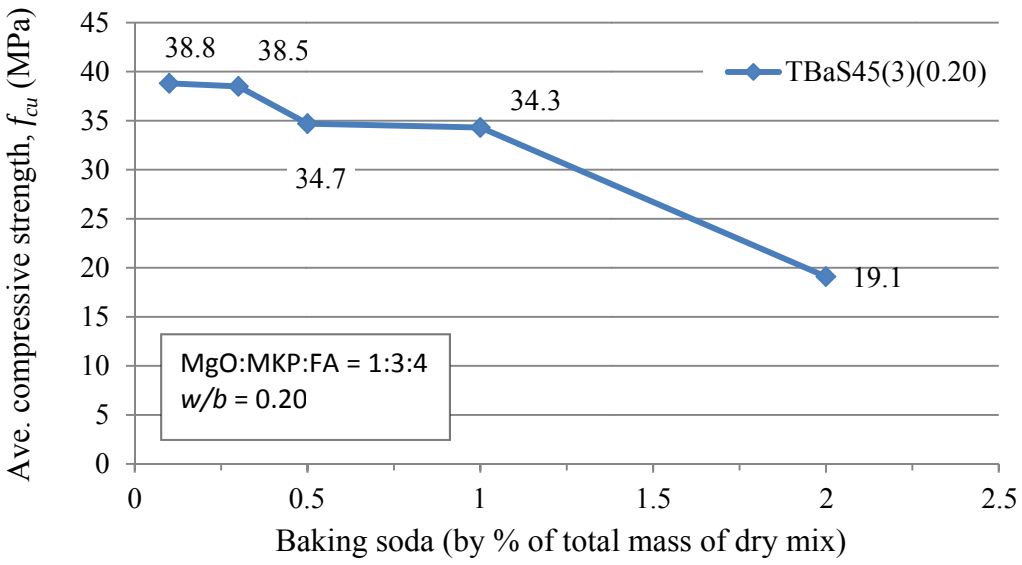

Figure 4-17: Compressive strength vs. baking soda content (at 3 days, sand 4)

Further trial mixes used a baking soda dosage at 1% of the total mass of dry mix. Test results are summarized in Table 4-10 and Table 4-11.

Table 4-10: Test results of sand-4 mortars at 3 days (w/b = 0.20)

Mix ID	*b/s* mass ratio	Average compressive strength, f_{cu} (MPa)	COV	Average density, γ (kg/m^3)	COV
TBa1S45(3)(0.20)	1:0.5	34.3	0.051	2107	0.008
TBa1S46(3)(0.20)	1:0.6	32.6	0.129	2062	0.039
TBa1S47(3)(0.20)	1:0.7	26.7	0.104	2042	0.012
TBa1S48(3)(0.20)	1:0.8	28.4	0.071	2125	0.022

Table 4-11: Test results of sand-3 mortars at 7 days (b/s = 1:1)

Mix ID	*w/b* mass ratio	Average compressive strength, f_{cu} (MPa)	COV	Average density, γ (kg/m^3)	COV
TBa1S31(7)(0.20)	0.20	29.8	0.083	2226	0.015
TBa1S31(7)(0.22)	0.22	28.0	0.037	2225	0.010
TBa1S31(7)(0.24)	0.24	26.9	0.094	2216	0.003
TBa1S31(7)(0.26)	0.26	27.6	0.078	2192	0.005

Fig. 4-18 compares the compressive strengths of cubes using different sand contents. In general, the cube compressive strength reduced slightly when more sand was added to the mix. When the *b/s* ratio changed from 1:0.5 to 1:0.6 (i.e. sand was increased by 10% of the total mass of binder), the compressive strength of the cubes decreased by 5%. There is an outlier point at *b/s* = 1:0.7. Between *b/s* = 1:0.6 and *b/s* = 1:0.8 (sand content increased by 20% of the total mass of binder), the strength of the cubes reduced by 13% (from 32.6 to 28.4 MPa). Ignoring the value at *b/s* = 1:0.7, the strength of sand mortars reduced by approximately 5 to 6.5% when 10% more sand was added to the mix.

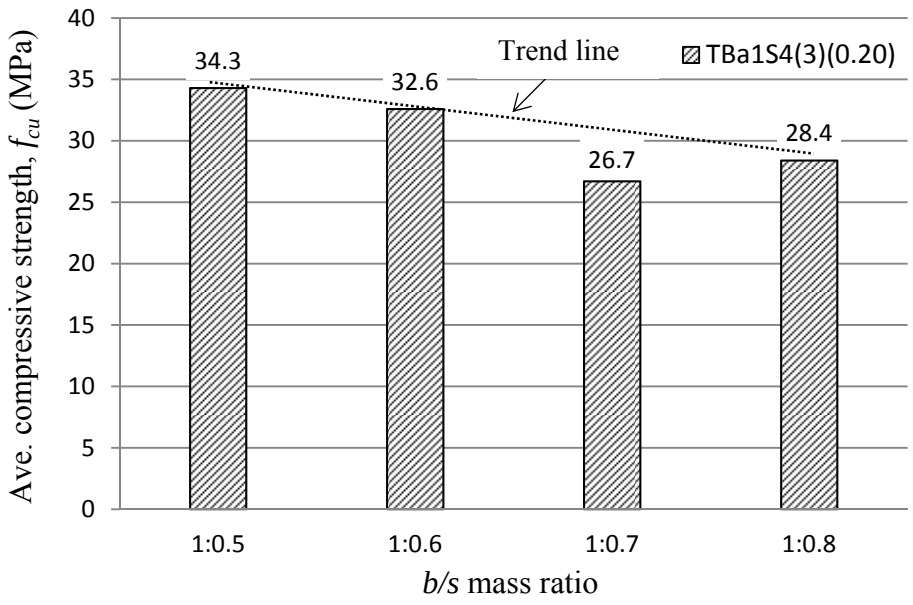

Figure 4-18: Compressive strength vs. b/s ratio

(at 3 days, sand 4, w/b = 0.2, 1% baking soda)

In addition to sand 4 used in the above mixes, mixes with sand 3 were also studied. In these mixes, sand 3 was included with the *b/s* ratio of 1:1 and the *w/b* ratio was varied. The results are summarized in Table 4-11 and plotted in Fig. 4-19. Figure 4-19 shows that the highest cube strength (29.8 MPa) was achieved when the *w/b* ratio was 0.20. Although there is a deviated point at *w/b* = 0.26, in general, adding more water to the mix resulted in a reduction in strength, as was also described in section 4.2.1.2.

During the specimen preparation, gas bubbles caused by the baking soda reacting with other components improved the flowability and so the workability of the fresh mixture. However, it was qualitatively observed that baking soda could make the fresh mixture swell after mixing and then shrink after setting. For example, for mixes containing 1% or 2% baking soda, the heights of the cubes measured at 3-day age were 2 mm to 5 mm shorter than the walls of the mold.

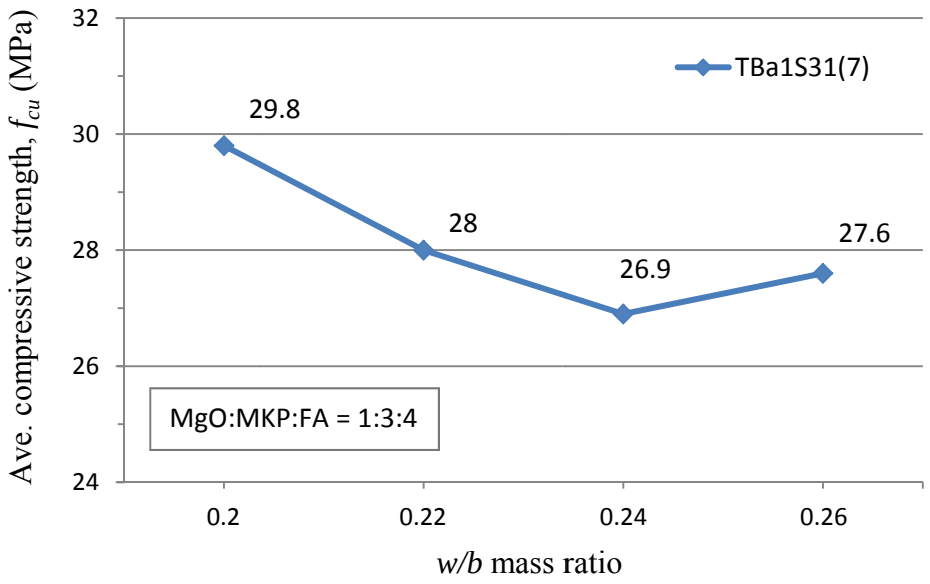

Figure 4-19: Effect of w/b ratio on compressive strength

(at 7 days, sand 3, 1% baking soda)

4.2.2 MPPC wood composites

4.2.2.1 Effect of w/b ratio on compressive strength of MPPC wood composites

The relationship between the *w/b* mass ratio and compressive strength of MPPC wood composites was examined in this study. Trial mixes named TSa were prepared with MgO:MKP:FA mass ratio of 1:3:4 and binder-to-sawdust mass ratio (*b/sdt*) of 1:0.2. Since the water absorption of sawdust is very high, *w/b* mass ratios from 0.32 to 0.50 were used for these mixes. These *w/b* mass ratios were much higher than the *w/b* mass ratios for the mixes without sawdust in Section 4.2.1 which were 0.16 to 0.28. Test results are summarized in Table 4-12.

Table 4-12: Test result of MPPC wood composites at 3-day age

Mix ID	*w/b* mass ratio	Average compressive strength, f_{cu} (MPa)	COV	Average density, γ (kg/m^3)	COV
TSa5(3)(0.32)	0.32	5.8	0.062	1431	0.004
TSa5(3)(0.36)	0.36	6.4	0.056	1468	0.015
TSa5(3)(0.40)	0.40	6.4	0.047	1481	0.012
TSa5(3)(0.46)	0.46	3.4	0.058	1393	0.020
TSa5(3)(0.50)	0.50	3.2	0.082	1504	0.008

Figure 4-20 shows the 3-day cube compressive strength of MPPC wood composites in which the highest strength (6.4 MPa) was achieved at *w/b* = 0.36. In general, the strength of the cubes reduced when the *w/b* ratio increased, as was described in sections 4.2.1.2 and 4.2.1.5. At *w/b* = 0.32, however, the compressive strength (5.8 MPa) was lower than that at *w/b* = 0.36 (6.4MPa). This can be explained by the reduction of water content in the mix which reduced the workability to a point where the uniformity of the fresh mixture was poor. When the *w/b* ratio was lower than 0.36, the fresh mixture was very dry and difficult to mix and cast. The *w/b* ratio of 0.36 was chosen for further mixes containing sawdust as it had reasonable workability and the highest strength among the trial mixes examined.

The densities of these mixes measured at 3-day age are shown in Table 4-12 in which the density of the mix using *w/b* = 0.36 was 1468 kg/m^3.

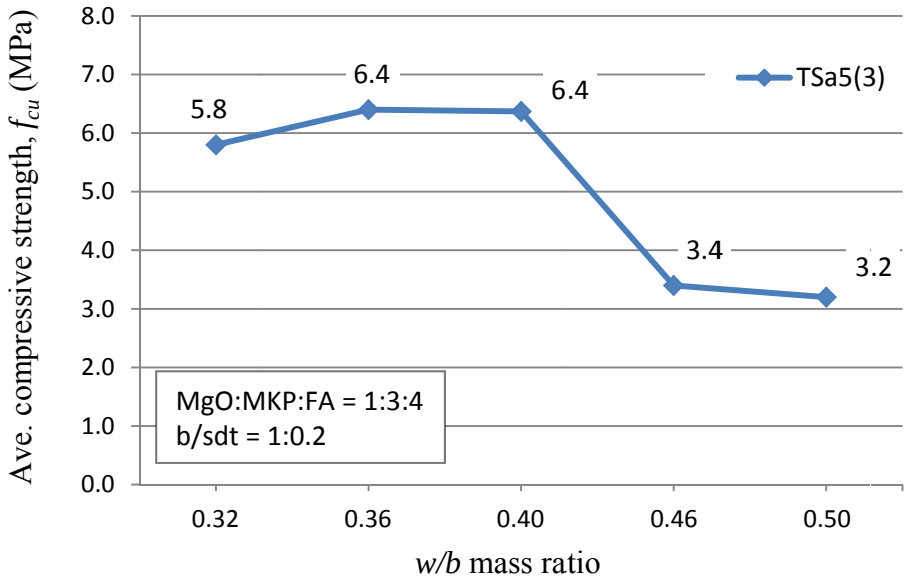

Figure 4-20: 3-day cube compressive strength of MPPC wood composites

4.2.2.2 Effect of fly ash on the compressive strength

Different FA contents affect the compressive strength of MPPC wood composites. This was examined through trial mixes named TSaS using *b/sdt* mass ratio of 1:0.20 and sand 4 with *b/s mass* ratio of 1:0.5. Among the FA dosages studied, Fig. 4-21 shows that the highest 7-day strength was obtained for mixes with the MgO:MKP:FA mass ratio of 1:3:1, where the FA dosage was 20% of the total mass of the binder including FA. The strength of the cubes reduced when more FA was included in the mix. With MgO:MKP:FA ratio = 1:3:2.67 (40% FA by weight of the binder), the lowest strength (11.7 MPa) was obtained. This contrasts with the strength of MPPC binders without sawdust which could reach the highest value at MgO:MKP:FA ratio of about 1:3:4 (50% FA) (see Section 3.3). The ratio of MgO:MKP:FA = 1:3:1 was selected for later mixes containing sawdust.

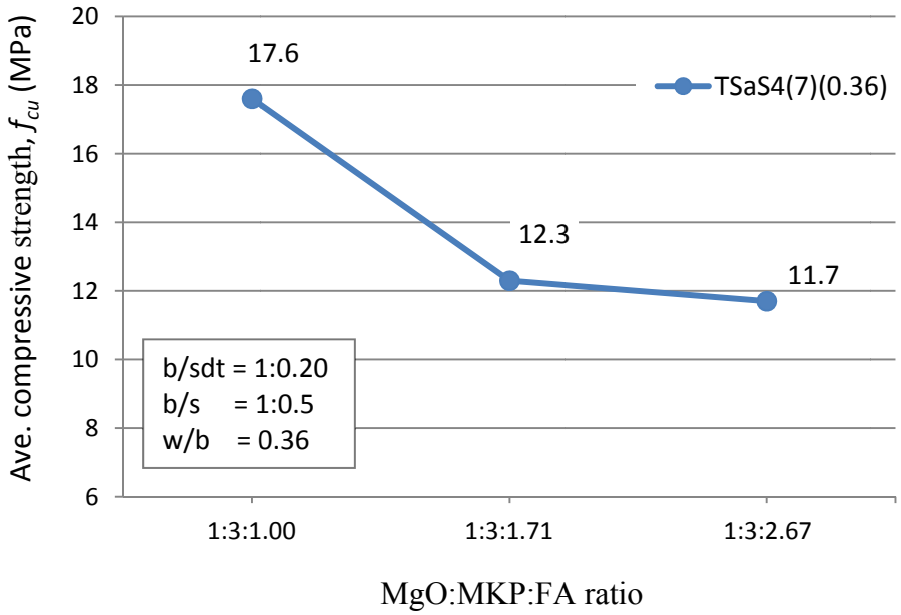

Figure 4-21: 7-day compressive strength of MPPC wood composites using sand 4

The measured densities for mixes in this series are shown in Table 4-13. It can be observed that the increase in the FA content decreased the compressive strength and the density of these mixes.

Table 4-13: Test results of MPPC wood composites (at 7 days, w/b = 0.36)

Mix ID	MgO:MKP:FA mass ratio	Average compressive strength, f_{cu} (MPa)	COV	Average density, (kg/m^3)	COV
TSa2S4(7)(0.36)	1:3:1.00	17.6	0.091	1691	0.015
TSa3S4(7)(0.36)	1:3:1.71	12.3	0.123	1624	0.004
TSa4S4(7)(0.36)	1:3:2.67	11.7	0.078	1586	0.021

4.2.2.3 Effect of baking soda on the compressive strength

In addition to sand 4, mixes in section 4.2.2.2 were also studied using sand 3 with *b/s* mass ratio of 1:0.5. In this study, different baking soda contents by total mass of the dry mix were examined. Figure 4-22 shows that, at 7 and 28 days

after casting, the cubes containing 3% baking soda achieved the highest strengths which were 7.1 MPa and 11.0 MPa, respectively.

For the period from 7 days to 28 days, however, the highest strength increase was achieved with mixes that used 2% baking soda (strength increased from 4.9 to 8.1 MPa, approximately 63%). For mixes with 3% and 1% baking soda, the strength increases were 54% (from 7.1 to 11.0 MPa) and 39% (from 4.7 to 6.5 MPa) for the same time period, respectively. In general, the compressive strength of MPPC wood composites increased when the baking soda content increased. This contrasts with the result obtained in Section 4.2.1.5 where the strength of mixes containing baking soda but without sawdust reduced when more baking soda was added.

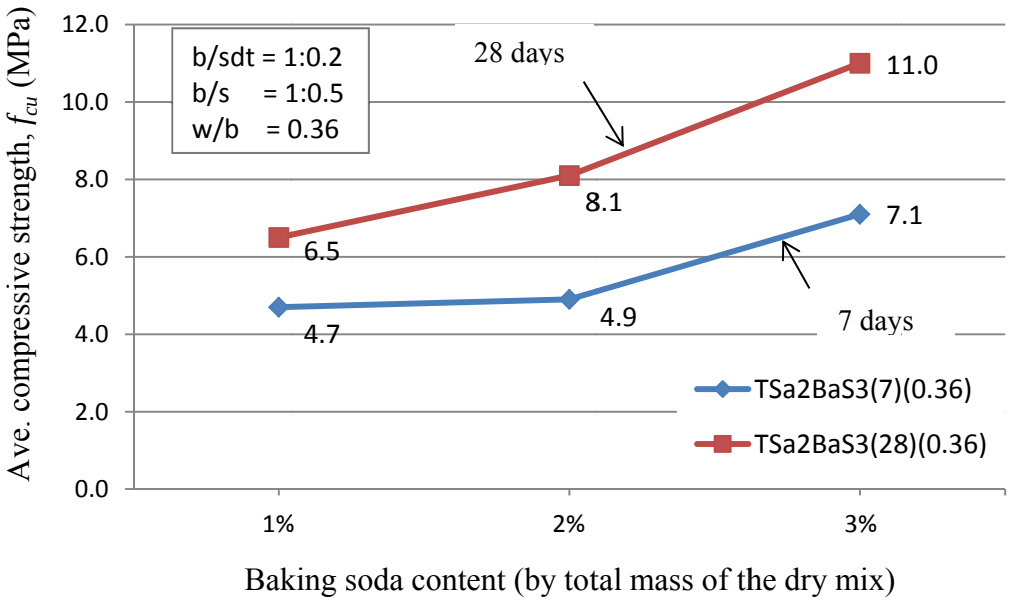

Figure 4-22: Effect of baking soda content on compressive strength

In terms of workability, the fresh mixtures could not flow but they were still workable and could be consolidated in the molds by tamping. In contrast with mixes containing baking soda but without sawdust described in section 4.2.1.5, no gas bubbles were readily observed during the mixing and the fresh mixture did not swell after casting for these mixes. After setting, the specimens with 3% baking soda exhibited some shrinkage (measured at 1-2 mm for 50x50x50 mm

cubes). For cubes made with mixes containing 1% or 2% baking soda, there was no visible shrinkage.

The measured densities for mixes in this series are shown in Table 4-14. It can be observed that the increase in baking soda content increased the compressive strength and the density for these mixes.

Table 4-14: Test results of MPPC wood composites using baking soda

Mix ID	Baking soda (%)	Age (days)	Average compressive strength, f_{cu} (MPa)	COV	Average density, γ (kg/m^3)	COV
TSa2Ba1S3(7)(0.36)	1	7	4.7	0.015	1494	0.014
TSa2Ba2S3(7)(0.36)	2	7	4.9	0.035	1543	0.011
TSa2Ba3S3(7)(0.36)	3	7	7.1	0.037	1662	0.020
TSa2Ba1S3(28)(0.36)	1	28	6.5	0.102	1479	0.026
TSa2Ba2S3(28)(0.36)	2	28	8.1	0.021	1540	0.012
TSa2Ba3S3(28)(0.36)	3	28	11.0	0.129	1621	0.022

4.3 Potential mixtures for further research

Trial mixes were developed for MPPC concretes/wood composites in this chapter. Evaluation of the trial mixes mainly focused on the cube compressive strengths and qualitative workability. Based on the results obtained from these trial mixes, six mixtures were selected to conduct further studies on the hardened and fresh properties. Selected mixes exhibited good characteristics in terms of compressive strength and workability for targeted construction applications. The mixes are summarized in Table 4-15 and briefly described as follows:

- Mixtures S5 and S10: MPPC binders with MgO:MKP:FA mass ratio of 1:3:4; *w/b* mass ratio of 0.20; and SF was used at 5% for mixture S5 or 10% for mixture S10 by mass of the binder. These mixes exhibited high compressive strengths and Sections 4.2.1.3 showed that the strength increase appeared to be negligible if more than 10% SF is added to the mix.

- Mixtures SS5 and SS10: sand mortars produced by adding sand 3 with *b/s* mass ratio of 1:1 to mixtures S5 and S10. The addition of sand can help reduce the cost of the product and could allow direct comparison of influence of sand on MPPC binders containing SF.

- Mixture Sa: MPPC wood composites with MgO:MKP:FA mass ratio of 1:3:1; *w/b* mass ratio of 0.36; and sawdust was used with the binder-to-sawdust ratio (*b/sdt*) of 1:0.2. This mixture exhibited high compressive strength and suitable workability.

- Mixture SaB: mixture Sa was used again with an inclusion of 2% baking soda by total mass of the mix. This mixture could allow direct study of influence of baking soda on MPPC wood composites. It exhibited high strength but no significant shrinkage.

Table 4-15: Mix compositions of MPPC concretes/wood composites for further studies

Mix ID	**MgO:MKP:FA ratio**	**Sand type**	***b/s* ratio**	***b/sdt* ratio**	**SF (%)**	**Baking soda (%)**	***w/b* ratio**
S5	1:3:4	-	-	-	5	-	0.20
S10	1:3:4	-	-	-	10	-	0.20
SS5	1:3:4	3	1:1.0	-	5	-	0.20
SS10	1:3:4	3	1:1.0	-	10	-	0.20
Sa	1:3:1	3	1:0.5	1:0.2	-	-	0.36
SaB	1:3:1	3	1:0.5	1:0.2	-	2	0.36

Chapter 5 MAGNESIUM POTASSIUM PHOSPHATE CERAMIC CONCRETES AND WOOD COMPOSITES

5.1 Introduction

This chapter reports the results of an expanded laboratory program for the six MPPC concretes/wood composite mixes indicated in Section 4.3. The mix compositions are shown in Table 5-1. Flow and setting time properties as well as compression and flexural properties of these mixes were evaluated. A summary of the analyzed data for each characteristic is reported in this chapter and detailed test results are reported in Appendix B.

Table 5-1: Mix compositions of MPPC concretes/wood composites

Mix ID	MgO:MKP:FA ratio	Sand type	*b/s* ratio	*b/sdt* ratio	SF (%)	Baking soda (%)	*w/b* ratio
S5	1:3:4	-	-	-	5	-	0.20
S10	1:3:4	-	-	-	10	-	0.20
SS5	1:3:4	3	1:1.0	-	5	-	0.20
SS10	1:3:4	3	1:1.0	-	10	-	0.20
Sa	1:3:1	3	1:0.5	1:0.2	-	-	0.36
SaB	1:3:1	3	1:0.5	1:0.2	-	2	0.36

5.2 Fresh properties of MPPC concretes/wood composites

5.2.1 Flow property

Experimental results of the flow test are shown in Fig. 5-1 for MPPC concretes. It is observed that mixture S5, which used only 5% SF, exhibited the highest flow (135%). Meanwhile, the flow of mixture S10, which used 10% SF, decreased significantly to 73%. This result indicates that the addition of a higher SF mass ratio in the mix increased the viscosity and reduced the flow.

For sand mortars, mixture SS5 exhibited lower flow (128%) when compared with mixture S5 which had the same SF content but did not contain sand. When the SF content increased to 10%, mixture SS10 showed a decrease in flow (97%) as was described above for mixes without sand. However, comparing mixes S10 and SS10, it is observed that the inclusion of sand increased the flow of mixes with 10% SF from 73% (S10) to 97% (SS10).

In summary, the flow as well as the workability of MPPC binders containing SF decreased when the SF content increased. This trend was also observed with sand mortars containing SF. In addition, the inclusion of sand increased the flow of mixes with 10% SF but decreased the flow of mixes with 5% SF.

Since the fresh mixtures of MPPC wood composites do not flow, flow-table tests could not be applied for mixes Sa and SaB.

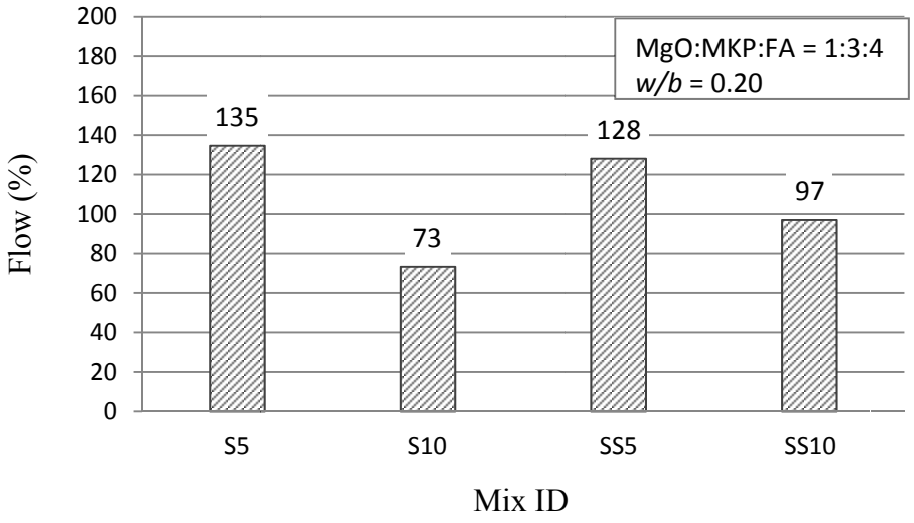

Figure 5-1: Flow test result of MPPC concretes

5.2.2 Setting time property

Tests were completed to determine the setting times of MPPC concretes/wood composites. Six mixtures in Table 5-1 were prepared with Delvo Stabilizer admixture at a dosage of 2% by mass of the binder. Figure 5-2

compares the initial and final setting time of these mixes. It is observed that SF reduced the initial setting time for MPPC binders containing SF. When the SF content increased from 5% to 10% by mass of the binder, the initial setting time reduced from 105 minutes (S5) to 85 minutes (S10). For sand mortars containing SF, however, an increase in SF content from 5% to 10% by mass of the binder resulted in an increase in the initial setting time from 65 to 80 minutes as can be observed for mixes SS5 and SS10.

For MPPC wood composites, the initial setting times were 90 minutes and 45 minutes for mixes Sa and SaB, respectively. This indicates that the addition of 2% baking soda by total mass of the mix significantly reduced the initial setting time for MPPC wood composites.

The differences between the initial and final setting times were 60 minutes for mix Sa and 20-30 minutes for the other mixes. The initial and final setting times for all mixes can be found in Table 5-2.

In a prior study, Tassew and Lubell (2013) indicated that the difference between the initial and final setting times of MPPCs was very short if Borax or Lignosulphonate was used as a retarder. It appears that Delvo Stabilizer may be a better retarder for MPPC concretes/wood composites if the application requires an extended finishing time.

Table 5-2: Setting time of MPPC concretes/wood composites

Mix	**Setting time (minutes)**	
	Initial	Final
S5	105	135
S10	85	105
SS5	65	85
SS10	80	100
Sa	90	150
SaB	45	75

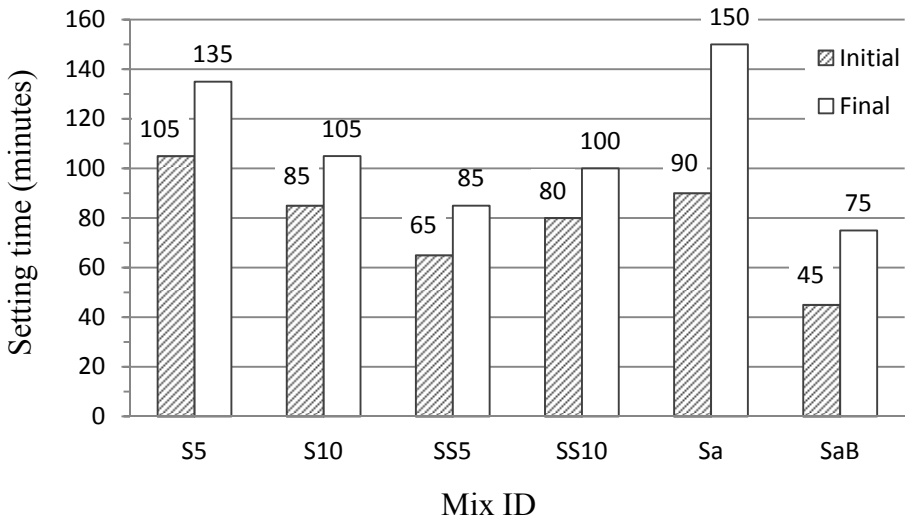

Figure 5-2: Setting time of MPPC concretes/wood composites

(w/b = 0.20 for S5, S10, SS5 and SS10; w/b = 0.36 for Sa and SaB)

5.3 Hardened properties of MPPC concretes/wood composites

This section describes the measured and analyzed test data to determine the properties of hardened MPPC concretes/wood composites. Density, compression properties and flexure properties were evaluated. Because of the limited availability of the laboratory test equipment, all specimens were tested at the age of 90 days after casting. At this age, the properties of MPPC concretes should have stabilized since Section 4.2.1.1 showed that continued strength development of MPPC concretes was insignificant at the age of 56 days. A summary of the test result of each characteristic is reported in this chapter.

5.3.1 Density

The densities of hardened MPPC concretes/wood composites were determined by testing cubes at 90 days after casting. These specimens were demolded at one day after casting and then cured at the ambient lab temperature (23±2^{o}C) and relative humidity (50±5%) until testing. Figure 5-3 compares the densities of the six mixtures considered. The coefficient of variation for the densities of these mixes can be found in Table 5-3. It can be observed that sand mortars containing SF (mixes SS5 and SS10) had the highest densities, at 2150 and 2173 kg/m^3, respectively. Mixes S5 and S10, containing only MPPC binder

and SF, had relatively lower densities (1751 and 1763 kg/m^3, respectively) when compared with the sand mortars. This occurred because the sand density was higher than the binder density.

Among the six mixtures, the MPPC wood composites (Sa and SaB) exhibited the lowest densities at 1315 and 1438 kg/m^3, respectively. This can be explained by the presence of sawdust which was low density material when compared with sand and MPPC binders. Another reason is that the MPPC wood composites had *w/b* ratios of 0.36 which were higher than that of the other four mixtures (*w/b* = 0.20). Tassew and Lubell (2012) also reported that the density of MPPC decreased when the *w/b* ratio increased.

Figure 5-3 also indicates that the weight percent of SF had negligible influence on the densities of MPPC binders containing SF (S5 and S10) and sand mortars containing SF (SS5 and SS10). Meanwhile, 2% baking soda by total mass of the mix slightly increased the density for MPPC wood composites from 1315 kg/m^3 (Sa) to 1438 kg/m^3 (SaB). This was unexpected because the baking soda was assumed to increase the voids in the structure which could result in a lighter material. However, improved mixing due to lubricating effect may have resulted in an improved mix consolidation.

Table 5-3: Coefficient of variation for densities of MPPC concretes/wood composites

Mix	Coefficient of variation
S5	0.001
S10	0.001
SS5	0.006
SS10	0.008
Sa	0.029
SaB	0.006

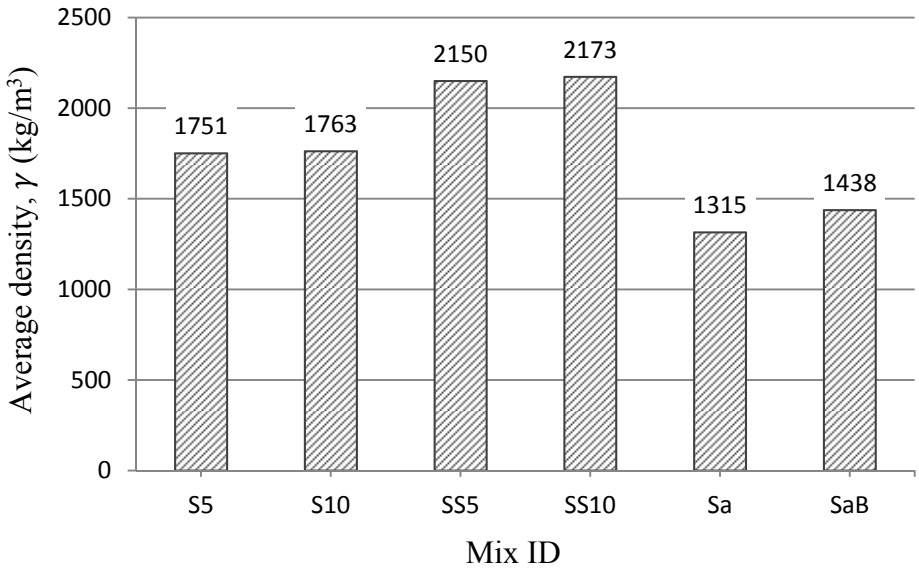

Figure 5-3: Density of MPPC concretes/wood composites at 90-day age

(w/b = 0.20 for S5, S10, SS5 and SS10; w/b = 0.36 for Sa and SaB)

5.3.2 Compression properties

The properties including compressive strength, modulus of elasticity and stress-strain relationship were determined in this section.

5.3.2.1 Compressive strength of cube and cylindrical specimens

Tests were conducted with 50x50x50 mm cube specimens. The cube compressive strength (f_{cu}) was determined from the maximum load indicated by the testing machine as was described in section 4.2, chapter 4. The description for the permissible range of variation between the specimens was also described in section 4.2. In this section, the cube compressive strengths for all mixes were within the permissible range of variation for three specimens which is 8.7%.

Detailed values of f_{cu} for each individual specimen, the average and the coefficient of variation for each mix series are shown in Appendix B.

Table 5-4 shows the average cube compressive strength and the coefficient of variation for each mixture. It can be observed that the coefficient of variation for mixes SS5, SS10 and Sa are higher than other mixes.

Table 5-4: Average cube and cylinder compressive strengths of MPPC concretes/wood composites at 90-day age

Mix	f_{cu} (MPa)	COV	f'_c(MPa)	COV	f'_c/f_{cu}	f'_c/f_{cu}*
S5	34.0	0.048	31.4	0.039	0.92	1.06
S10	33.9	0.006	32.6	0.049	0.96	1.10
SS5	41.1	0.089	31.5	0.038	0.76	0.88
SS10	46.8	0.095	33.2	0.051	0.71	0.82
Sa	7.0	0.089	13.3	0.083	1.90	2.18
SaB	14.5	0.043	12.7	0.047	0.88	1.01

**cube compressive strengths f_{cu} multiplied by the factor of 0.87*

Figure 5-4 shows the average cube compressive strengths for the six mixtures considered. It is observed that mixes SS5 and SS10 had the highest strengths at 41.1 and 46.8 MPa, respectively. The increase in SF content from 5% to 10% by mass increased the strength of sand mortars containing SF but it had negligible influence on the strength of MPPC binders containing SF.

For MPPC wood composites, the strengths of mixes Sa and SaB were low compared with the other four mixes. The addition of 2% baking soda by mass of the total mix significantly increased the strength of these mixes from 7.0 MPa (Sa) to 14.5 MPa (SaB).

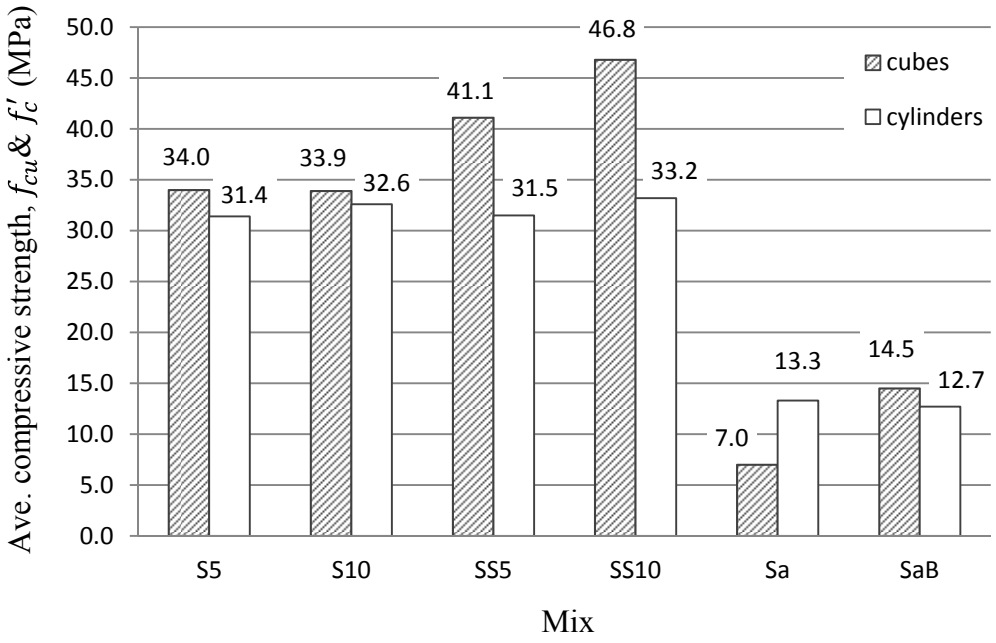

Figure 5-4: Cube and cylinder compressive strength of MPPC concretes/wood composites at 90-day age

(w/b = 0.20 for S5, S10, SS5 and SS10; w/b = 0.36 for Sa and SaB)

Cylinders with the dimension of 100 x 200 mm (diameter x height) were also examined to determine the compressive strengths for the six mixtures considered. The maximum compressive strength f_c' for each cylinder was found by:

$$f_c' = \frac{P}{A_{cyl}} \qquad (5\text{-}1)$$

where f_c' : maximum compressive strength (MPa)

P : maximum load (N)

A_{cyl} : cross-sectional area of cylinder; calculated based on averaging two measurements of diameter taken at right angles to each other at mid-height of the cylinder (mm^2)

Detailed values of f_c' for each individual specimen as well as the coefficient of variation for each series can be found in Appendix B.

According to ASTM C39/C39M-12, the variation between specimens of the same batch produced under laboratory conditions should not exceed 10.67% of the average when three cylinders were tested at the same age and 9.0% when two cylinders were tested at the same age. Only the cylinder compressive strengths for mixes S5, Sa and SaB were within the permissible range of variation for three specimens. Thus, the cylinder compressive strengths for these mixes are the average strengths of three specimens in the same mix. Meanwhile, the cylinder compressive strengths for mixes S10, SS5 and SS10 are the average strengths of two specimens in the same mix.

The average cylinder compressive strengths for the six mixtures are plotted in Fig. 5-4. There was a negligible difference between the compressive strengths of sand mortars containing SF and MPPC binders containing SF. This contrasts with the cube compressive strengths where sand mortars containing SF had significantly lower strength than MPPC binders containing SF (see Fig. 5-4).

Figure 5-4 also shows that, for MPPC binders containing SF, an increase of SF by mass of the binder from 5% to 10% slightly increased the strength from 31.4 MPa (S5) to 32.6 MPa (S10). This trend was similar for sand mortar containing SF where the strength increased from 31.5 (SS5) to 33.2 MPa (SS10).

Mixes Sa and SaB, which contained sawdust, showed significantly lower cylinder compressive strengths than the other four mixes without sawdust. The addition of baking soda slightly decreased the strength from 13.3 (Sa) to 12.7 MPa (SaB). This is also in contrast with the cube compressive strengths for these mixes which increased significantly when baking soda was added as shown in Fig. 5-4.

Typical failures of cylinder specimens at the age of 90 days after casting are shown in Fig. 5-5 to Fig. 5-7 for the six mixtures considered. Figure 5-5 and 5-6 indicate that the failures were due to shear fracture with the failure plane starting from one end and almost intersecting the other end of the specimen. Figure 5-7 shows another type of shear fracture where the crack developed from

one side to the other side at approximately mid-height of the specimen. These broken cylinders using MPPC concretes/wood composites did not exhibit the typical conical fracture type of cylinders using conventional concrete made with Portland cement and rock aggregates (ASTM International, 2003). According to Neville (2012), the typical cone fracture occurs due to the friction between the platens of the testing machine and the cylinder ends which restrains the lateral expansion of the cylinder when it is loaded vertically. Thus, the concrete near the platens is confined and this results in two cone-shape zones (Neville, 2012). These cone-shape zones are relatively undamaged when the cyliner is tested to fracture (Neville, 2012).

Poor testing could be a possibility for the type of fracture shown in Fig. 5-5 and 5-6. According to Kosmatka et al. (2002), when the test does not meet the requirements for perpendicularity of the cylinder ends or vertical alignment during, load applied to the cylinder may be concentrated on one side of the specimen. This can cause a short shear fracture in which the failure plane intersects the end of the cylinder as shown in Fig. 5-5 for cylinder of MPPC binders containing SF and Fig. 5-6 for cylinder of sand mortars containing SF. This type of failure usually indicates the cylinder failed prematurely, yielding results lower than the actual strength of the concrete. However, the coefficients of variation for the cylinder strengths of these mixes shown in Table 5-4 demonstrate that insignificant differences occurred between the strengths of each specimen. This indicates that poor testing may not be the main reason for the type of fracture of these specimens.

The difference in type of shear fracture of MPPC wood composites compared to MPPC concretes was believed to be caused by the different mix compositions and different types of compaction during the mixing procedure. Vibration was used for consolidating fresh MPPC concretes. Meanwhile, fresh MPPC wood composites needed to be compacted by tamping. Thus, it was difficult to achieve good consolidation for fresh MPPC wood composites.

The fracture type of MPPC wood composites shows that the failure occurred at approximately mid-height of the specimen where the material is subjected to almost-pure uniaxial vertical compression (i.e. outside the conical zones where the material is under multiaxial stresses) and the cylinder ends were not damaged. This is quite similar to typical cone failure mode of conventional concrete where the cones are not damaged. Thus, the fracture mode of MPPC wood composties can be considered as a good failure mode.

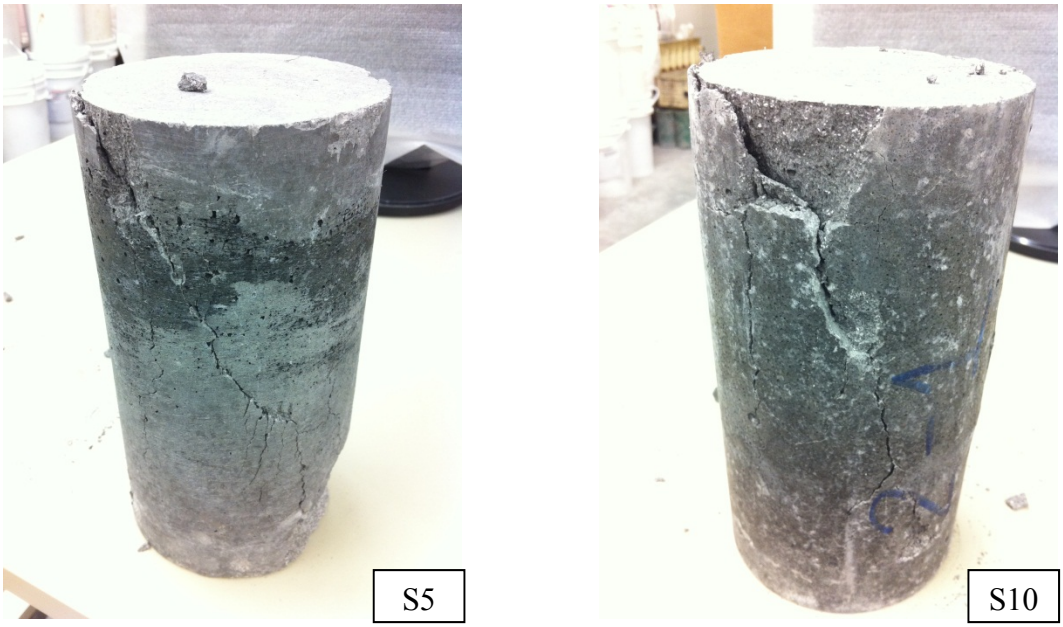

Figure 5-5: Typical failure of cylinder specimens of mixes S5 and S10

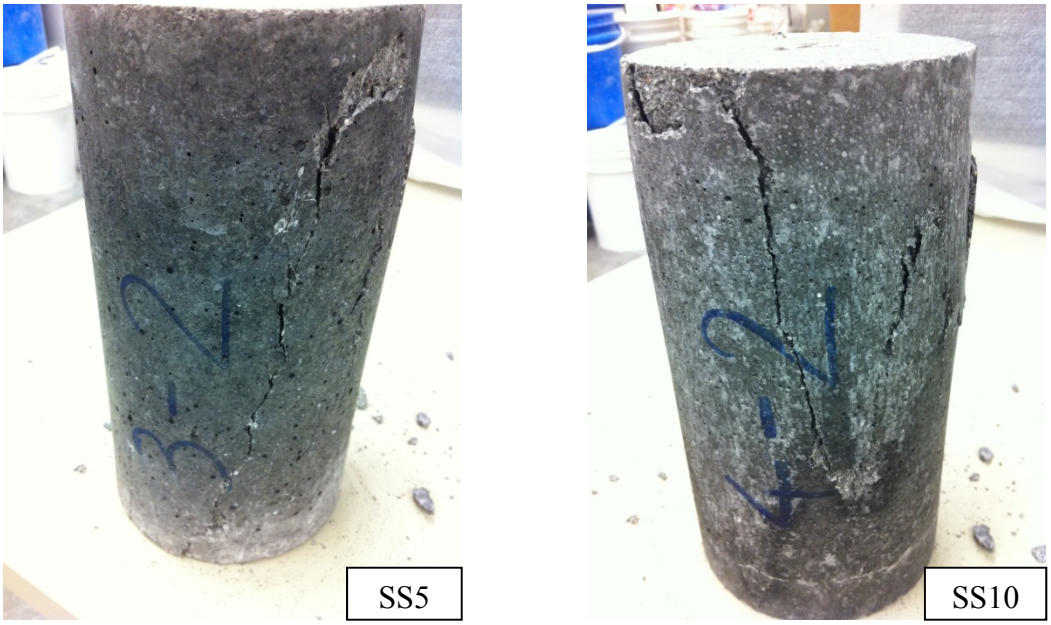

Figure 5-6: Typical failure of cylinder specimens of mixes SS5 and SS10

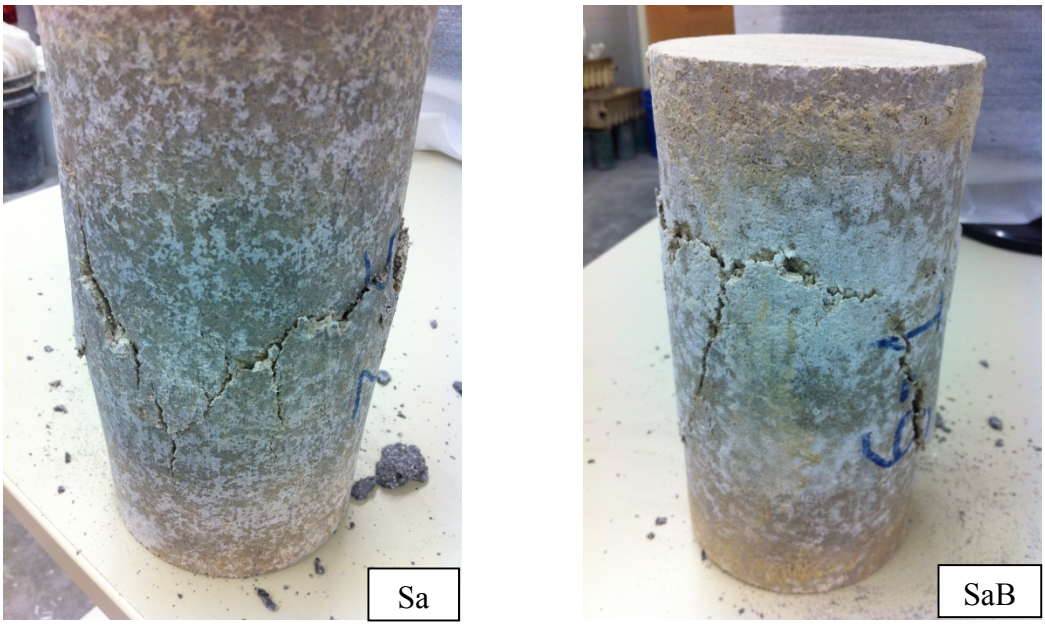

Figure 5-7: Typical failure of cylinder specimens of mixes Sa and SaB

For the same mixture, the compressive strength values varied depending on the types of specimen tested as shown in Fig. 5-4. The cylinder/cube compressive strength ratios can be found in Table 5-4. According to BS

1881:1986, the cylinder compressive strength is typically about 80% of the cube compressive strength but the relation of strengths obtained from the two specimen types can not be expressed by a simple function. The difference between the compressive strengths of cube and cylinder specimens depends on many factors such as: shape of specimen, level of strength of concrete, direction of loading and aggregate grading (Neville, 2012). The cubes and cylinders used in this study had the height-to-maximum-lateral-dimension (*h/d*) ratios of 1.0 and 2.0, respectively. ASTM C39/C39M-12 suggests that the ratio of the cylinder to cube compressive strength should be approximately 0.87 to account for the difference between the *h/d* ratios of the cubes and cylinders.

Table 5-4 shows the cylinder/cube compressive strength ratios where the cube compressive strengths were corrected by the factor of 0.87. It is observed that the cylinder/cube compressive strength ratios of mixes S5 and SaB were closer to unity than other mixes.

In addition to *h/d* ratio, the uniformity of the mixes can also influence the cylinder/cube strength ratios. According to Sigvaldason (1966), smaller cylinder/cube strength ratios could be found for segregating concretes than for more uniform concrete. He reported that the cylinder/cube strength ratios for segregating concretes were about 0.71 to 0.77 while they were about 0.76 to 0.84 for more uniform concretes (Sigvaldason, 1966). The addition of sand in mixes SS5 and SS10 could increase the segregation of the fresh mixtures under the vibration used for consolidation and thereby decrease the uniformity of the fresh mixtures. Thus, it was believed that the addition of sand decreased the cylinder/cube strength ratios for mixes SS5 and SS10 and made them lower when compared with mixes S5 and S10 (without sand).

The addition of baking soda was believed to increase the uniformity of mix SaB through a lubrication effect during mixing compared to mix Sa which did not contain baking soda. As shown in Table 5-4, the cylinder/cube strength ratio for mix SaB was closer to unity than for mix Sa.

5.3.2.2 Stress-strain relationship

The compression stress-strain relationships obtained from cylinder tests of MPPC concretes/wood composites were determined based on the displacement (d_i) measured by three LVDTs and the corresponding load (P_i) indicated by the machine. The stress and strain values were calculated as following:

$$f_c = \frac{P_i}{A_{cyl}} \quad (5\text{-}2)$$

$$\varepsilon_c = \frac{d_i}{L_g} \quad (5\text{-}3)$$

where f_c = compressive stress (MPa)

P_i = corresponding load (N)

A_{cyl} = cross-sectional area of cylinder; calculated based on averaging two measurements of diameter taken at right angles to each other at mid-height of the cylinder (mm^2)

ε_c = strain corresponding to f_c (mm/mm)

d_i = average value of three vertical displacements recorded by LVDTs

L_g = gauge length between the top and bottom collar which is 100mm in this case.

The 90-day stress-strain response curves for the six mixtures considered are plotted in Fig. 5-8 to Fig. 5-13. The tests were stopped at failure when the load-deflection curve exhibited a sudden drop and the specimen showed significant cracks.

From Fig. 5-8 and 5-9, it can be observed that the stress-strain responses of mixes S5 and S10 were almost linear up to the peak stress. Meanwhile, mixes SS5, SS10, Sa and SaB only exhibited the linearity up to approximately 40% of

the peak stress as shown in Fig. 5-10 to Fig. 5-13. After 40% of the peak stress, the stress-strain responses of these mixes became non-linear with a parabolic shape. According to Collins and Mitchell (1997), the interaction between the paste and the aggregate causes the nonlinearity for the stress-strain response curve of concrete. This explains why the stress-strain response curves of MPPC binders containing SF were more linear than those of sand mortars containing SF. Collins and Mitchell (1997) also stated that when the strength of concrete increases, the stress-strain response curve exhibits more linearity, less ductility and increase in initial stiffness. MPPC wood composites had lower compressive strengths than other mixes. The stress-strain curves of mixes Sa and SaB exhibited less linearity and more ductility.

The average peak stress (f_c') and strain at peak stress values (ε_c') for these mixes are shown in Table 5-5. MPPC concretes (S5, S10, SS5 and SS10) had strain at peak stress magnitudes from $3.24\text{x}10^{-3}$ to $3.72\text{x}10^{-3}$ (mm/mm). Sand mortars containing SF (SS5 and SS10) exhibited lower strains at peak stress than MPPC binders contaning SF. The increase in SF from 5% to 10% slightly decreased the strain at peak stress of MPPC binders containing SF from $3.72\text{x}10^{-3}$ mm/mm (S5) to $3.47\text{x}10^{-3}$ mm/mm (S10). However, the same increase in SF content had negligible influence on strains at peak stress of sand mortars containing SF.

With the addition of 2% baking soda by total mass of the dry ingredients, the strains at peak stress of MPPC wood composites increased from $\varepsilon_c' = 9.72\text{x}10^{-3}$ mm/mm (Sa) to $\varepsilon_c' = 10\text{x}10^{-3}$ mm/mm (SaB).

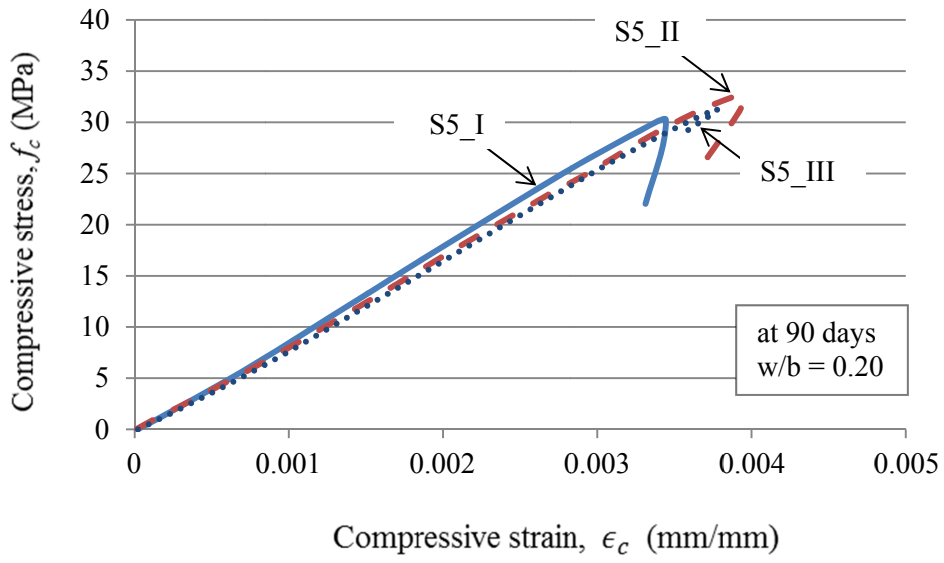

Figure 5-8: Compressive stress-strain response for mix S5

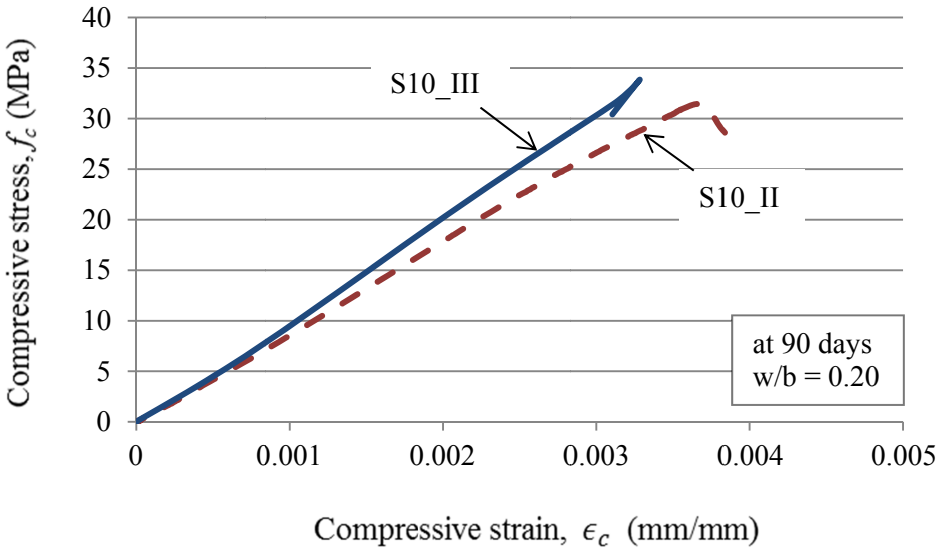

Figure 5-9: Compressive stress-strain response for mix S10

(S10_I is omitted for high deviation from the average strength)

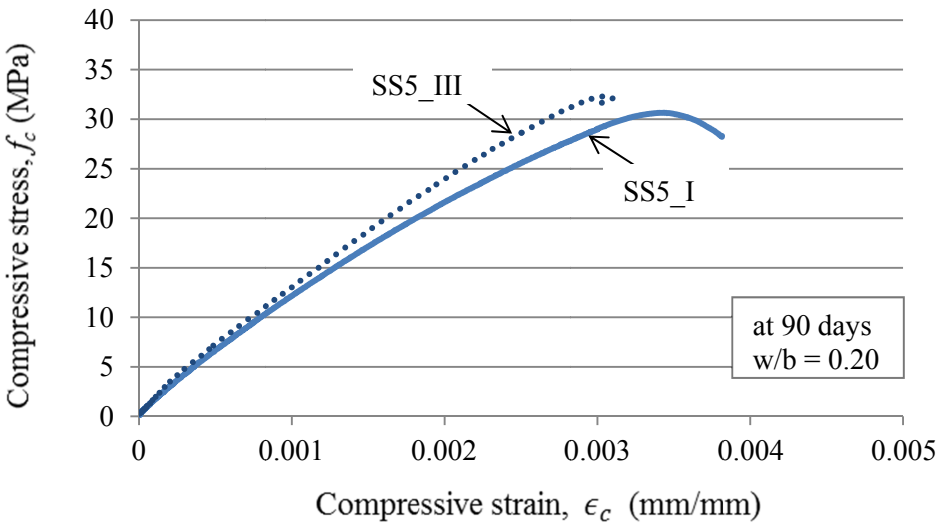

Figure 5-10: Compressive stress-strain response for mix SS5

(SS5_II is omitted for high deviation from the average strength)

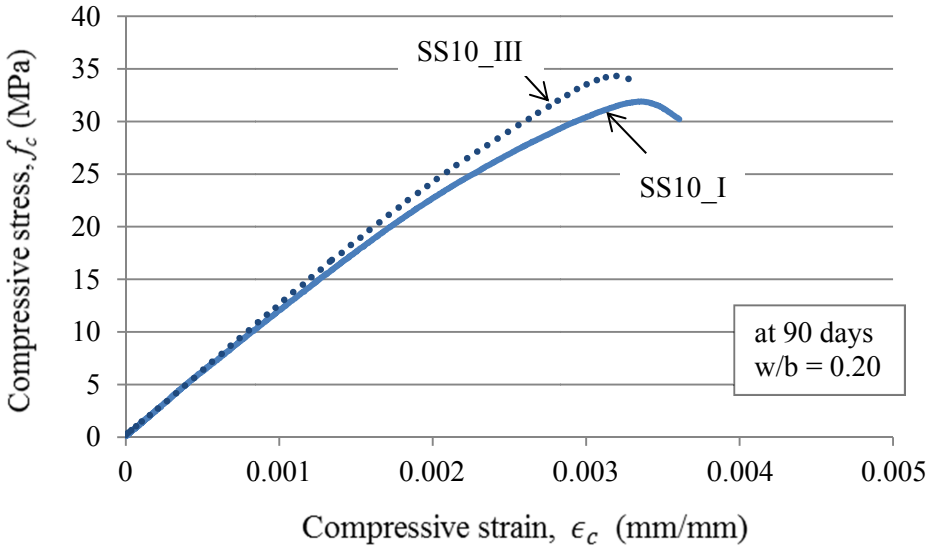

Figure 5-11: Compressive stress-strain response for mix SS10

(SS10_II is omitted for high deviation from the average strength)

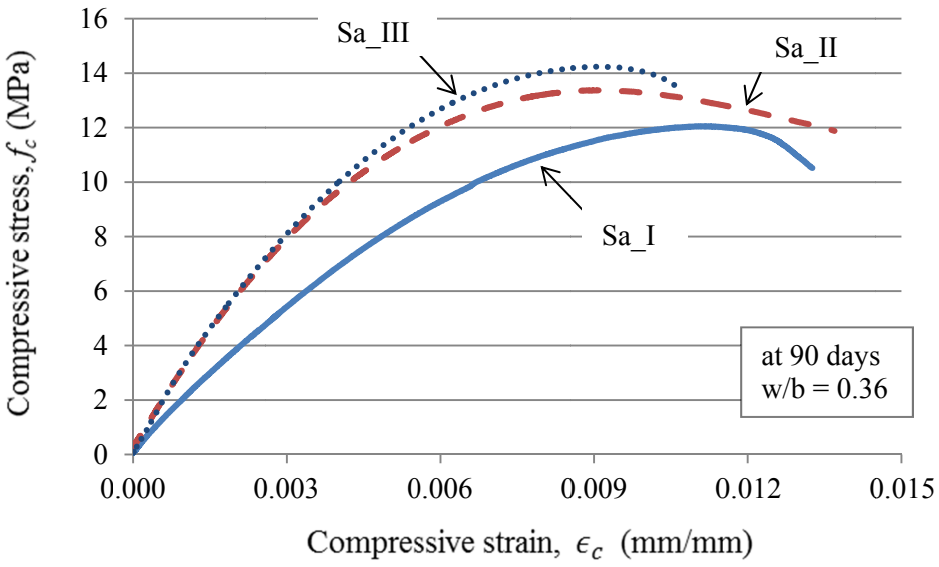

Figure 5-12: Compressive stress-strain response for mix Sa

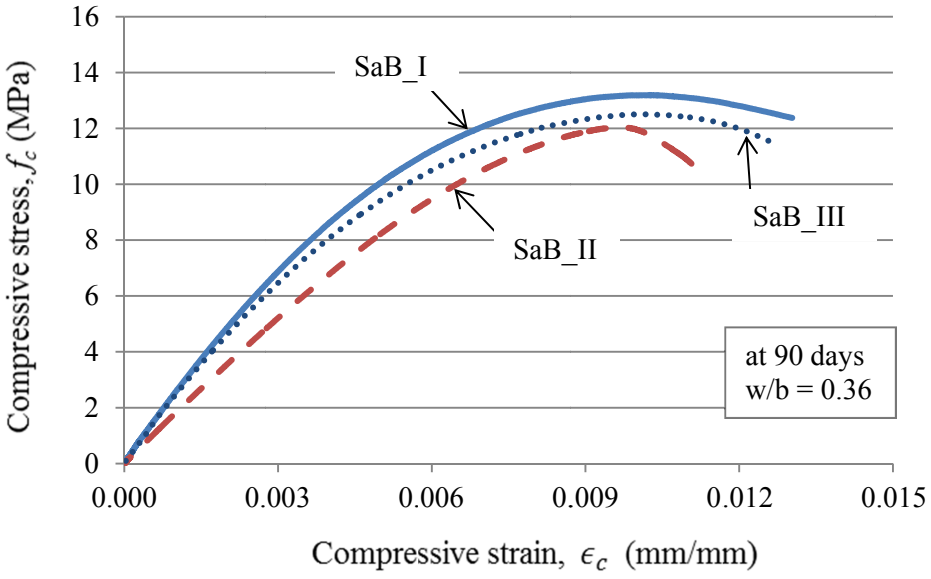

Figure 5-13: Compressive stress-strain response for mix SaB

Table 5-5: Average compressive stress and strain of MPPC concretes/wood composites

Mix	Average cylinder compressive strength, f'_c (MPa)	Average strain at peak stress, ε'_c (mm/mm)
S5	31.4	3.72×10^{-3}
S10	32.6	3.47×10^{-3}
SS5	31.5	3.24×10^{-3}
SS10	33.2	3.28×10^{-3}
Sa	13.3	9.72×10^{-3}
SaB	12.7	10.00×10^{-3}

5.3.2.3 Modulus of elasticity

According to ASTM C 469-02, the secant modulus of elasticity was calculated as follows:

$$E = \frac{(\sigma_2 - \sigma_1)}{(\varepsilon_2 - 0.00005)} \qquad (5\text{-}4)$$

where E = modulus of elasticity (MPa)

σ_2 = stress corresponding to 40% of ultimate strength (MPa)

σ_1 = stress corresponding to a longitudinal strain of 5×10^{-5} (MPa)

ε_2 = longitudinal strain at σ_2 (mm/mm)

Table 5-6 shows the average moduli of elasticity at 90-day age for the six mixtures considered. Values of *E* for each specimen can be found in Appendix B. Table 5-6 shows that sand mortars containing SF had the highest values of *E* which were 12.23 GPa and 12.16 GPa for SS5 and SS10, respectively. The increase in SF from 5% to 10% decreased the values of *E* for sand mortars from 12.23 to 12.16 GPa but increased those for MPPC binders containing SF from 8.47 to 9.28 GPa.

Among the six mixtures considered, MPPC wood composites had the lowest values of *E*. The addition of 2% baking soda by total mass of the dry mix decreased the value of *E* from 2.86 GPa (Sa) to 2.32 GPa (SaB).

Table 5-6: Average modulus of elasticity of MPPC concretes/wood composites

Mix	Average cylinder strength, f'_c (MPa)	Average density, γ (kg/m^3)	Average modulus of elasticity, E (GPa)		
			From test	Predicted by Eqn. 5-5	Predicted by Eqn. 5-6
S5	31.4	1751	8.47	17.65	12.73
S10	32.6	1763	9.28	18.17	13.10
SS5	31.5	2150	12.23	24.06	17.35
SS10	33.2	2173	12.16	25.10	18.09
Sa	13.3	1315	2.51	7.48	5.39
SaB	12.7	1438	2.13	8.36	6.02

The relationship between modulus of elasticity and compressive strength of MPPC concretes/wood composites is shown in Fig. 5-14. It is observed that the moduli of elasticity of all mixes increased when the compressive strength increased.

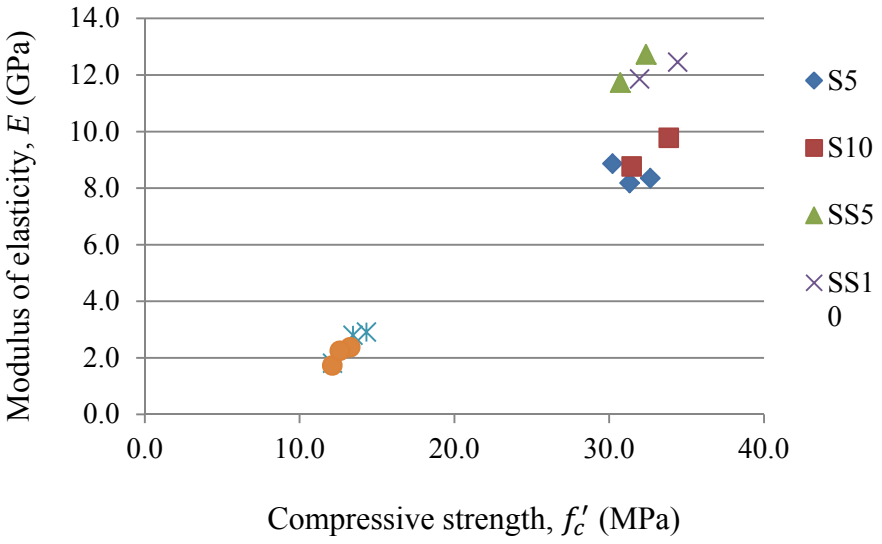

Figure 5-14: Modulus of Elasticity vs. Cylinder compressive strength

(at 90 days; w/b = 0.20 for S5, S10, SS5 and SS10; w/b = 0.36 for Sa and SaB)

ACI 213 (2009) predicts the modulus of elasticity of Portland cement lightweight concrete (in MPa) by an equation based on its density (w_c, in kg/m^3) and compressive strength (f'_c, in MPa) as follows:

$$E_c = 0.043 w_c^{1.5} \sqrt{f_c'} \qquad (5\text{-}5)$$

Based on a least square error analysis method of test data for lightweight MPPC concretes, Tassew and Lubell (2012) suggested that the modulus of elasticity was better captured by:

$$E = 0.031 \gamma^{1.5} \sqrt{f_c'} \qquad (5\text{-}6)$$

where E is the modulus of elasticity (MPa), γ is the density (kg/m^3), and f_c' is the cylinder compressive strength (MPa).

Table 5-6 compares the moduli of elasticity obtained from the tests and predictions by Eqn. 5-5 and Eqn. 5-6 for the six mixtures considered. The ratios of Test/Prediction values for modulus of elasticity can be found in Table 5-7. It can be seen that the Tassew and Lubell model better predicted the test results for MPPC concretes (S5, S10, SS5 and SS10) but all test/prediction ratios were less than 0.70. Both models by ACI 213 (2009) and by Tassew and Lubell did not predict well the modulus of elasticity for MPPC wood composites (mixes Sa and SaB).

Table 5-7: Test/Prediction ratios for modulus of elasticity of MPPC concretes/wood composites

Mix	Test/Predicted by Eqn. 5-5	Test/Predicted by Eqn. 5-6
S5	0.48	0.66
S10	0.51	0.70
SS5	0.51	0.70
SS10	0.48	0.67
Sa	0.34	0.46
SaB	0.25	0.35

5.3.3 Flexural properties

This section reports the test results used to determine the flexural properties of MPPC concretes/wood composites. Both prism and panel specimens were examined for the six mixtures considered.

5.3.3.1 Modulus of rupture using prism specimens

Prism specimens were tested by the 4-point bending test. The modulus of rupture of the prisms was calculated as the stress at the bottom fiber of the specimen produced by maximum load applied as follows:

$$f_{r-pr} = \frac{PL}{bd^2} \qquad (5\text{-}7)$$

where f_{r-pr} = modulus of rupture of prism specimen (MPa)

P = maximum load indicated by the testing machine (N)

L = span length which is 150mm in this case

b, d = average width and depth (notch accounted) of prism, respectively (mm)

According to ASTM C78/C78M-10, the test results of specimens in the same batch produced under laboratory conditions should not differ from each other by more than 16%. In this section, only the prism flexural strengths for mixes S5, SS5 and SaB met this criterion. Thus, the prism flexural strengths for these mixes are the average strengths of three specimens in the same mix. Meanwhile, the prism flexural strengths for mixes S10, SS10 and Sa are the average strengths of two specimens in the same mix.

The modulus of rupture for each mixture is shown in Fig. 5-15 and summarized in Table 5-8. The test results for each specimen can be found in Appendix B. Figure 5-15 shows that MPPC binders containing SF had the lowest flexural strengths. The increase in SF from 5% to 10% increased the modulus of rupture for MPPC binders containing SF from 0.8 MPa (S5) to 1.3 MPa (S10).

The same increase in SF content also increased the modulus of rupture for sand mortars containing SF from 1.6 MPa (SS5) to 1.8 MPa (SS10).

MPPC wood composites exhibited relatively high flexural strengths when compared with the other mixes. This contrasts with the results obtained from the cube and cylinder tests where the compressive strengths of MPPC wood composites were lowest compared with the others. The addition of 2% baking soda by mass significantly increased the modulus of rupture for these mixes from 1.5 MPa (Sa) to 2.7 MPa (SaB).

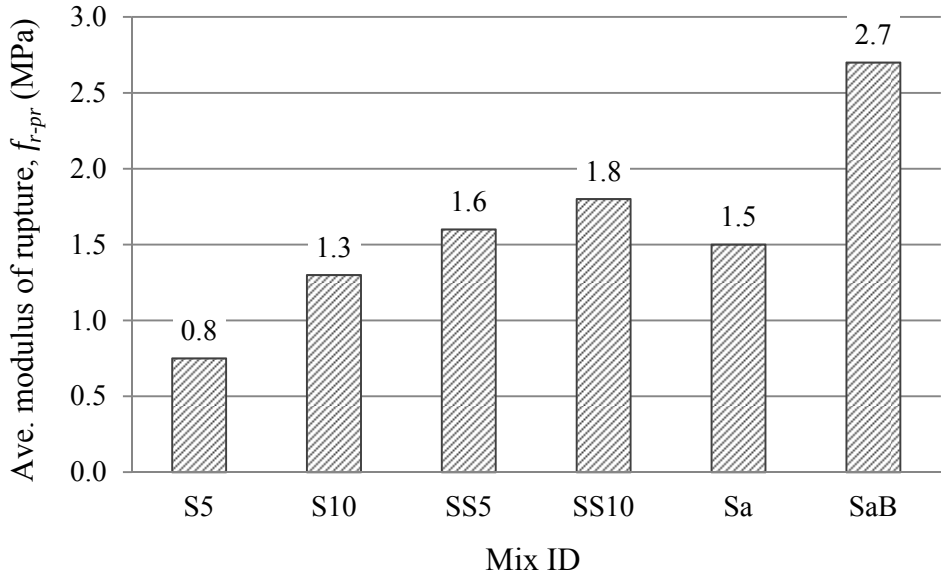

Figure 5-15: Modulus of rupture of MPPC concretes/wood composites from prsim test

(at 90 days; w/b = 0.20 for S5, S10, SS5 and SS10; w/b = 0.36 for Sa and SaB)

The load-deflection behaviors of MPPC concretes/wood composites are shown in Fig. 5-16 to Fig. 5-21. The average mid-span deflections at peak stress and the average slopes obtained from the load-deflection curves can be found in Table 5-8. These slopes (MPa/mm) were calculated by dividing the stress (MPa) corresponding to 40% of ultimate strength of each specimen by the corresponding mid-span displacement (mm) at that stress.

It can be observed in Table 5-8 that the load-deflection curves of sand mortars containing SF exhibited the steepest slopes. The increase in SF from 5% to 10% increased the slope of sand mortars containing SF from 19.9 MPa/mm (SS5) to 25.4 MPa/mm (SS10). The same increase in SF content also increased the slope of MPPC binders containing SF from 8.7 MPa/mm (S5) to 14.7 MPa/mm (S10). For MPPC wood composites, the addition of 2% baking soda by mass increased the slope of these mixes from 2.8 MPa/mm (Sa) to 6.9 MPa/mm (SaB).

In general, sand mortars containing SF exhibited the highest bending stiffness and MPPC wood composites showed the lowest bending stiffness. The increase in SF and the addition of baking soda increased the stiffness of MPPC concretes and MPPC wood composites, respectively.

The post-peak behavior of all MPPC concretes/wood composites exhibited a rapid drop in load carrying capcity after the first flexural crack forms in the high bending moment region of the specimens.

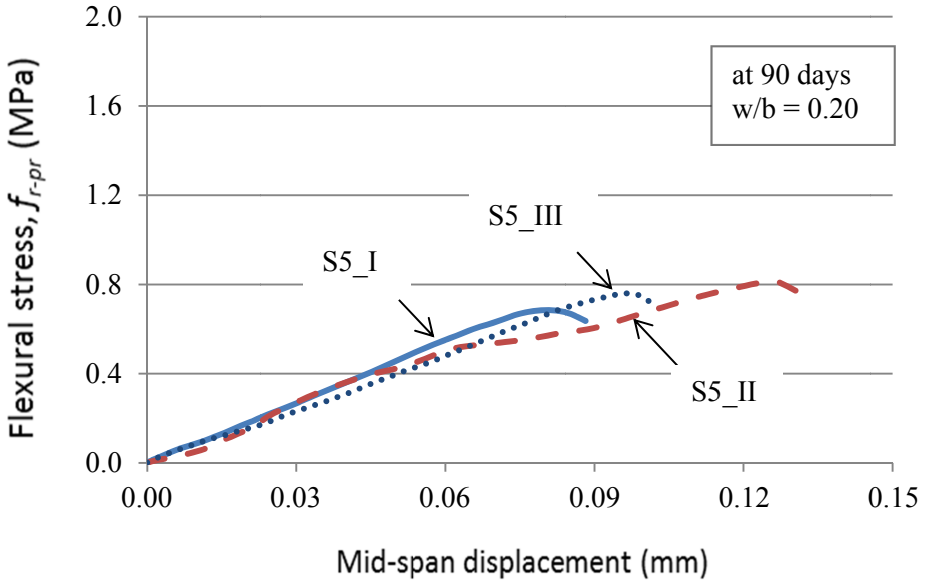

Figure 5-16: Flexural stress vs. mid-span displacement of prism for mix S5

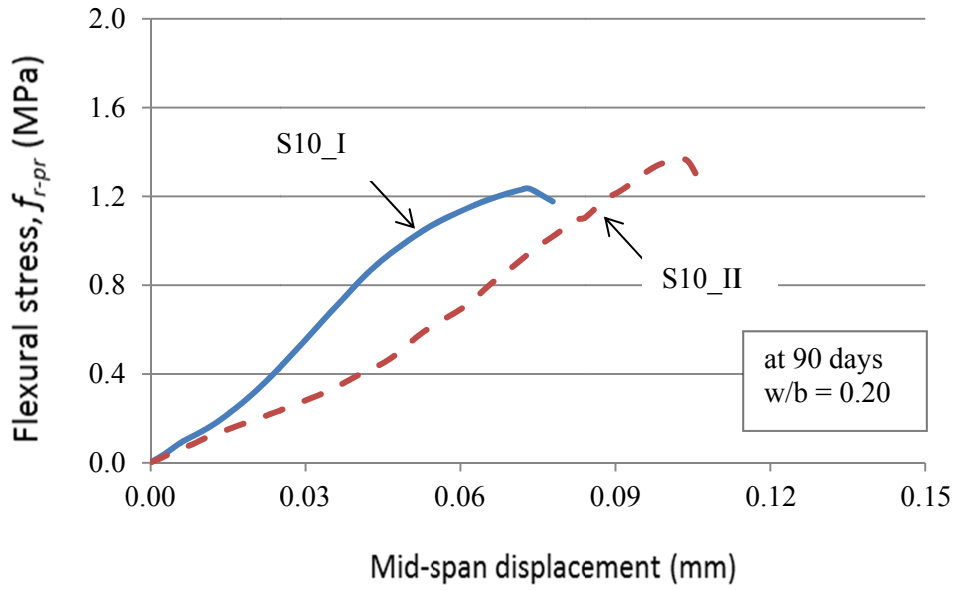

Figure 5-17: Flexural stress vs. mid-span displacement of prism for mix S10

(S10_III is omitted for high deviation from the average strength)

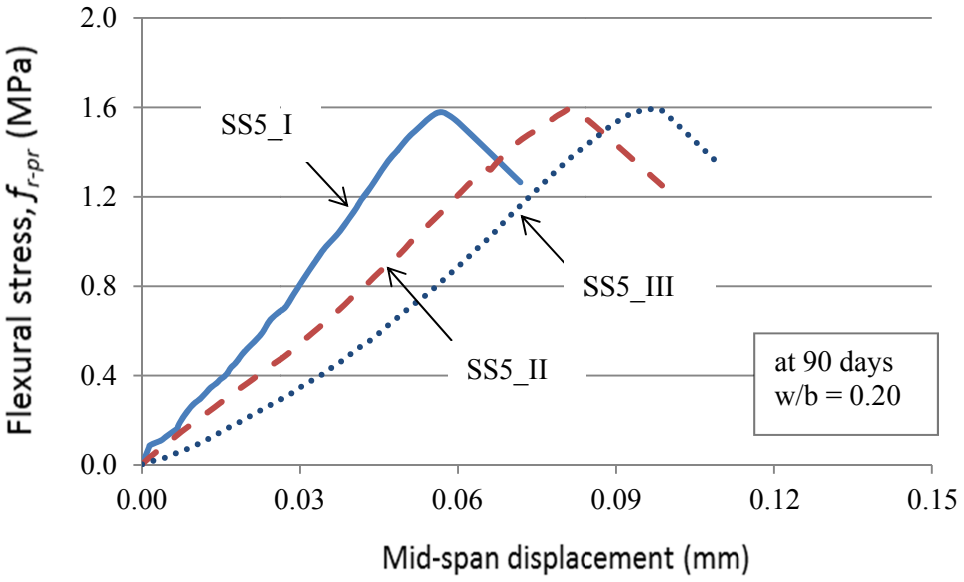

Figure 5-18: Flexural stress vs. mid-span displacement of prism for mix SS5

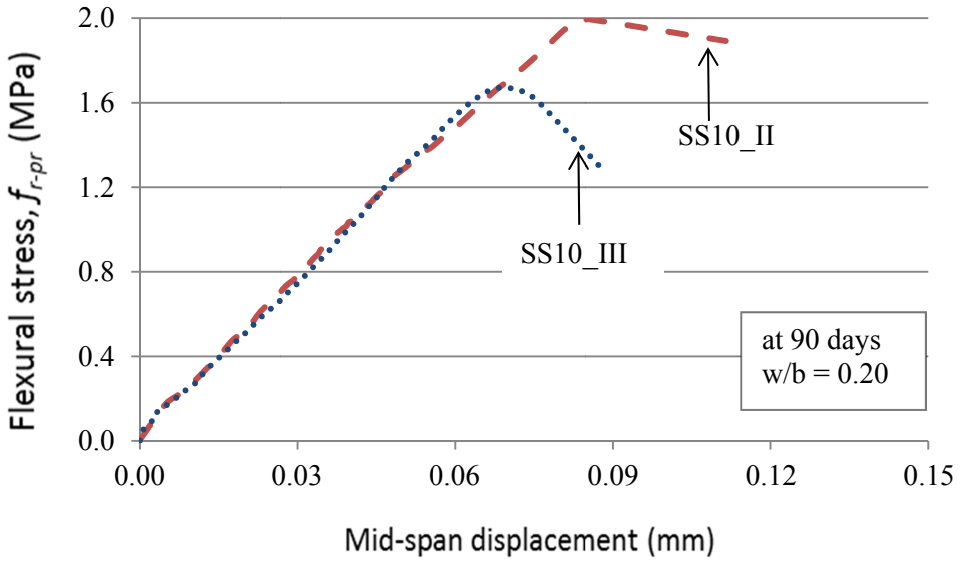

Figure 5-19: Flexural stress vs. mid-span displacement of prism for mix SS10

(SS10_I is omitted for high deviation from the average strength)

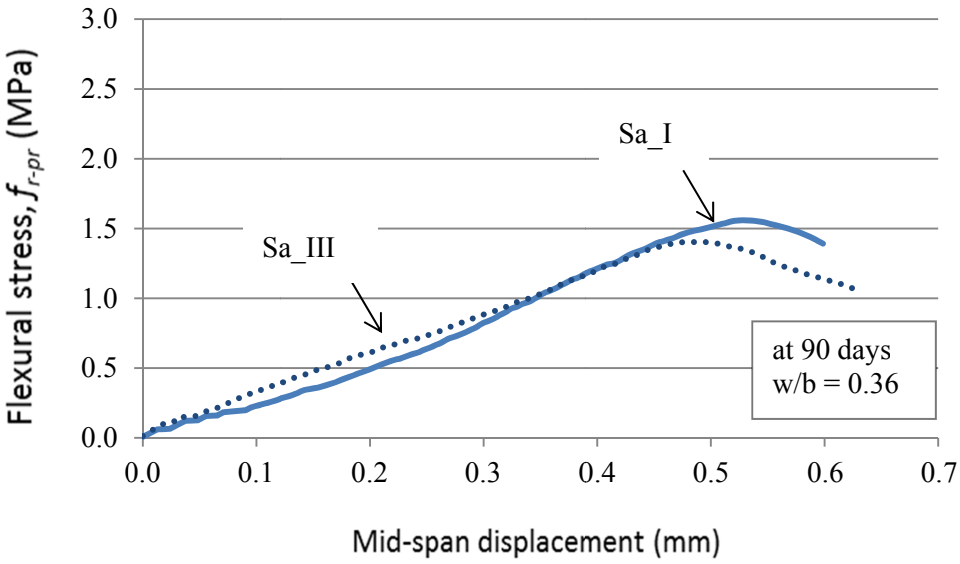

Figure 5-20: Flexural stress vs. mid-span displacement of prism for mix Sa

(Sa_II is omitted for high deviation from the average strength)

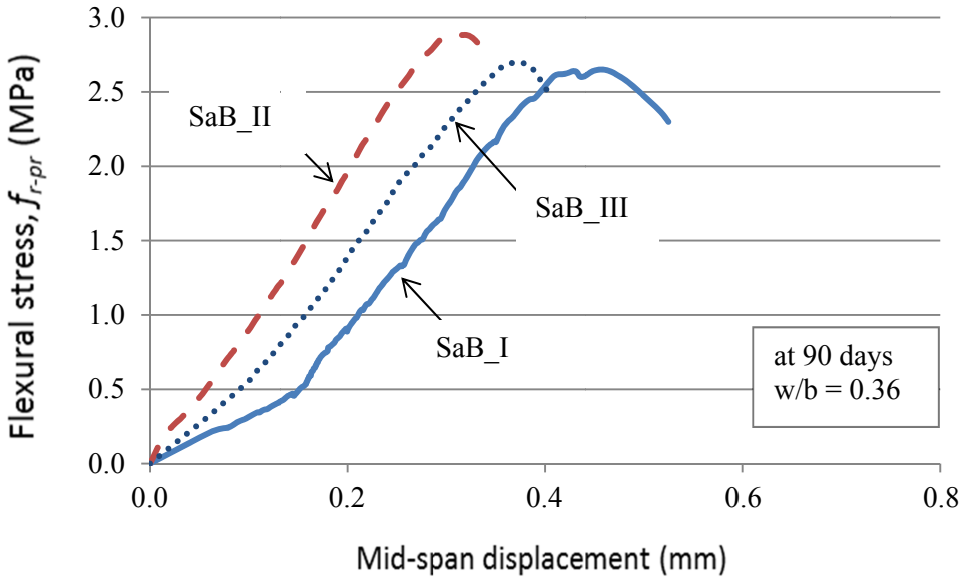

Figure 5-21: Flexural stress vs. mid-span displacement of prism for mix SaB

Table 5-8: Average modulus of rupture and mid-span deflection from prism tests

Mix	(MPa)	COV	(MPa)	(mm)	Slope (MPa/mm)	(%)	
S5	0.8	0.087	31.4	0.101	8.7	2.6	1/1485
S10	1.3	0.076	32.6	0.088	14.7	3.9	1/1704
SS5	1.6	0.004	31.5	0.078	19.9	5.1	1/1923
SS10	1.8	0.123	33.2	0.077	25.4	5.4	1/1948
Sa	1.5	0.076	13.3	0.503	2.8	11.3	1/298
SaB	2.7	0.044	12.7	0.383	6.9	21.3	1/391

$f_{r\text{-}pr}$: average modulus of rupture of prism; : average cylinder compressive strength; : average mid-span deflection; L: span length = 150 mm.

As shown in Table 5-8, the flexural strengths of MPPC concretes from the prism tests ranged between 2.6% and 5.4% of the corresponding cylinder compressive strengths. Meanwhile, the flexural strengths of MPPC wood composites were 11.3% (Sa) and 21.3% (SaB) of the corresponding cylinder compressive strength. ACI 213 (2009) expresses the relationship between the modulus of rupture ( ) and the compressive strength (of Porland Cement lightweight concrete by the following equation:

(5-8)

Based on a least square error analysis method of test data for lightweight MPPC concretes, Tassew and Lubell (2012) suggested that the modulus of rupture was better captured by:

$$f_{r-pr} = 0.33\sqrt{f_c'} \qquad (5\text{-}9)$$

where f_{r-pr} is the modulus of rupture obtained from prism test (MPa), and f_c' is the cylinder compressive strength (MPa).

Table 5-9 compares the values of modulus of rupture obtained from the tests and predictions by Eqn. 5-8 and Eqn. 5-9 for the six mixtures considered. The ratios of Test/Prediction values for modulus of rupture obtained from Eqn. 5-8 and Eqn. 5-9 can be found in Table 5-10. It can be seen that the Tassew and Lubell model gave good predictions for sand mortars containing SF (SS5 and SS10). The ACI 213 model (2009) also gave good prediction for mix Sa. The other predictions by both the ACI 213 model (2009) and Tassew and Lubell model (2012) did not show good correlations to the test values.

Table 5-9: Average modulus of rupture of MPPC concretes/wood composites from the prism tests and predictions

Mix	**Average cylinder compressive strength, f_c' (MPa)**	**Average modulus of rupture, $f_{r\text{-}pr}$ (MPa)**		
		From test	Predicted by Eqn. 5-8	Predicted by Eqn. 5-9
S5	31.4	0.8	2.52	1.85
S10	32.6	1.3	2.57	1.88
SS5	31.5	1.6	2.53	1.85
SS10	33.2	1.8	2.59	1.90
Sa	13.3	1.5	1.64	1.20
SaB	12.7	2.7	1.60	1.18

Table 5-10: Test/Prediction ratio for modulus of rupture of MPPC concretes/wood composites from the prism tests and predictions

Mix	Test/Predicted by Eqn. 5-8	Test/Predicted by Eqn. 5-9
S5	0.32	0.43
S10	0.51	0.69
SS5	0.63	0.86
SS10	0.69	0.95
Sa	0.91	1.25
SaB	1.69	2.29

5.3.3.2 Modulus of Rupture using panel specimens

Panel specimens were tested by the 3-point bending test. The modulus of rupture of each panel was calculated as the stress at the bottom fiber of the specimen produced by maximum load applied as follows:

$$f_{r-pa} = \frac{3PL}{2bd^2} \qquad (5\text{-}10)$$

where f_{r-pa} = modulus of rupture of panel specimen (MPa)

P = maximum load indicated by the tesing machine (N)

L = span length which is 450 mm in this case

b, d = average width and depth of panel , respectively (mm)

According to ASTM C78/C78M-10, the test results of specimens in the same batch produced under laboratory conditions should not differ from each other by more than 16%. In this section, the panel flexural strengths for mixes S10, SS5, SS10 and Sa met this criterion. Thus, the panel flexural strengths for these mixes are the average strengths of three specimens in the same mix. Meanwhile, the panel flexural strengths for mixes S5 and SaB are the average strengths of two specimens in the same mix.

The average moduli of rupture from the panel tests for each mixture are shown in Fig. 5-22. The test results for each specimen can be found in Appendix

B. Figure 5-22 shows that the MPPC binders containing SF had the lowest flexural strengths. The increase in SF from 5% to 10% slightly decreased the modulus of rupture for these mixes from 3.5 MPa (S5) to 3.3 MPa (S10). A similar trend can be observed for sand mortars containing SF where the same increase in SF content slightly decreased the modulus of rupture from 5.3 MPa (SS5) to 5.2 MPa (SS10).

MPPC wood composites exhibited relatively high flexural strengths when compared with other mixes. This contrasts with the results obtained from the cube and cylinder tests where the compressive strengths of MPPC wood composites were lowest. The addition of 2% baking soda by mass increased the modulus of rupture for these mixes from 4.1 MPa (Sa) to 5.9 MPa (SaB).

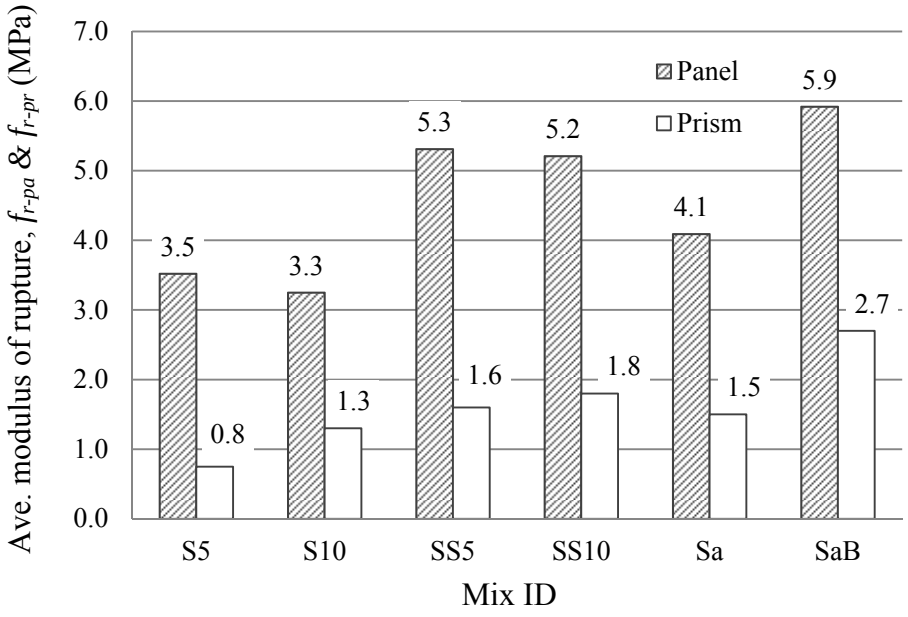

Figure 5-22: Modulus of Rupture of MPPC concretes/wood composites from the panel and prism tests at 90-day age

(w/b = 0.20 for S5, S10, SS5 and SS10; w/b = 0.36 for Sa and SaB)

Figure 5-22 compares the moduli of rupture of MPPC concretes/wood composites obtained from the panel and prism tests. It is observed that the moduli of rupture from the panel tests were significantly higher than from the prism tests for all mixes. This can be explained by the difference between the 3-point bending

test for the panel and the 4-point bending test for the prism. In the 4-point bending test the peak tensile stress occurs over a long constant moment region between the load points whereas in the 3-point bending test the peak stress only occurs at the load point. Since the region under peak stress in the 4-point bending test is longer, there is more chance of a local defect being subjected to a load sufficient to break it than in the 3-point bending test (Tucker, 1941). However, this effect was partially offset by the presence of the notch in the prisms which forced a failure location.

The difference in the depths between the panel and prism specimens was also believed to influence the modulus of rupture bobtained from the two types of test. Accoding to Carpinteri and Chiaia (2002), the flexural strength depends upon the strain gradient over the member cross-section. Higher flexural strengths would occur in shallower beams due to the larger strain decrease with respect to the depth (steep gradient) (Carpinteri & Chiaia, 2002). Since the depths of panel and prism specimens used in this study were 20 mm and 50 mm, respectively, higher flexural strengths could be expected for panel specimens. However, additional research is needed to better explain the influence that causes the difference in the moduli of rupture obtained from the prisms and the panels.

The load-deflection behaviors of MPPC concretes/wood composites are shown in Fig. 5-23 to Fig. 5-28. The average mid-span deflections at peak stress and the average slopes obtained from the load-deflection curves can be found in Table 5-11. The calculation for these slopes was described in Section 5.3.3.1.

It can be observed in Table 5-11 that the load-deflection curves of sand mortars containing SF exhibited the steepest slopes. The increase in SF from 5% to 10% increased the slopes of sand mortars containing SF from 6.5 MPa/mm (SS5) to 7.3 MPa/mm (SS10). The same increase in SF content also increased slightly the slopes of MPPC binders containing SF from 3.7 MPa/mm (S5) to 3.8 MPa/mm (S10). For MPPC wood composites, the addition of 2% baking soda by mass increased the slope of these mixes from 1.6 MPa/mm (Sa) to 2.5 MPa/mm (SaB).

In general, sand mortars containing SF exhibited the highest bending stiffness and MPPC wood composites showed the lowest bending stiffness. The increase in SF and the addition of baking soda increased the stiffness of MPPC concretes and MPPC wood composites, respectively. This trend is similar to the result from prism test as discussed in section 5.3.3.1.

The post-peak behaviors of all MPPC concretes/wood composites exhibited the significant drop in load after the first flexural crack forms in the high bending moment region of the specimens.

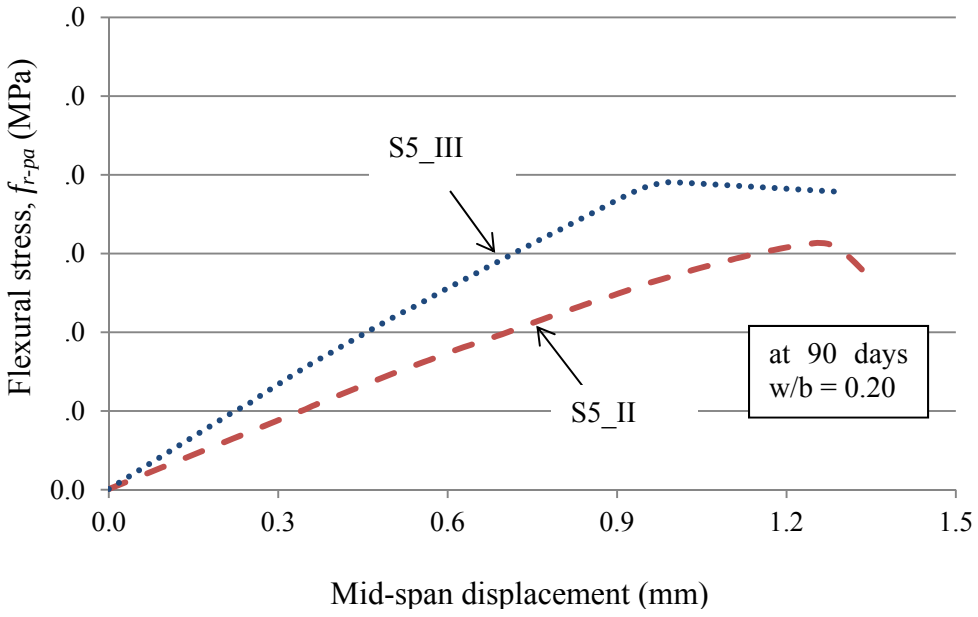

Figure 5-23: Flexural stress vs. mid-span displacement of panels for mix S5

(S5_I is omitted for high deviation from the average strength)

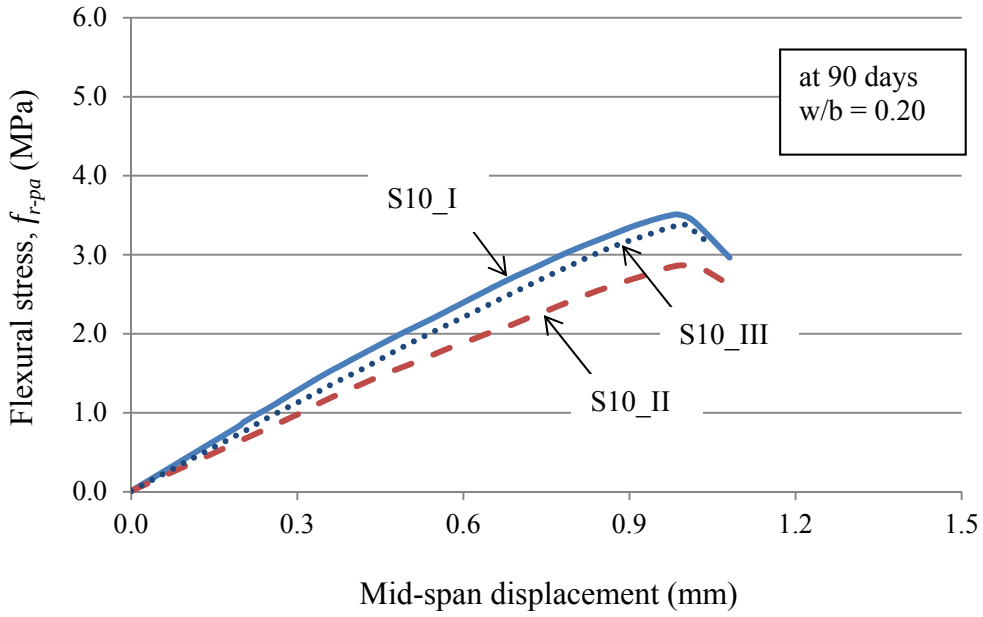

Figure 5-24: Flexural stress vs. mid-span displacement of panels for mix S10

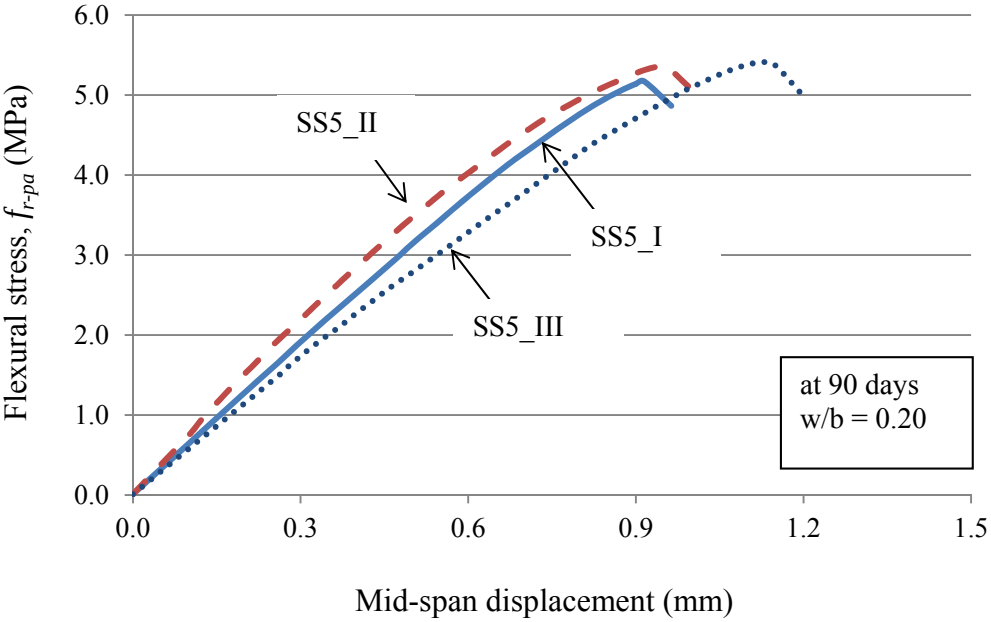

Figure 5-25: Flexural stress vs. mid-span displacement of panels for mix SS5

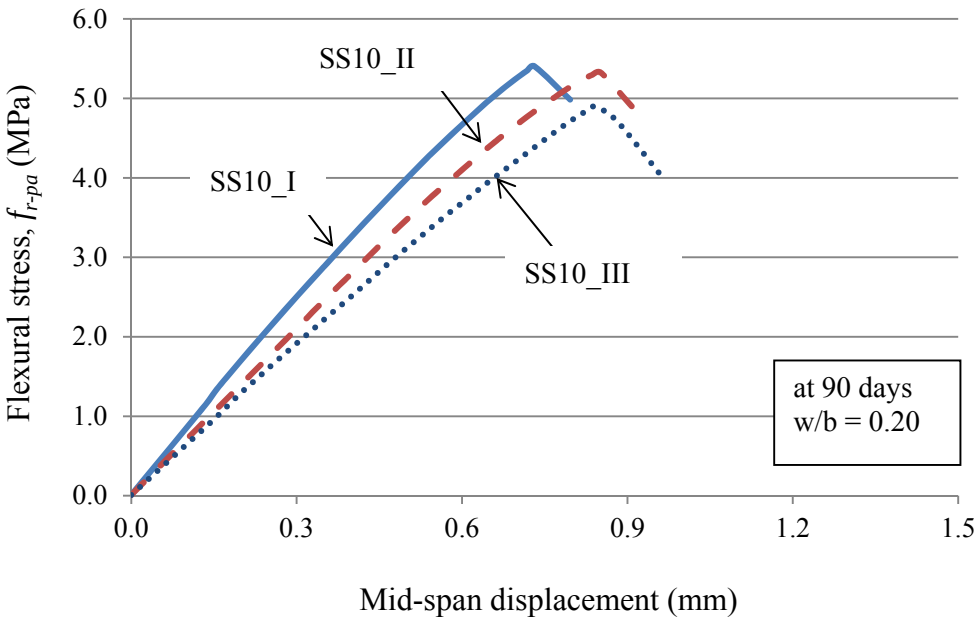

Figure 5-26: Flexural stress vs. mid-span displacement of panels for mix SS10

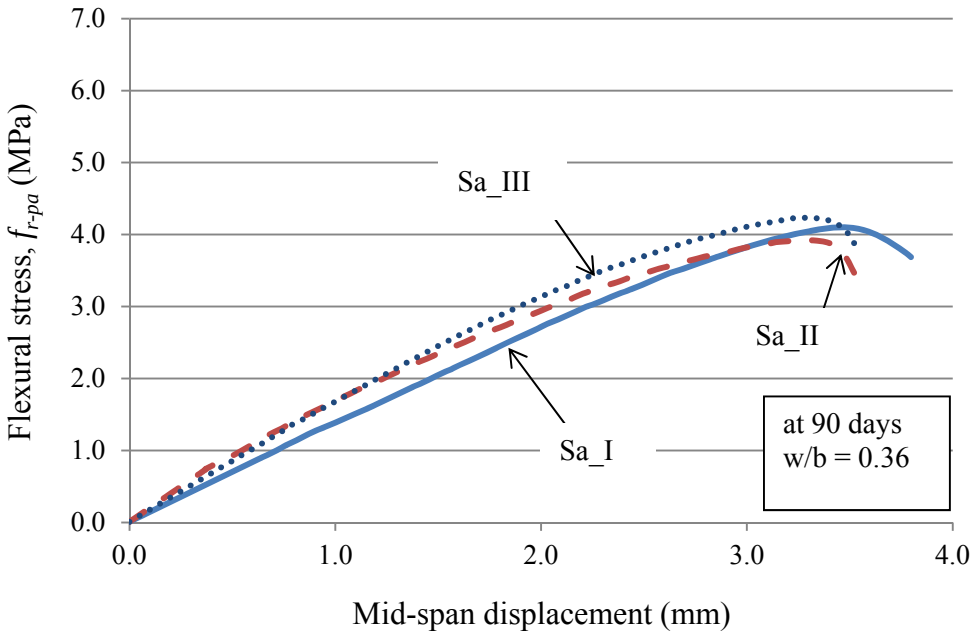

Figure 5-27: Flexural stress vs. mid-span displacement of panels for mix Sa

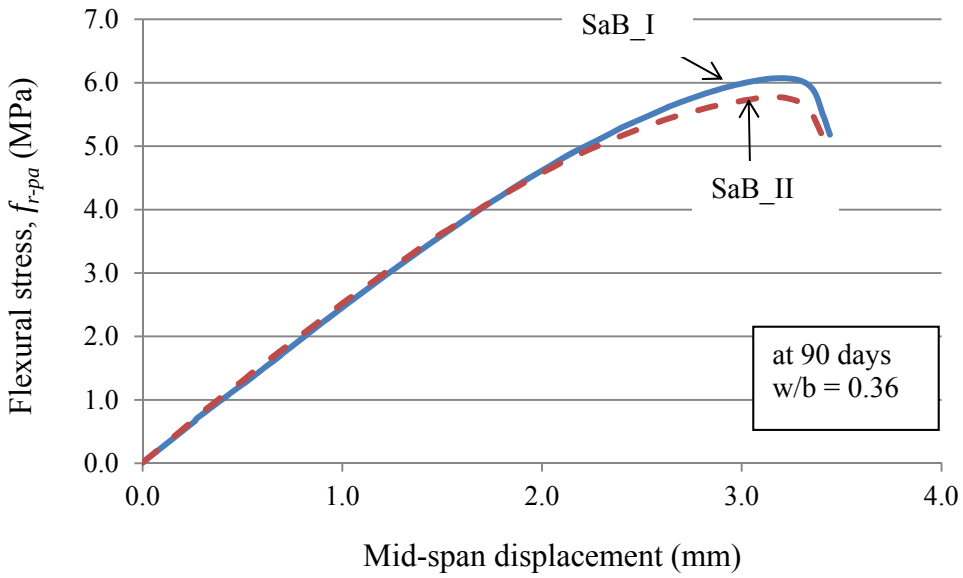

Figure 5-28: Flexural stress vs. mid-span displacement of panels for mix SaB

(SaB_III is omitted for high deviation from the average strength)

Table 5-11: Average modulus of rupture and mid-span deflection from panel tests

Mix	f_{r-pa} (MPa)	COV	f'_c (MPa)	δ (mm)	Slope, (Mpa/mm)	f_{r-pa}/f'_c (%)	δ/L
S5	3.5	0.154	31.4	1.129	3.7	11.2	1/398
S10	3.3	0.104	32.6	0.993	3.8	10.1	1/453
SS5	5.3	0.023	31.5	0.998	6.5	16.8	1/450
SS10	5.2	0.051	33.2	0.808	7.3	15.6	1/556
Sa	4.1	0.036	13.3	3.329	1.6	30.8	1/135
SaB	5.9	0.035	12.7	3.184	2.5	46.5	1/141

$f_{r\text{-}pa}$: average modulus of rupture of panel; f'_c: average cylinder compressive strength; δ: average mid-span deflection; L: span length = 450 mm;

As shown in Table 5-11, the flexural strengths of MPPC concretes from the panel tests ranged between 10.1% and 16.8% of the corresponding cylinder compressive strength. Meanwhile, the flexural strengths of MPPC wood composites were 30.8% (Sa) and 46.5% (SaB) of the corresponding cylinder compressive strength.

Equations 5-8 and 5-9 were used again to predict the moduli of rupture for the panel tests. Table 5-12 compares the moduli of rupture obtained from the tests and predictions by Eqn. 5-8 and Eqn. 5-9 for the six mixtures considered. The

ratios of Test/Prediction values for modulus of rupture can be found in Table 5-13. It can be seen that all the predictions were lower than the test values. The ACI 213 model only gave good predictions for MPPC binders containing SF (S5 and S10). The other predictions by either the ACI 213 model or the Tassew and Lubell model showed a significant difference with the test results. The coefficient of variation of Test/Predicted ratios by Eqn. 5-8 was smaller than by Eqn. 5-9.

Table 5-12: Average modulus of rupture of MPPC concretes/wood composites from the panel tests and predictions at 90-day age

Mix	Average cylinder compressive strength, f'_c (MPa)	Average modulus of rupture, $f_{r\text{-}pa}$ (MPa)		
		From test	Predicted by Eqn. 5-8	Predicted by Eqn. 5-9
S5	31.4	3.5	2.5	1.9
S10	32.6	3.3	2.6	1.9
SS5	31.5	5.3	2.5	1.9
SS10	33.2	5.2	2.6	1.9
Sa	13.3	4.1	1.6	1.2
SaB	12.7	5.9	1.6	1.2

Table 5-13: Test/Prediction ratio for modulus of rupture of MPPC concretes/wood composites from the panel tests and predictions

Mix	Test/Predicted by Eqn. 5-8	Test/Predicted by Eqn. 5-9
S5	1.4	1.8
S10	1.3	1.7
SS5	2.1	2.8
SS10	2.0	2.7
Sa	2.6	3.4
SaB	3.7	4.9

5.4 Summary

The following conclusions can be drawn from this chapter:

- Fresh mixture of MPPC binders and sand mortars exhibited good slump flow property. An increase in SF content decreased the slump flow for these mixtures. Fresh mixtures of MPPC wood composites did not exhibit flow property but they were still workable.
- MPPC concrete/wood composites exhibited rapid strength gain with initial setting times of 45 to 105 minutes. The differences between the initial setting time and the final setting time for these mixtures were about 20 to 60 minutes. An increase in SF content increased the setting time of sand mortars containing SF but decreased those of MPPC binders containing SF. The addition of baking soda decreased the setting times of MPPC wood composites.
- The compressive strengths of MPPC concretes/wood composites increased as their densities increased. The 90-day cylinder compressive strengths and densities ranged from 12.7 MPa to 33.2 MPa and 1315 kg/m^3 to 2173 kg/m^3, respectively. The increase in SF content had negligible influence on the densities of MPPC concretes. Meanwhile, the addition of baking soda slightly increased the densities of MPPC wood composites from 1315 kg/m^3 to 1438 kg/m^3.
- An increase in SF content from 5% to 10% by mass had negligible influence on the compressive strengths of MPPC concretes. The addition of baking soda increased the cube compressive strengths but decreased the cylinder compressive strengths of MPPC wood composites.
- The increase in SF content decreased the strains at peak stress for MPPC binders containing SF but had negligible influence on sand mortars containing SF. The addition of baking soda increased the strains at peak stress for MPPC wood composites.
- The moduli of elasticity increased for MPPC binders containing higher mass percent of SF but decreased slightly for sand mortars containing SF

as the SF content increased. The addition of baking soda decreased the modulus of elasticity for MPPC wood composites. The equation by Tassew and Lubell (2012) gave better predictions for the moduli of elasticity but all test/prediction ratios were less than 0.70.

- MOR values of MPPC concretes and wood composites from the prism tests were about 2.6 to 5.4% and 11.3 to 21.3% of their corresponding cylinder compressive strengths, respectively. These MOR values increased as the SF content increased or when baking soda was added. The equation by Tassew and Lubell (2012) gave good predictions for test values of sand mortars containing SF. Meanwhile, the equation by ACI 213 (2009) gave better prediction for MPPC wood composites without baking soda.
- MOR values of MPPC concretes and wood composites from the panel tests were 10.1 to 16.8% and 30.8% to 46.5% of their corresponding cylinder compressive strengths, respectively. These MOR values decreased slightly as the SF content increased and they increased when baking soda was added. The equation by ACI 213 (2009) gave better predictions for MPPC binders containing SF.

Chapter 6 MPPC CONCRETES AND WOOD COMPOSITES REINFORCED WITH GLASS-FIBERS OR TEXTILE GLASS-FABRICS

6.1 Introduction

The six MPPC concretes/wood composite mixtures examined in chapter 5 were re-examined in this chapter after being reinforced with chopped glass-fibers or textile glass-fibers. Flow property, compression and flexural properties were evaluated. A summary of the analyzed data for each characteristic is reported in this chapter. Detailed test data for each specimen can be found in Appendix C.

Each mixture in chapter 6 can be differentiated with the corresponding mixture in chapter 5 by a letter F prefix to designate a mix with "fibers". The mix compositions of MPPC concretes/wood composites used in chapter 6 for cube, cylinder and prism specimens are shown in Table 6-1. An amount of 1% chopped glass-fibers by total mass of the mix was added in mixes for cube, cylinder and prism specimens. It is noted that for panel specimens, the chopped glass-fibers were replaced by two layers of textile glass-fibers as described in section 3.2.3.

Table 6-1: Mix compositions of MPPC concretes/wood composites reinforced with chopped glass-fibers

Mix ID	MgO:MKP:FA ratio	Binder-to-sand mass ratio (*b/s*)	Binder-to-sawdust mass ratio (*b/sdt*)	Silica fume (%)	Baking soda (%)	Glass-fibers (%)
FS5	1:3:4	-	-	5	-	1
FS10	1:3:4	-	-	10	-	1
FSS5	1:3:4	1:1.0	-	5	-	1
FSS10	1:3:4	1:1.0	-	10	-	1
FSa	1:3:1	1:0.5	1:0.2	-	-	1
FSaB	1:3:1	1:0.5	1:0.2	-	2	1

silica fume and baking soda contents are by mass percent of the binder
glass-fiber content is by mass percent of the whole mix

6.2 Flow property of MPPC concretes using glass-fibers

Experimental results of the flow test are shown in Fig. 6-1 for MPPC concretes with and without fibers. For mixes containing chopped glass-fibers, mixture FS5 (with 5% by mass SF) exhibited the highest flow at 137%. Meanwhile, the flow of mixture FS10, which used 10% SF, decreased significantly to 93%. This result indicates that an increase of SF in the mix increased the viscosity and reduced the flow.

For sand mortars, mixture FSS5 exhibited lower flow (90%) when compared with mixture FS5 which had the same SF content but without sand. When the SF content increased to 10%, mixture FSS10 showed a decrease in flow (69%) as was described above for mixes without sand. Comparing mixes FS10 and FSS10, it is observed that the inclusion of sand decreased the flow from 93% (S10) to 69% (SS10).

In summary, the flow as well as the workability of MPPC binders containing SF decreased when the SF content increased. This trend was also observed with sand mortars containing SF. The inclusion of sand decreased the flow of mixes regardless of the SF content.

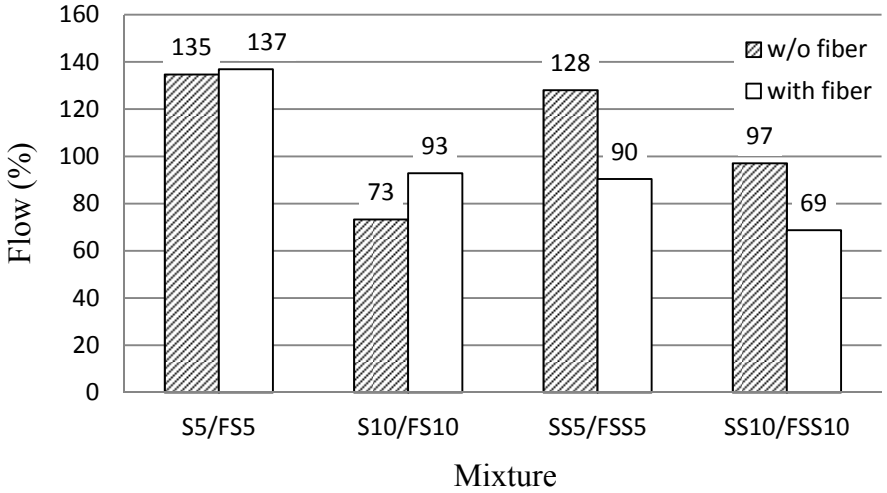

Figure 6-1: Flow test results of MPPC concretes

(w/b = 0.20; MgO:MKP:FA = 1:3:4)

Figure 6-1 also compares the flow between mixtures with and without chopped glass-fibers. It can be seen that mixtures FS5 and S5 had similar flow. The addition of glass-fibers decreased the flow of mixtures FSS5 and FSS10 from 128% to 90% and from 97% to 69%, respectively. However, it was unexpected that the flow of mixture FS10 increased from 73% to 93% when glass-fibers were added.

Since the fresh mixtures of MPPC wood composites do not flow, flow-table tests could not be applied for mixes FSa and FSaB.

6.3 Hardened properties of MPPC concretes using glass fibers

6.3.1 Density

Figure 6-2 compares the densities of the six mixtures considered. Detailed values can be found in Table 6-2. It can be observed that the addition of 1% fiber by total mass of the mix had negligible influence on the densities of mixes FS5, FS10, FSa and FSaB compared to mixes S5, S10, Sa and SaB. However, it slightly decreased the density of mixes FSS5 and FSS10. For mixes containing glass-fibers, sand mortars containing SF had the highest densities which were 2026 kg/m^3 (FSS5) and 2040 kg/m^3 (FSS10). Meanwhile, MPPC wood composites containing glass-fibers had the lowest densities which were 1339 and 1509 kg/m^3 for mixes FSa and FSaB, respectively.

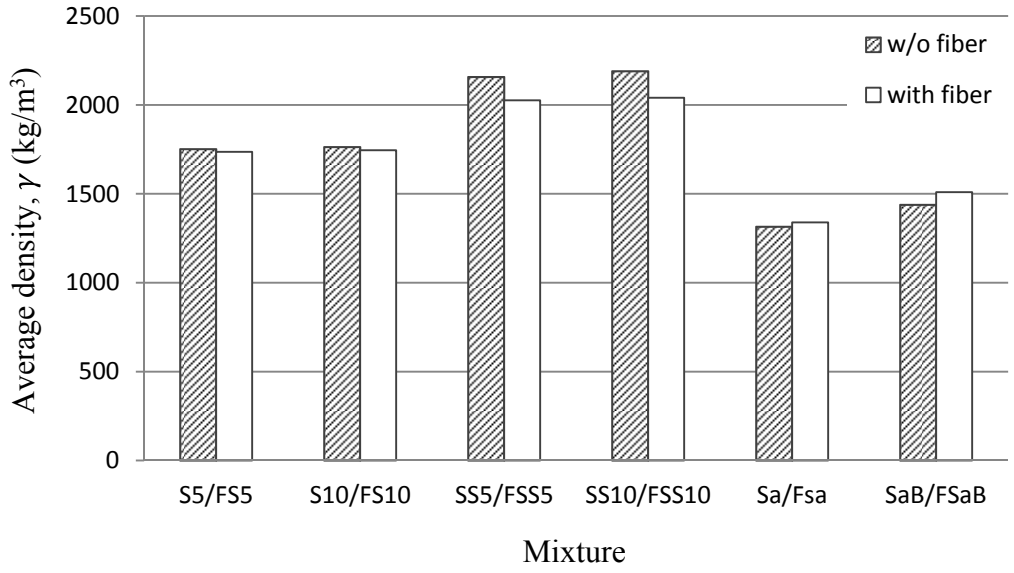

Figure 6-2: Density of MPPC concretes/wood composites

(w/b = 0.20 for FS5, FS10, FSS5 and FSS10; w/b = 0.36 for FSa and FSaB)

Table 6-2: Average density of MPPC concretes/wood composites with and without chopped glass- fibers

Mix	Average density, γ (kg/m^3)		Coefficient of variation	
	Without glass-fibers	With glass-fibers	Without glass-fibers	With glass-fibers
S5/FS5	1751	1736	0.001	0.003
S10/FS10	1763	1745	0.001	0.003
SS5/FSS5	2150	2026	0.006	0.003
SS10/FSS10	2173	2040	0.008	0.003
Sa/FSa	1315	1339	0.029	0.033
SaB/FSaB	1438	1509	0.006	0.009

6.3.2 Compression properties

The properties including compressive strength, modulus of elasticity and stress-strain relationship of MPPC concretes/wood composites reinforced with fibers are reported in this section.

6.3.2.1 Compressive strength of cube and cylindrical specimens

Tests were conducted with 50x50x50 mm cube specimens. The cube compressive strength (f_{cu}) can be found based on the maximum load indicated by the testing machine as was described in section 4.2, chapter 4. The permissible range of variation between the specimens was also described in section 4.2. In this section, the cube compressive strengths for all mixes were within the permissible range of variation for three specimens which is 8.7%.

Detailed values of f_{cu} for each individual specimen, the average and the coefficient of variation for each mix series are shown in Appendix C.

Figure 6-3 shows the cube compressive strength of the six mixtures with and without chopped glass-fibers. Detailed values of compressive strength can be found in Table 6-3. For MPPC concretes/wood composites containing chopped glass-fibers, mixes FSS5 and FSS10 exhibited the highest compressive strengths which were 50.7 MPa (FSS5) and 52.3 MPa (FSS10). It can be seen that an increase in SF from 5% to 10% slightly increased the strengths of both sand mortars and MPPC binders.

The compressive strengths of MPPC wood composites containing chopped glass-fibers were the lowest when compared with the other mixes containing chopped glass-fibers. When 2% baking soda by total mass of the dry ingredients was added, the strength of these mixes increased from 12.0 MPa (FSa) to 19.4 MPa (FSaB).

Figure 6-3 also compares the strengths of mixes with and without chopped glass-fibers. It can be observed that the inclusion of glass-fibers increased the strength of all mixtures. When glass-fibers were added, sand mortars containing SF had the highest strength gains which were 23% and 12% for mixes FSS5 and FSS10, respectively, when compared with mixes without glass-fibers.

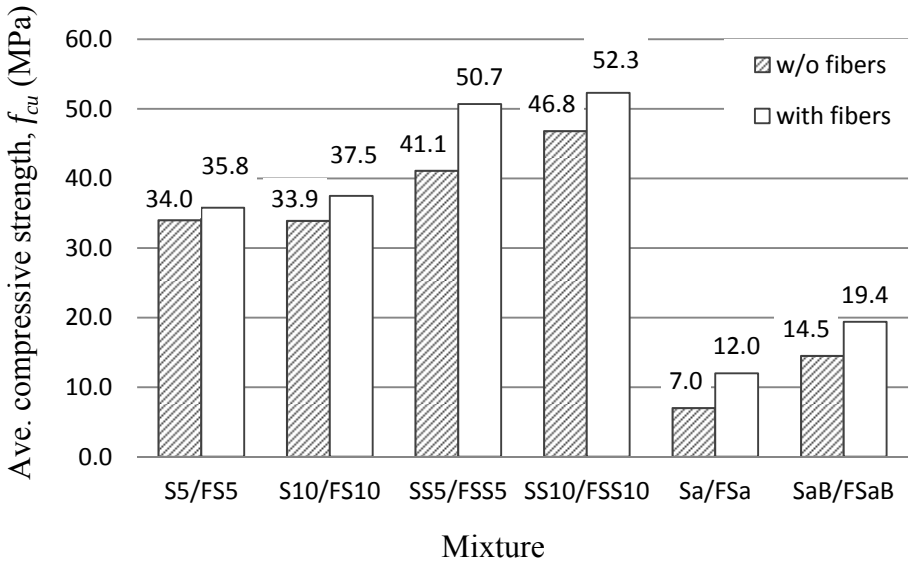

Figure 6-3: Cube compressive strength of MPPC concretes/wood composites at 90-day age

(w/b = 0.20 for FS5, FS10, FSS5 and FSS10; w/b = 0.36 for FSa and FSaB)

Table 6-3: Average cube strength of MPPC concretes/wood composites

Mix	Average cube strength, f_{cu}(MPa)		Coefficient of variation	
	Without glass-fibers	With glass-fibers	Without glass-fibers	With glass-fibers
S5/FS5	34.0	35.8	0.048	0.062
S10/FS10	33.9	37.5	0.006	0.055
SS5/FSS5	41.1	50.7	0.089	0.018
SS10/FSS10	46.8	52.3	0.095	0.025
Sa/FSa	7.0	12.0	0.089	0.100
SaB/FSaB	14.5	19.4	0.043	0.048

Cylinders with the dimension of 100 x 200 mm (diameter x height) were examined to determine the compressive strengths for the six mixtures considered. The compressive strength f_c' for each cylinder can be found based on the load indicated by the testing machine as was described in Section 5.3.2.1, chapter 5. The permissible range of variation between the specimens was also described in the same section. In this section, the cylinder compressive strengths for all mixes

were within the permissible range of variation for three specimens which is 10.67%.

Detailed values of f_c' for each individual specimen as well as the coefficient of variation for each series can be found in Appendix C.

The results of the compressive strength from the cylinder tests for six mixtures with and without fibers were plotted in Fig. 6-4. Detailed values of compressive strength for each mixture can be found in Table 6-4. For mixes using glass-fibers, sand mortars containing SF had the highest compressive strengths which were 37.4 MPa (FSS5) and 35.9 MPa (FSS10). MPPC wood composites exhibited the lowest strengths which were 12.7 MPa (FSa) and 14.3 MPa (FSaB).

Figure 6-4 indicates that, for mixes with glass-fibers, an increase in SF from 5% to 10% slightly reduced the strength of sand mortars and had no influence on the strength of MPPC binders containing SF. This contrasts with the results obtained for cylinders without glass-fibers as can be seen in Fig. 6-4. The addition of baking soda increased the strengths of MPPC wood composites from 12.7 MPa (FSa) to 14.3 MPa (FSaB). This is also contrary to the results obtained for cylinders without glass-fibers as can be seen in Fig. 6-4.

When comparing between mixes with and without glass-fibers, the addition of glass-fibers increased the cylinder compressive strength (8-19%) for all mixes but FSa. The inclusion of glass-fibers reduced the cylinder compressive strength of mix FSa by 5%.

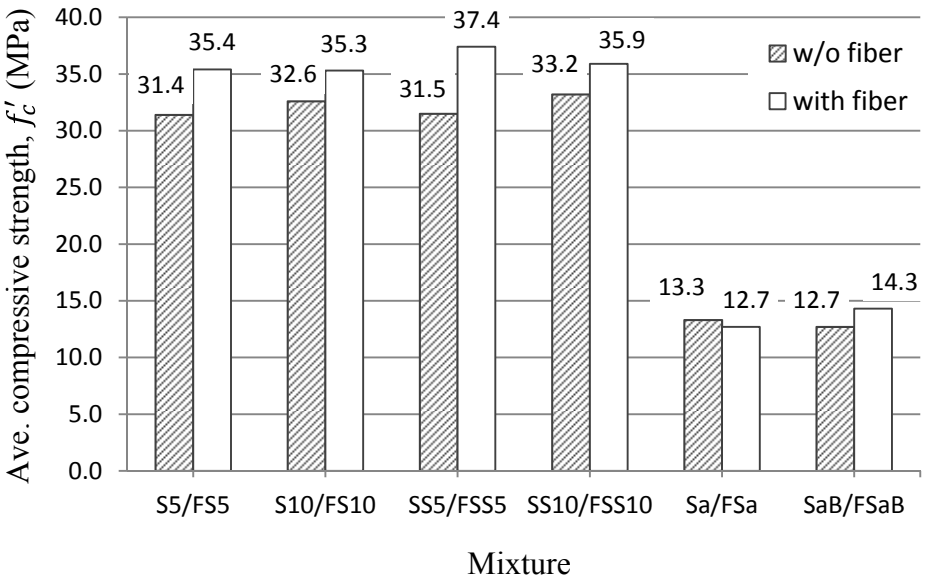

Figure 6-4: Cylinder compressive strength of MPPC concretes/wood composites at 90-day age

(w/b = 0.20 for FS5, FS10, FSS5 and FSS10; w/b = 0.36 for FSa and FSaB)

Table 6-4: Average cylinder strength of MPPC concretes/wood composites

Mix	**Average cylinder strength, f_c' MPa)**		**Coefficient of variation**	
	Without glass-fibers	With glass-fibers	Without glass-fibers	With glass-fibers
S5/FS5	31.4	35.4	0.039	0.060
S10/FS10	32.6	35.3	0.049	0.060
SS5/FSS5	31.5	37.4	0.038	0.071
SS10/FSS10	33.2	35.9	0.051	0.054
Sa/FSa	13.3	12.7	0.083	0.075
SaB/FSaB	12.7	14.3	0.047	0.055

It is observed that the typical failures of cylinders containing glass-fibers at the age of 90 days after casting were similar to those of specimens without glass-fibers as described in Section 5.3.2.1.

Similar to the test results obtained for mixes without glass-fibers, the compressive strengths for mixes containing glass-fibers varied depending on the

types of specimen tested as shown in Fig. 6-5. Compressive strengths from the two specimen types can be found in Table 6-5.

Figure 6-5 shows that, for mixes containing glass-fibers, the cube compressive strengths of all mixes but FSa were higher than their corresponding cylinder compressive strengths. This is similar to the result obtained for mixes without glass-fibers as described in Section 5.3.2.1.

The average cylinder compressive strength of mix FSa was slightly higher than its corresponding cube compressive strength. This is similar to the result described in Section 5.3.2.1 for mixes without glass-fibers.

Table 6-5 shows that the cylinder/cube compressive strength ratios varied from 0.69 to 1.06 for mixes with glass-fibers. For mixes without glass-fibers, those ratios varied from 0.88 to 1.90. Except for mixes FSa and FSaB, there was a small difference between the cylinder/cube compressive strength ratios obtained from mixes with or without glass-fibers.

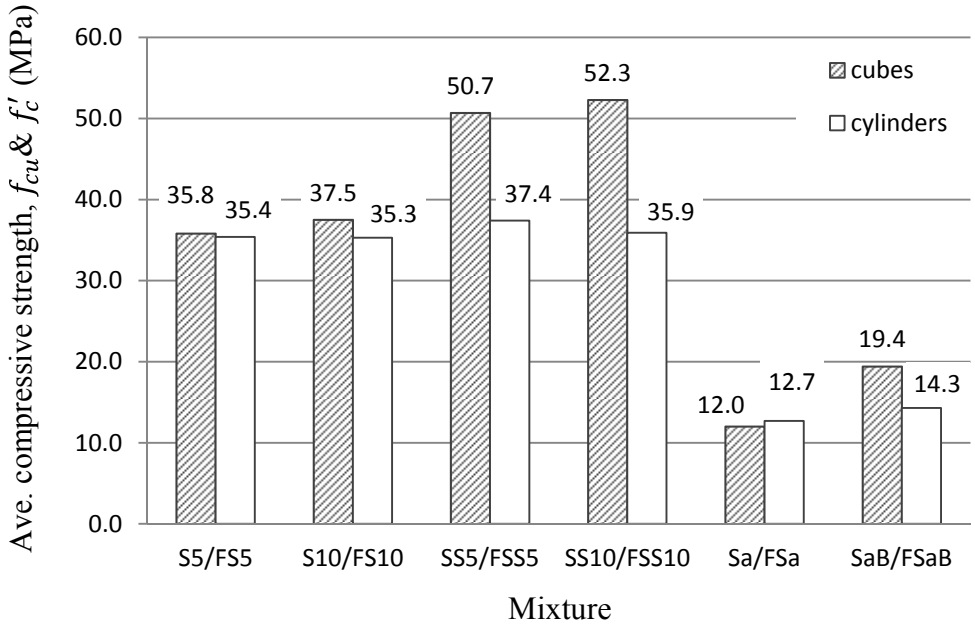

Figure 6-5: Cube and cylinder compressive strength of MPPC concretes/wood composites containing glass-fibers at 90-day age

(w/b = 0.20 for FS5, FS10, FSS5 and FSS10; w/b = 0.36 for FSa and FSaB)

Table 6-5: Average cube and cylinder compressive strength of MPPC concretes/wood composites containing glass-fibers

Mix	Average cube strength, f_{cu} (MPa)	Average cylinder strength, f'_c (MPa)	Cylinder/cube strength ratio (with fibers)	Cylinder/cube strength ratio (w/o fiber)
FS5	35.8	35.4	0.99	0.92
FS10	37.5	35.3	0.94	0.96
FSS5	50.7	37.4	0.74	0.76
FSS10	52.3	35.9	0.69	0.71
FSa	12.0	12.7	1.06	1.90
FSaB	19.4	14.3	0.74	0.88

6.3.2.2 Stress-strain relationship

The stress-strain relationship for MPPC concretes/wood composites containing chopped glass-fibers was determined based on the displacement (d_i) and the correponding load (P_i) as described in section 5.3.2.2.

The 90-day stress-strain curves for the six mixtures containing chopped glass-fibers are plotted in Figures 6-6 to 6-11. The average strains at peak stress (ε'_c) for these mixes are shown in Table 6-6. MPPC concretes had strains at peak stress of $2.99x10^{-3}$ to $3.96x10^{-3}$ (mm/mm). The increase in SF from 5% to 10% slightly decreased the strain of MPPC binders containing SF from $3.96x10^{-3}$ mm/mm (FS5) to $3.80x10^{-3}$ mm/mm (FS10). This trend is similar to mixes without glass-fibers as described in Section 5.3.2.2. For sand mortars containing SF, however, the increase in SF from 5% to 10% increased the strain from $2.99x10^{-3}$ mm/mm (FSS5) to $3.08x10^{-3}$ mm/mm (FSS10). This is also similar to the trend observed for sand mortars containing SF but without glass-fibers as described in Section 5.3.2.2.

MPPC wood composites containing glass-fibers had the highest strains at peak stress. Contrasting with MPPC wood composites without glass-fibers, the addition of 2% baking soda by total mass of the dry ingredients decreased the strains from $15.7x10^{-3}$ mm/mm (FSa) to $12.0x10^{-3}$ mm/mm (FSaB).

Table 6-6 compares the strains at peak stress for mixes with and without glass-fibers. Except for mixes FSS5 and FSS10, the strains at peak stress of all mixes increased when glass-fibers were added.

It can also be observed from Fig. 6-6 to 6-11 that the stress-strain response curves of mixes containing glass-fibers were similar to those of mixes without glass-fibers as described in Section 5.3.2.2.

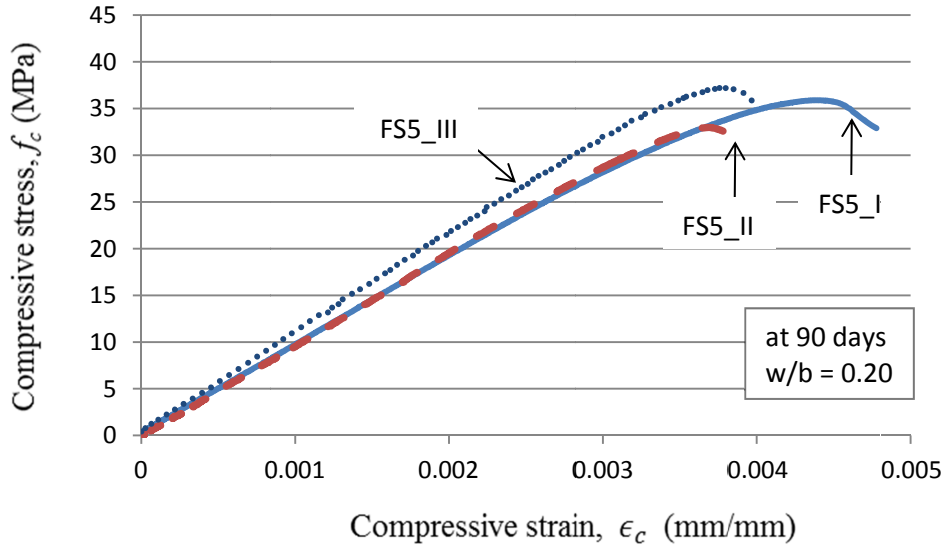

Figure 6-6: Compressive stress-strain response of mix FS5

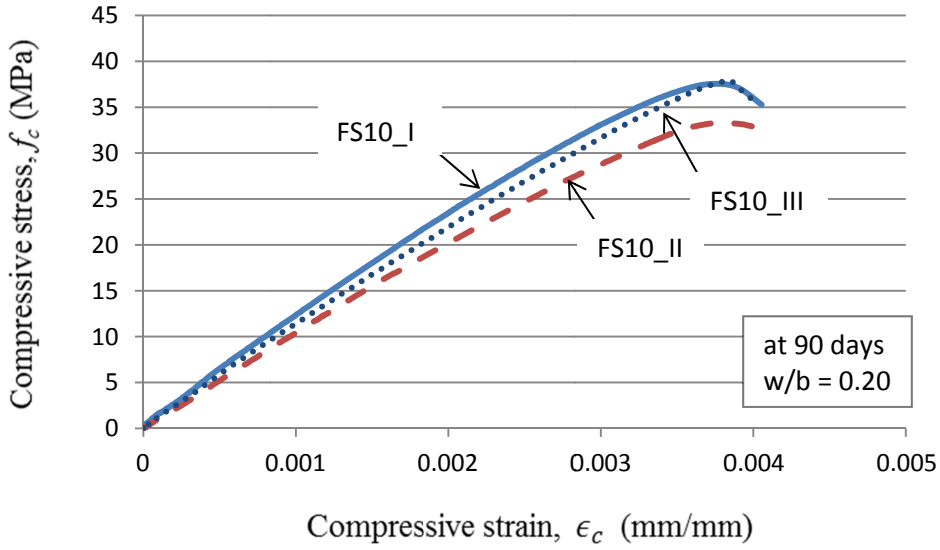

Figure 6-7: Compressive stress-strain response of mix FS10

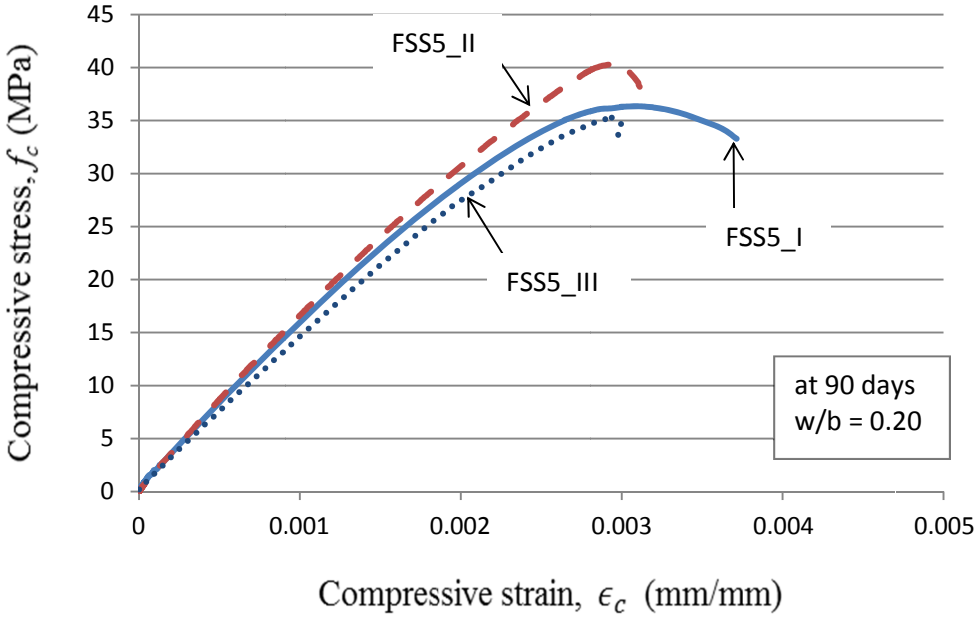

Figure 6-8: Compressive stress-strain response of mix FSS5

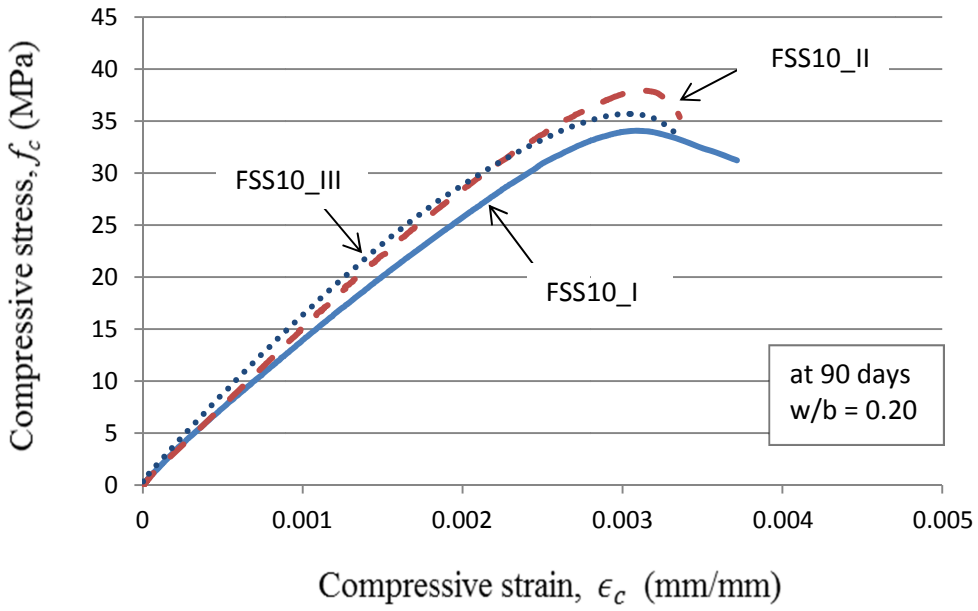

Figure 6-9: Compressive stress-strain response of mix FSS10

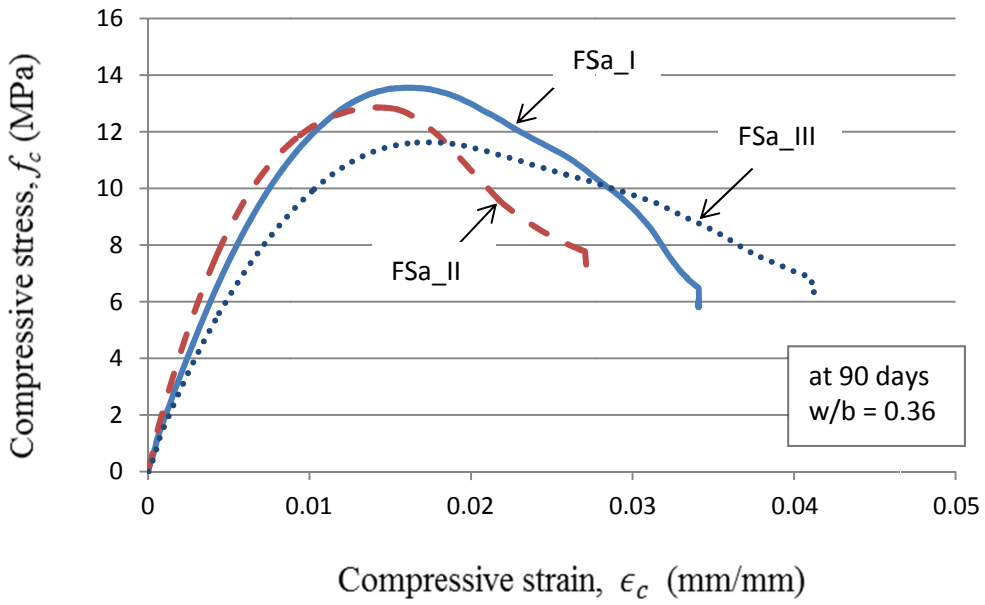

Figure 6-10: Compressive stress-strain response of mix Fsa

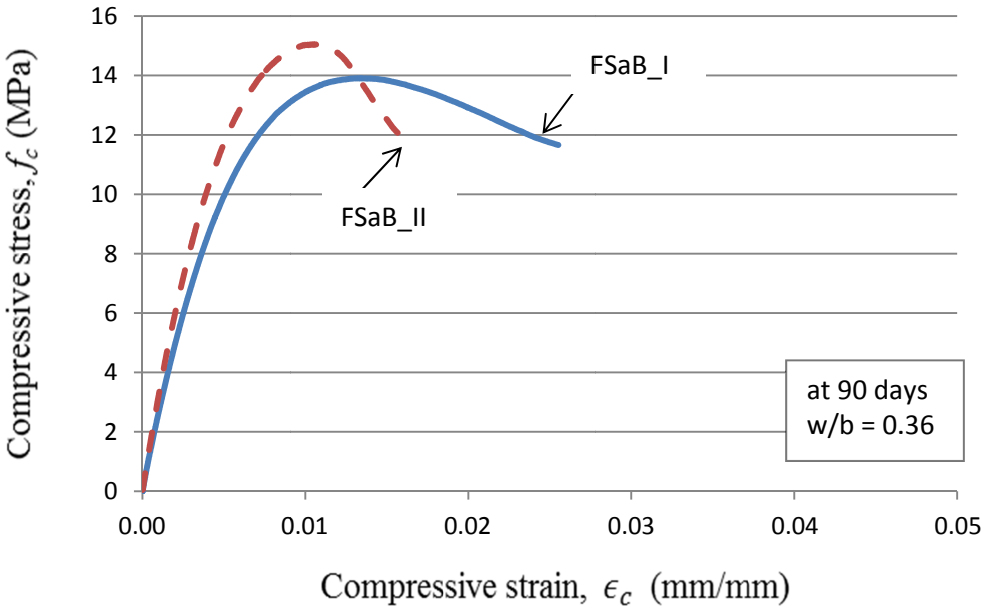

Figure 6-11: Compressive stress-strain response of mix FSaB

(FSaB_III is omitted for high deviation from the average strength)

Table 6-6: Average strain at peak stress of MPPC concretes/wood composites at 90 days

Mix	Average strain at peak stress, ε'_c (mm/mm)	
	Without glass-fibers	With glass-fibers
S5/FS5	3.72×10^{-3}	3.96×10^{-3}
S10/FS10	3.55×10^{-3}	3.80×10^{-3}
SS5/FSS5	3.17×10^{-3}	2.99×10^{-3}
SS10/FSS10	3.25×10^{-3}	3.08×10^{-3}
Sa/FSa	9.72×10^{-3}	15.70×10^{-3}
SaB/FSaB	10.00×10^{-3}	12.00×10^{-3}

6.3.2.3 Modulus of elasticity

The secant modulus of elasticity (*E*) of MPPC concretes/wood composites containing chopped glass-fibers was determined from the cylinder tests as described in Section 5.3.2.3.

Table 6-7 shows the average values of *E* at 90 days for mixtures with and without glass-fibers. Values of *E* for each specimen can be found in Appendix C. For mixes containing glass-fibers, it can be seen that sand mortars containing SF had the highest values of *E*. The increase in SF from 5% to 10% decreased the values of *E* for sand mortars containing SF from 16.02 to 15.51 GPa but increased those for MPPC binders containing SF from 9.58 to 11.56 GPa. These trends are similar to MPPC concretes without glass-fibers.

MPPC wood composites had the lowest values of *E*. The addition of 2% baking soda by total mass of the dry ingredients increased the values of *E* from 1.78 to 2.69 GPa. This contrasts to MPPC wood composites without glass-fibers where the addition of baking soda resulted in a decrease in modulus of elasticity.

It can also be observed in Table 6-7 that the moduli of elasticity of all mixtures, except for FSa, increased when glass-fibers were added.

Table 6-7: Average modulus of elasticity of MPPC concretes/wood composites at 90 days

Mix	Average modulus of elasticity, E (GPa)	
	Without glass-fibers	With glass-fibers
S5/FS5	8.47	9.58
S10/FS10	9.28	11.56
SS5/FSS5	12.23	16.02
SS10/FSS10	12.16	15.51
Sa/FSa	2.86	1.78
SaB/FSaB	2.32	2.69

The relationship between the modulus of elasticity and the cylinder compressive strength of mixtures with and without glass-fibers was plotted in Fig. 6-12. The figure shows that the modulus of elasticity increased as the cylinder compressive strength increased.

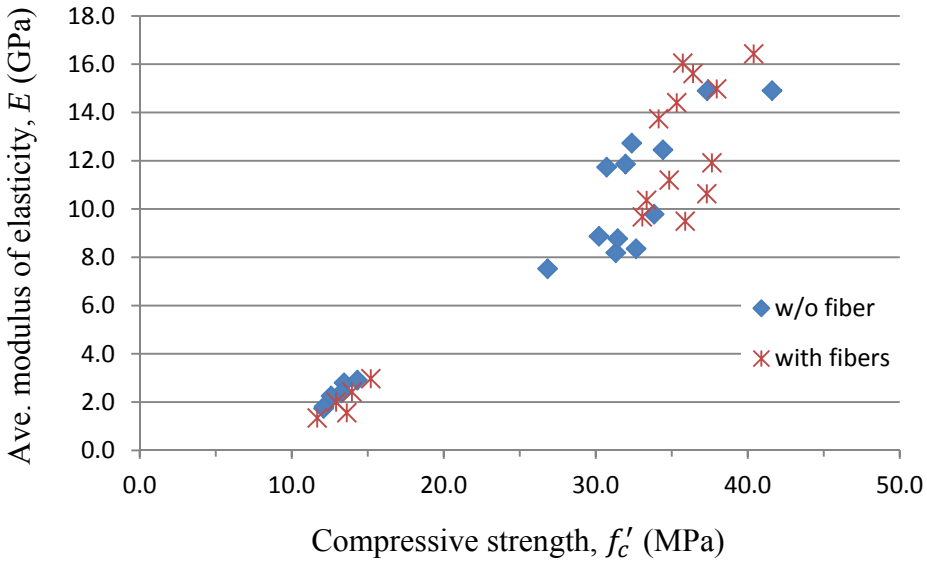

Figure 6-12: Modulus of elasticity vs. compressive strength of MPPC concretes/wood composites with and without fibers

Equations by ACI 213 (2009) and Tassew and Lubell (2011) used in Section 5.3.2.3 were employed again in this section. Table 6-8 compares the

values of modulus of elasticity obtained from the tests and predictions by Eqn. 5-5 and 5-6 for the six mixtures containing glass-fibers. The Test/Prediction ratios for modulus of elasticity can be found in Table 6-9.

It can be seen that the Tassew and Lubell model (Eqn. 5-6) gave better predictions for the values of E of MPPC concretes. However, Eqn. 5-6 did not show good predictions for MPPC wood composites. This is similar to the result obtained from Section 5.3.2.3 where Eqn. 5-6 also gave better predictions for the values of E of MPPC concretes without glass-fibers but resulted in poor predictions for E in MPPC concretes without glass-fibers.

Table 6-8: Average modulus of elasticity of MPPC concretes/wood composites containing glass-fibers at 90 days

Mix	**Average cylinder strength, f'_c (MPa)**	**Average density, γ (kg/m^3)**	**Average modulus of elasticity, E (GPa)**		
			From test	Predicted by Eqn. 5-5	Predicted by Eqn. 5-6
FS5	35.4	1670	9.58	17.46	12.58
FS10	35.3	1679	11.56	17.58	12.67
FSS5	37.4	1950	16.02	22.64	16.32
FSS10	35.9	1964	15.51	22.42	16.17
FSa	12.7	1289	1.78	7.09	5.11
FSaB	14.3	1453	2.69	9.01	6.49

Table 6-9: Test/Prediction ratios for modulus of elasticity of MPPC concretes/wood composites containing fibers

Mix	**Test/Predicted by Eqn. 5-5**	**Test/Predicted by Eqn. 5-6**
FS5	0.55	0.76
FS10	0.66	0.91
FSS5	0.71	0.98
FSS10	0.69	0.96
FSa	0.25	0.35
FSaB	0.29	0.41

6.3.3 Flexural properties

This section reports the test results used to determine the flexural properties of MPPC concretes/wood composites containing glass-fibers. Both prism and panel specimens were examined for the six mixtures considered. Comparisons are made to properties of the six similar mixes from chapter 5 that did not contain glass-fibers.

6.3.3.1 Flexural strength using prism specimens

Prism specimens containing chopped glass-fibers were tested using a 4-point bending setup. The flexural strength of prisms was calculated as the stress at the bottom fiber of the specimen produced by the maximum load applied as follows:

$$f_{b-pr} = \frac{PL}{bd^2} \qquad (5\text{-}7)$$

where f_{b-pr}= flexural strength at first crack of prism specimen (MPa)

P = maximum load indicated by the testing machine (N)

L = span length which is 150mm in this case

b, d = average width and depth (notch accounted) of prism, respectively (mm)

Three specimens were tested for each mix. The test results for each specimen can be found in Appendix C. The permissible range of variation between the test results was described in Section 5.3.3.1. In this section, only the prism flexural strengths for mixes S10, SS5, SS10 and SaB met this criterion. Thus, the prism flexural strengths for these mixes are the average strengths of three specimens in the same mix. Meanwhile, the prism flexural strengths for mixes S5 and Sa are the average strengths of two specimens in the same mix.

Figure 6-13 shows the average peak stress for the six mixtures considered. Figure 6-13 shows that when glass-fibers were added, the flexural strengths of all

mixes increased significantly compared to similar mixes without glass-fibers. The increase ranged from 51% (FSaB) to 325% (FS5).

For mixes containing glass-fibers, sand mortars containing SF exhibited the highest flexural strengths. The increase in SF from 5% to 10% slightly increased the flexural strengths of sand mortars containing SF from 4.8 MPa (FSS5) to 5.1 MPa (FSS10). However, the same increase in SF content decreased the flexural strength of MPPC binders containing SF from 3.4 MPa (FS5) to 3.0 MPa (FS10). This trend was different to the trend for MPPC concretes without glass-fibers as can be observed in Fig. 6-13.

MPPC wood composites containing glass-fibers exhibited relatively high flexural strengths when compared with the other mixes. This contrasts with the results obtained from the cube and cylinder tests for mixes with glass-fibers where the compressive strengths of MPPC wood composites containing glass-fibers were the lowest. The addition of 2% baking soda by total mass of the dry ingredients also increased the peak flexural stress for these mixes from 2.7 MPa (FSa) to 4.1 MPa (FSaB).

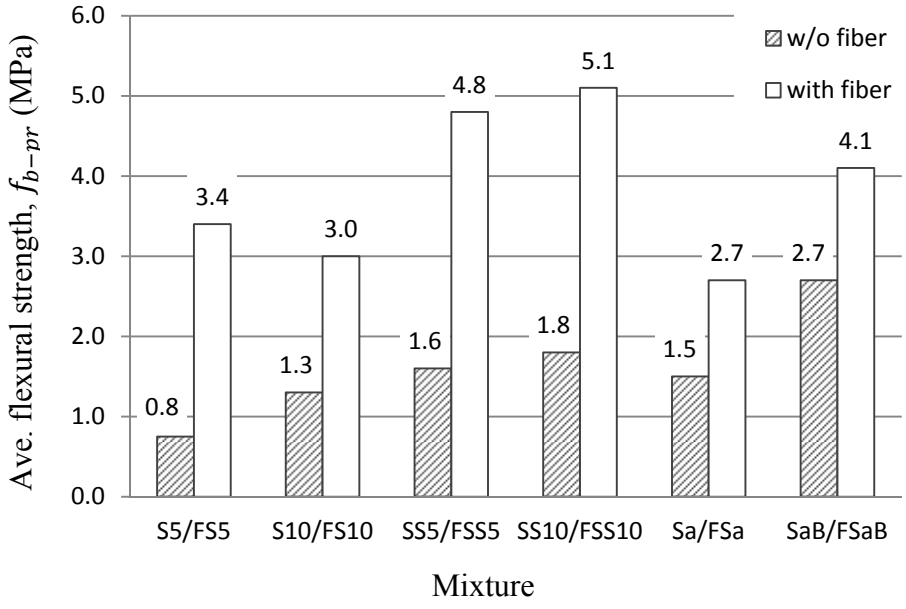

Figure 6-13: Flexural strength of prisms for MPPC concretes/wood composites

(w/b = 0.20 for FS5, FS10, FSS5 and FSS10; w/b = 0.36 for FSa and FSaB)

Table 6-10: Average flexural strength of prisms for MPPC concretes/wood composites at 90 days

Mix	Average flexural strength, f_{b-pr} (MPa)		Coefficient of variation	
	Without glass-fibers	With glass-fibers	Without glass-fibers	With glass-fibers
S5/FS5	0.8	3.4	0.087	0.153
S10/FS10	1.3	3.0	0.076	0.067
SS5/FSS5	1.6	4.8	0.004	0.056
SS10/FSS10	1.8	5.1	0.123	0.114
Sa/FSa	1.5	2.7	0.076	0.120
SaB/FSaB	2.7	4.1	0.044	0.074

The load-deflection behaviors of prisms made of MPPC concretes/wood composites containing chopped glass-fibers are shown in Figures 6-14 to 6-19. The mid-span deflections at the peak stress and the slopes obtained from the ascending branch of the load-deflection curves can be found in Table 6-11. The calculation for the slopes was described in Section 5.3.3.1.

It can be observed in Table 6-11 that, for all mixes containing glass-fibers, the load-deflection curves of sand mortars containing SF exhibited the steepest slopes and this is similar to the result described in Section 5.3.3.1 for sand mortars containing SF but without glass-fibers. The increase in SF from 5% to 10% decreased the slopes for sand mortars containing SF from 23.3 MPa/mm (FSS5) to 18.8 MPa/mm (FSS10). The same increase in SF content also decreased the slopes for MPPC binders containing SF from 14.0 MPa/mm (FS5) to 11.9 MPa/mm (FS10). This contrasts to the result obtained for mixes without glass-fibers as can be seen in Table 6-12.

For MPPC wood composites containing glass-fibers, the addition of 2% baking soda by mass increased the slope of these mixes from 8.1 MPa/mm (FSa) to 10.5 MPa/mm (FSaB). This trend is similar to that of MPPC wood composites without glass-fibers as shown in Table 6-12.

It can also be observed in Table 6-12 that when glass-fibers were added, the slopes of mixes containing 5% SF (i.e. FS5 and FSS5) and MPPC wood composites increased. At 10% SF by mass of the binder, the addition of glass-fibers decreased the slopes of mixes FS10 and FSS10.

The post-peak behaviors of all MPPC concretes/wood composites containing glass-fibers exhibited a softening behavior after the first flexural crack formed in the high bending moment region of the specimens as shown in Fig. 6-14 to Fig. 6-19. Comparing these softening behaviors with those of the corresponding mixes without glass-fibers in Section 5.3.3.1, the areas under the load-deformation curves of MPPC binders containing SF were larger when glass-fibers were added. The post-peak deflections shown in Fig. 6-14 and 6-15 were 2-3 times the corresponding deflections at peak stress for these mixes. Meanwhile, the prisms made of MPPC binders containing SF but without glass-fibers exhibited small post-peak deflections before they failed as can be observed in Fig. 5-16 and 5-17. This indicates that the specimens containing glass-fibers need more energy to fracture than the ones without fibers (Chen & Lui, 2005). The other four mixes showed negligible difference in post-peak behavior when glass-fibers were added.

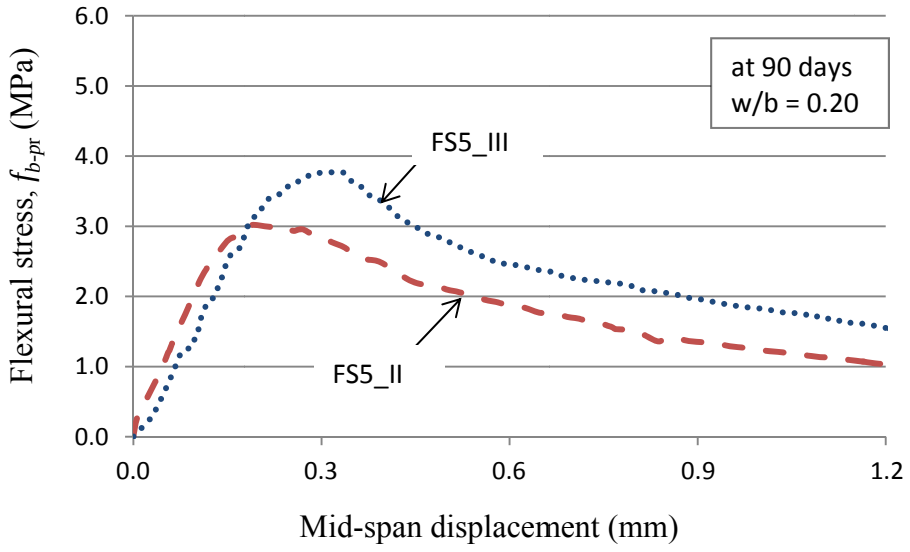

Figure 6-14: Flexural stress vs. mid-span displacement of prisms for mix FS5

(FS5_I is omitted for high deviation from the average strength)

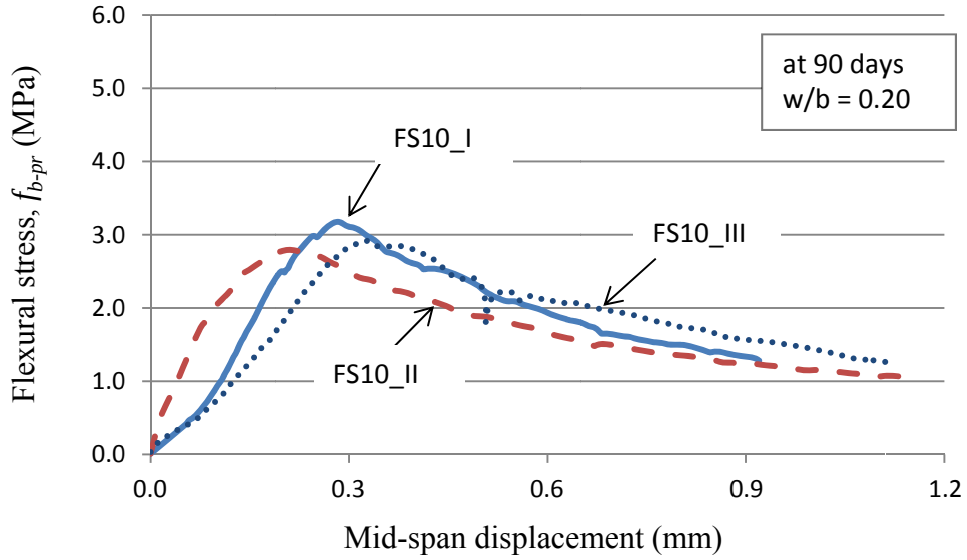

Figure 6-15: Flexural stress vs. mid-span displacement of prisms for mix FS10

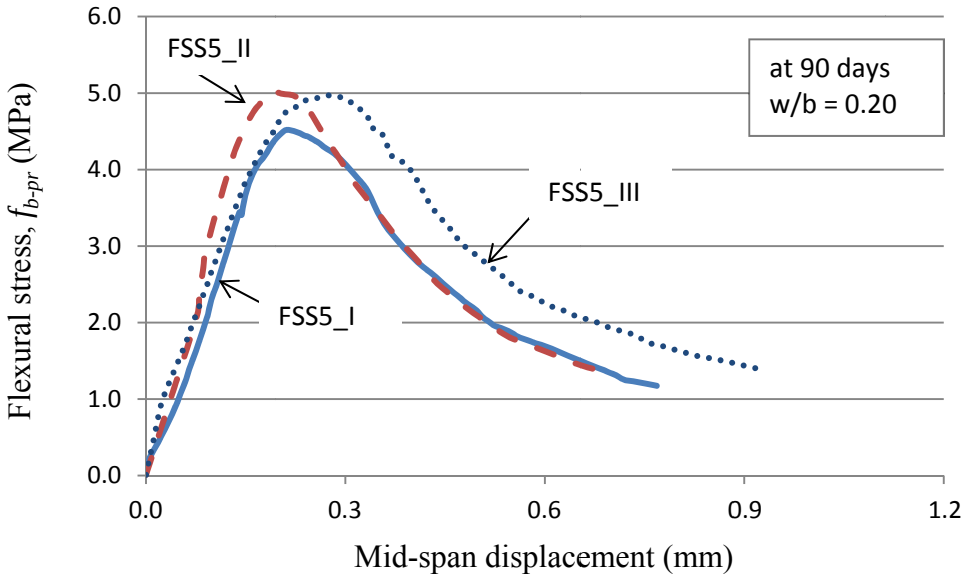

Figure 6-16: Flexural stress vs. mid-span displacement of prisms for mix FSS5

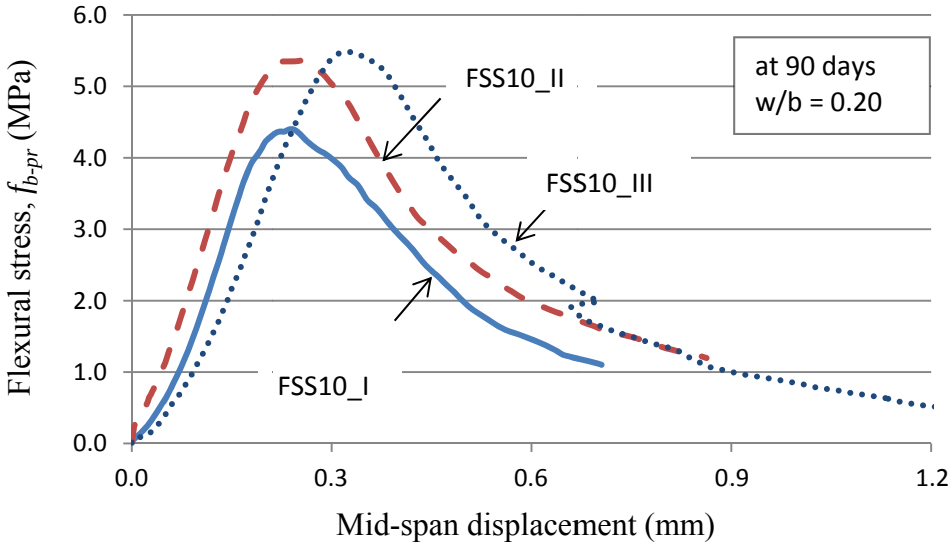

Figure 6-17: Flexural stress vs. mid-span displacement of prisms for mix FSS10

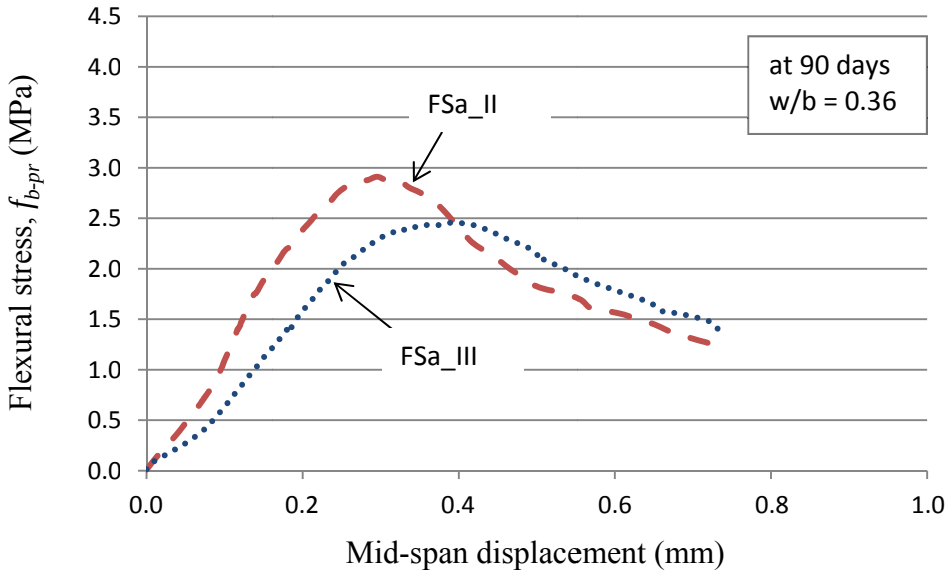

Figure 6-18: Flexural stress vs. mid-span displacement of prisms for mix FSa

(FSa_I is omitted for high deviation from the average strength)

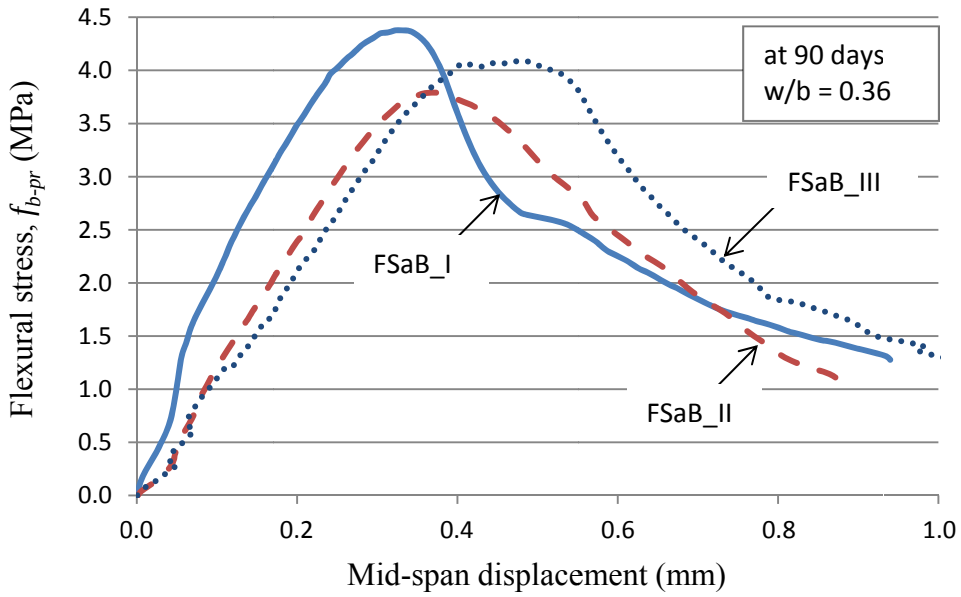

Figure 6-19: Flexural stress vs. mid-span displacement of prisms for mix FsaB

Table 6-11: Average flexural strength and mid-span deflection of prisms for MPPC concretes/wood composites containing glass-fibers at 90 days

Mix	$f_{b\text{-}pr}$ (MPa)	(MPa)	(mm)	Slope (MPa/mm)	$f_{b\text{-}pr}$/ (%)	
FS5	3.4	35.4	0.245	19.0	9.6	1/612
FS10	3.0	35.3	0.271	14.5	8.5	1/553
FSS5	4.8	37.4	0.227	25.9	12.8	1/660
FSS10	5.1	35.9	0.271	18.9	14.2	1/553
FSa	2.7	12.7	0.342	9.2	21.3	1/438
FSaB	4.1	14.3	0.392	14.9	28.7	1/382

$f_{b\text{-}pr}$: average flexural strength of prism; : average cylinder compressive strength; : average mid-span deflection; L: span length = 150 mm.

Table 6-12: Average mid-span displacement at peak stress of prisms for MPPC concretes/wood composites

Mix	Average mid-span displacement (mm)		Average slope (MPa/mm)		δ/L*	
	w/o glass-fibers	with glass-fibers	w/o glass-fibers	with glass-fibers	w/o glass-fibers	with glass-fibers
S5/FS5	0.101	0.245	8.7	19.0	1/1485	1/612
S10/FS10	0.088	0.271	14.7	14.5	1/1705	1/553
SS5/FSS5	0.078	0.227	19.9	25.9	1/1923	1/660
SS10/FSS10	0.077	0.271	25.4	18.9	1/1948	1/553
Sa/FSa	0.503	0.342	2.8	9.2	1/298	1/438
SaB/FSaB	0.383	0.392	6.9	14.9	1/391	1/382

* *L: span length = 150 mm.*

The flexural strengths of prisms for MPPC concretes containing glass-fibers ranged from 8.5% to 14.2% of the corresponding cylinder compressive strength. Meanwhile, the flexural strengths of MPPC wood composites containing glass-fibers ranged from 21.3% to 28.7% of the corresponding cylinder compressive strength. Equation 5-8 by ACI 213 (2009) and Eqn. 5-9 by Tassew and Lubell (2011) used in Section 5.3.3.1 were employed again in this section to express the relationship between the flexural strength and the cylinder compressive strength.

It can be seen in Table 6-13 and 6-14 that Eqn. 5-8 gave good predictions for MPPC binder containing SF (FS5 and FS10). Other predictions for sand mortars containing SF and MPPC wood composites either by Eqn. 5-8 or Eqn. 5-9 did not show good correlation with the test results.

Table 6-13: Average flexural strength of MPPC concretes/wood composites containing fibers from the prism tests and predictions

Mix	Average cylinder strength, f'_c (MPa)	Average flexural strength, $f_{b\text{-}pr}$ (MPa)		
		From test	Predicted by Eqn. 5-8	Predicted by Eqn. 5-9
FS5	35.4	3.4	2.7	2.0
FS10	35.3	3.0	2.7	2.0
FSS5	37.4	4.8	2.8	2.0
FSS10	35.9	5.1	2.7	2.0
FSa	12.7	2.7	1.6	1.2
FSaB	14.3	4.1	1.7	1.2

Table 6-14: Test/Prediction ratio for flexural strength of MPPC concretes/wood composites containing fibers

Mix	Test/Predicted by Eqn. 5-8	Test/Predicted by Eqn. 5-9
FS5	1.25	1.70
FS10	1.11	1.50
FSS5	1.71	2.40
FSS10	1.88	2.55
FSa	1.69	2.25
FSaB	2.41	3.41

6.3.3.2 Flexural strength using panel specimens

Panel specimens reinforced with textile glass-fibers were tested by the 3-point bending test. The mixes were similar to those used in Section 6.3.3.1 but did not contain the chopped glass-fibers. The flexural strength of each panel was determined based on the stress at the bottom fiber of the specimen produced by the load applied to cause the flexural crack (i.e. first loading peak) as follows:

$$f_{b-pa} = \frac{3PL}{2bd^2} \quad (5\text{-}10)$$

where f_{b-pa} = flexural strength at first peak of the panel specimen (MPa)

P = load corresponding to the first peak indicated by the tesing machine (N)

L = span length which is 450mm in this case

b, d = average width and depth of panel, respectively (mm)

The permissible range of variation between the test results was described in Section 5.3.3.2. In this section, only the panel flexural strengths for mixes S10, SS5 and SS10 met this criterion. Thus, the panel flexural strengths for these mixes are the average strengths of three specimens in the same mix. Meanwhile, the panel flexural strengths for mixes S5, Sa and SaB are the average strengths of two specimens in the same mix.

The test result for each specimen can be found in Appendix C. The average flexural strength at first peak for each mixture with and without textile glass-fibers is shown in Fig. 6-20. When the textile glass-fibers were added, panels with MPPC binders containing SF had the lowest flexural strengths. The increase in SF from 5% to 10% significantly increased the flexural strength for these panels from 1.9 MPa (FS5) to 3.5 MPa (FS10). The same increase in SF content also increased the flexural strength for panels with sand mortars containing SF from 5.5 MPa (FSS5) to 6.9 MPa (FSS10). This contrasts to the results obtained from the panel tests for MPPC concretes without textile glass-fibers as can be seen in Fig. 6-20.

Panels from MPPC wood composites reinforced with textile glass-fibers exhibited relatively high flexural strengths when compared with the panels using other mixes. The addition of 2% baking soda by total mass of the dry ingredients decreased the flexural strength from 5.8 MPa (FSa) to 4.9 MPa (FSaB). This trend contrasts to the trend for mixes without textile glass-fibers as can be observed in Fig. 6-20.

Figure 6-20 also shows that when the textile glass-fibers were added, the flexural strengths of all panels, except for those using mixes FS5 and FSaB, increased by 3% to 41%. Meanwhile, the addition of textile glass-fibers decreased

the flexural strengths of panels with FS5 and FSaB by 45% and 16%, respectively.

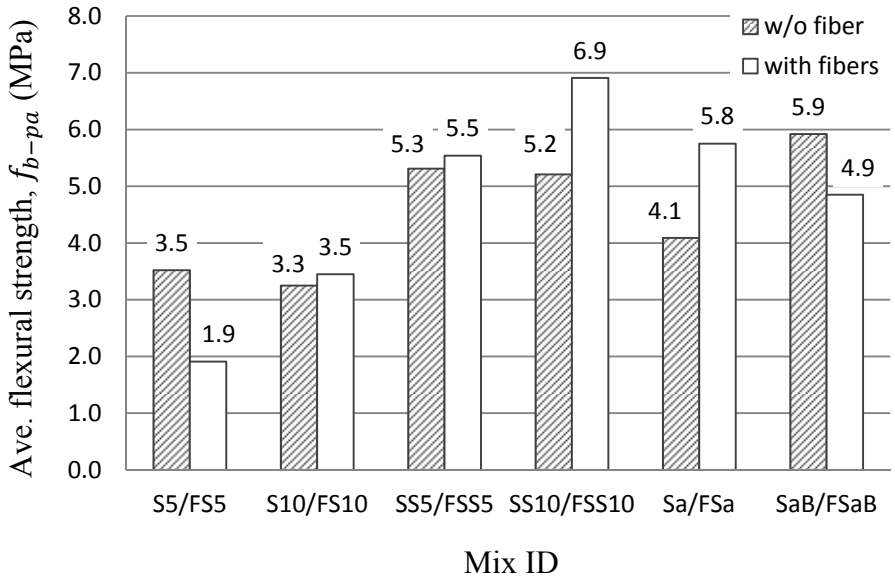

Figure 6-20: Flexural strength of panels for MPPC concretes/wood composites
(w/b = 0.20 for FS5, FS10, FSS5 and FSS10; w/b = 0.36 for FSa and FSaB)

Table 6-15: Average flexural strength of panels for MPPC concretes/wood composites at 90 days

Mix	**Average flexural strength, f_{b-pa} (MPa)**		**Coefficient of variation**	
	W/o textile glass-fibers	With textile glass-fibers	W/o textile glass- fiber	With textile glass-fibers
S5/FS5	3.5	1.9	0.154	0.005
S10/FS10	3.3	3.5	0.104	0.041
SS5/FSS5	5.3	5.5	0.023	0.103
SS10/FSS10	5.2	6.9	0.051	0.076
Sa/FSa	4.1	5.8	0.036	0.111
SaB/FSaB	5.9	4.9	0.035	0.075

The load-deflection behaviors of panels with MPPC concretes/wood composites reinforced with textile glass-fibers are shown in Fig. 6-21 to 6-26. The mid-span deflections at the first peak stress and the slopes obtained from the load-

deflection curves can be found in Table 6-16. The calculation for these slopes was described in Section 5.3.3.1.

It can be seen in Table 6-16 that panels with sand mortars containing SF resulted in the steepest slopes. The increase in SF from 5% to 10% increased the slopes for panels with sand mortars containing SF from 6.8 MPa/mm (FSS5) to 10.8 MPa/mm (FSS10). The same increase in SF content also increased the slopes for panels with MPPC binders containing SF from 2.3 MPa/mm (FS5) to 4.6 MPa/mm (FS10). This trend is similar to that of MPPC concretes without textile glass-fibers as described in Section 5.3.3.2.

For MPPC wood composite panels, the addition of 2% baking soda by mass increased the slope of these mixes from 2.0 MPa/mm (FSa) to 2.1 MPa/mm (FSaB).

The post initial-peak behaviors of all MPPC concretes/wood composites reinforced with textile-fabrics are shown in Fig. 6-21 to 6-26. After the first tension crack occurred at the initial peak, the specimens experienced additional deflection before the fabric was engaged to take significant load. A large deflection was needed before the load again reached the value corresponding to the initial peak. The average strengths lost after the first tension crack occurred are shown in Table 6-18. The mid-span displacements at the initial peak and when the load again reached the value corresponding to the initial peak can also be found in Table 6-18.

It is observed that panels with mix FSS5 only exhibited a 12% strength loss and it rapidly gained strength after that. Meanwhile, the strength loss and the deflection after the initial peak were significant for the panels with other mix type. This indicates that the fabrics only had sufficient stiffness to maintain the performance after initial peak for mix FSS5.

The flexural strengths of MPPC concrete panels reinforced with the textile glass-fibers ranged from 5% to 19% of the corresponding fiber-containing-cylinder compressive strengths. They also ranged from 6% to 21% of the

corresponding cylinder compressive strengths of mixes without glass-fibers. Meanwhile, the flexural strengths of MPPC wood composite panels reinforced with the textile glass-fibers were 34% to 46% of the corresponding fiber-containing-cylinder compressive strengths and were 39% to 44% of the corresponding cylinder compressive strengths of mixes without glass-fibers.

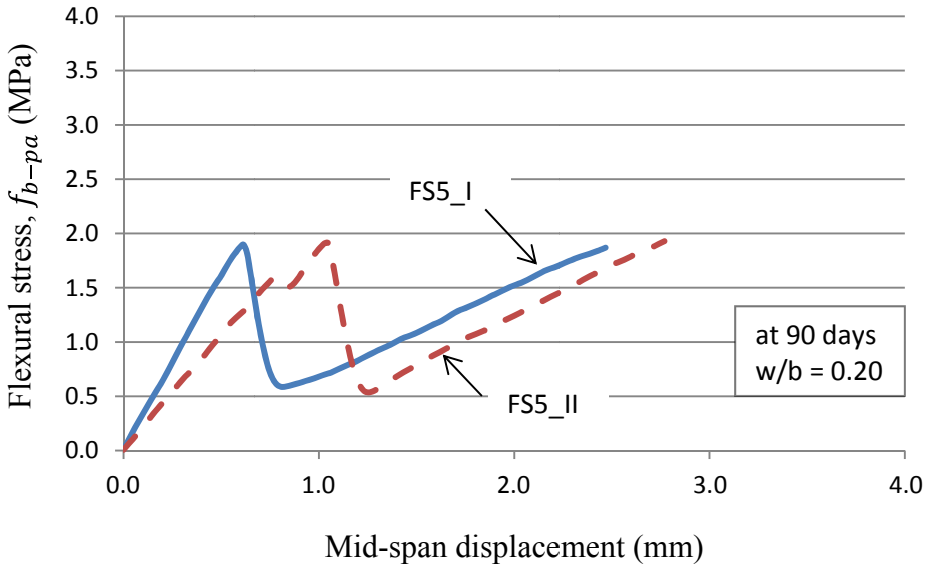

Figure 6-21: Flexural stress vs. mid-span displacement of panels for mix FS5

(FS5_III is omitted for high deviation from the average strength)

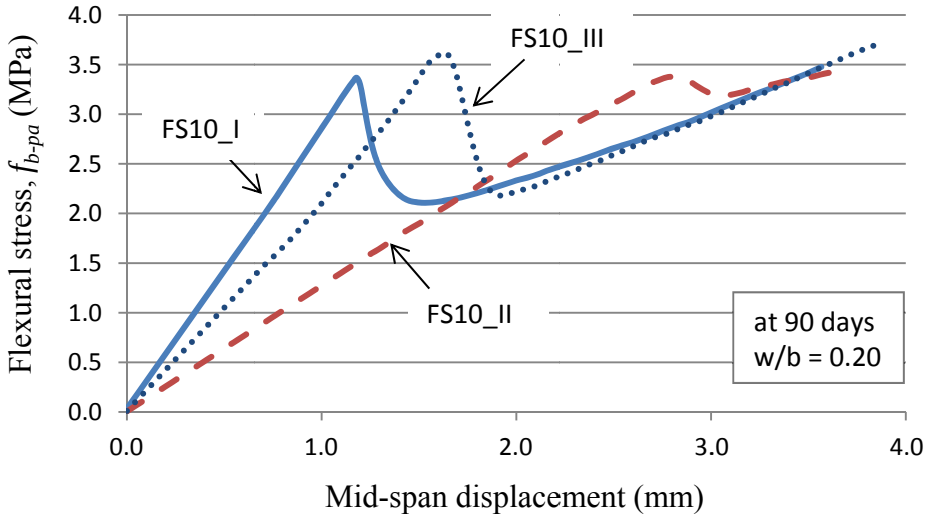

Figure 6-22: Flexural stress vs. mid-span displacement of panels for mix FS10

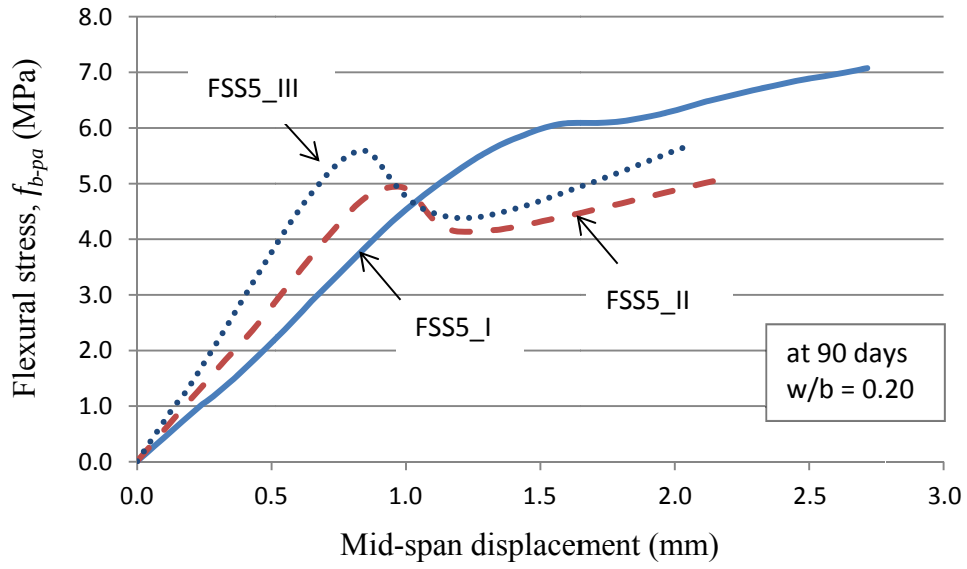

Figure 6-23: Flexural stress vs. mid-span displacement of panels for mix FSS5

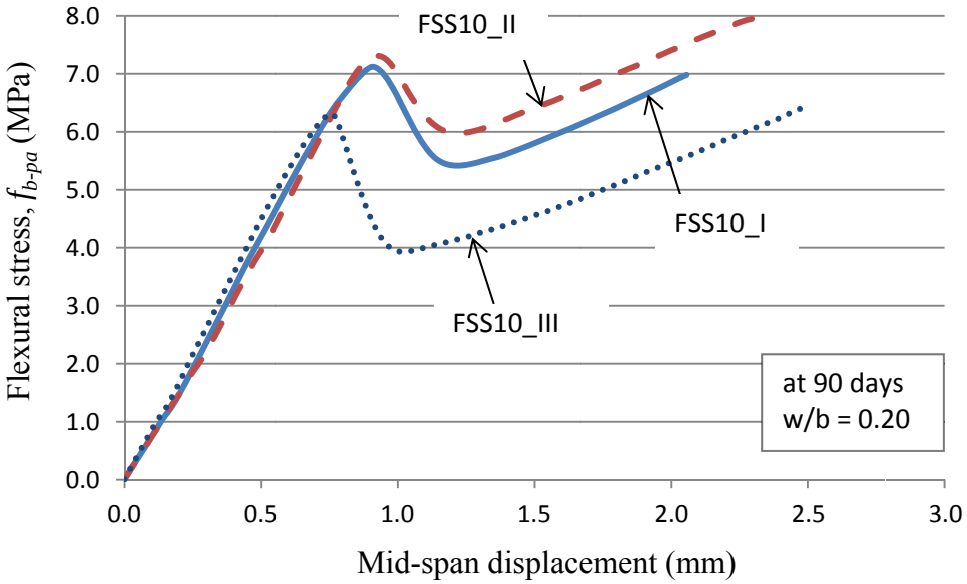

Figure 6-24: Flexural stress vs. mid-span displacement of panels for mix FSS10

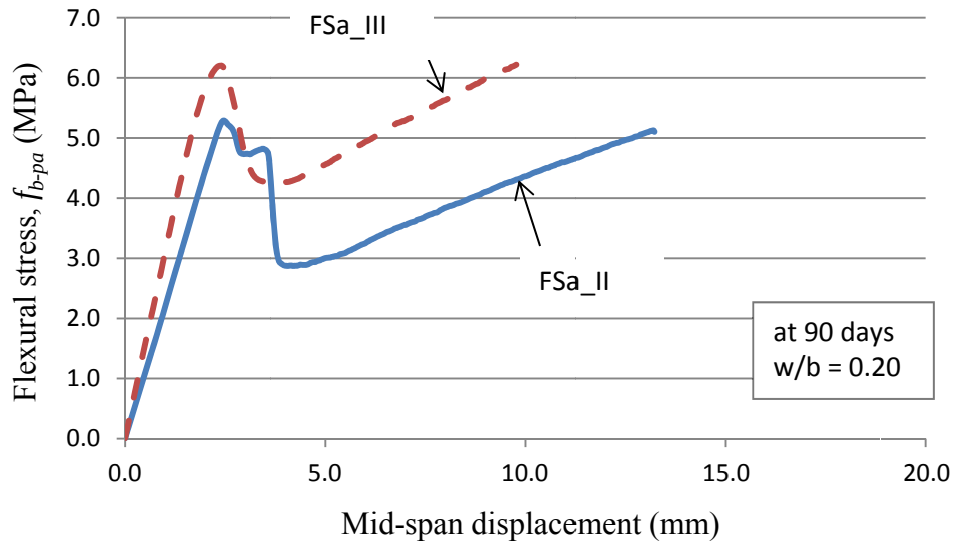

Figure 6-25: Flexural stress vs. mid-span displacement of panels for mix FSa

(FSa_I is omitted for high deviation from the average strength)

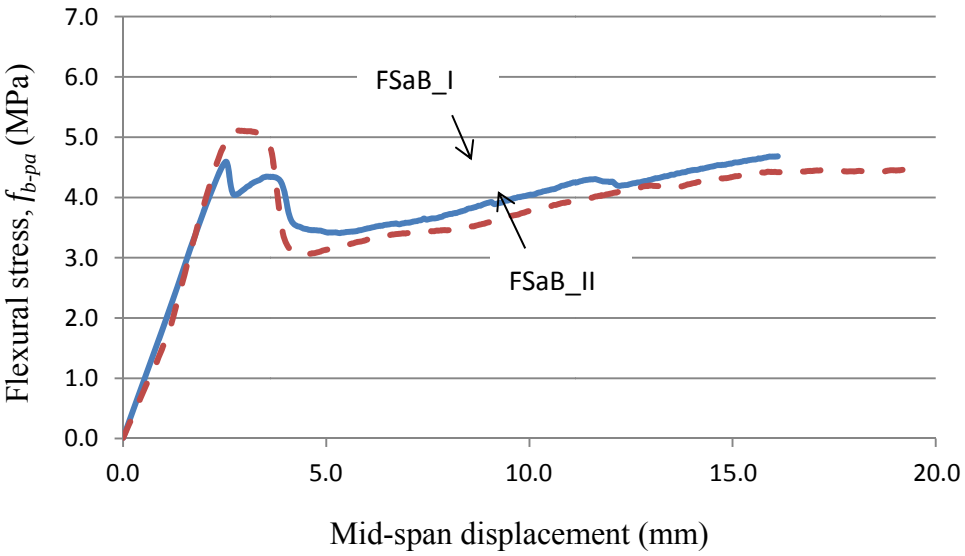

Figure 6-26: Flexural stress vs. mid-span displacement of panels for mix FSaB

(FSa_III is omitted for high deviation from the average strength)

Table 6-16: Average flexural strength and mid-span deflection from the panel tests of MPPC concretes/wood composites reinforced with textile glass-fibers

Mix	$f_{b\text{-}pa}$ (MPa)	f'_c (MPa)	δ (mm)	Slope (MPa/mm)	$f_{b\text{-}pa}/f'_c$ (%)	δ/L
FS5	1.9	35.4	0.831	2.7	5.4	1/270
FS10	3.5	35.3	1.900	1.5	9.9	1/236
FSS5	5.5	37.4	1.586	2.2	14.7	1/283
FSS10	6.9	35.9	0.867	4.3	19.2	1/519
FSa	5.8	12.7	2.436	2.6	45.7	1/184
FSaB	4.9	14.3	2.680	1.8	34.3	1/168

$f_{b\text{-}pa}$: average flexural strength of panel; f'_c: average cylinder compressive strength; δ: average mid-span deflection; L: span length = 450 mm;

Table 6-17: Average mid-span displacement at initial peak from the panel tests of MPPC concretes/wood composites with and without textile glass-fabrics

Mix	Average mid-span displacement (mm)		δ/L	
	W/o textile glass-fabrics	With textile glass-fabrics	W/o textile glass-fabrics	With textile glass-fabrics
S5/FS5	1.129	0.831	1/398	1/270
S10/FS10	0.993	1.900	1/453	1/236
SS5/FSS5	0.998	1.586	1/450	1/283
SS10/FSS10	0.808	0.867	1/556	1/519
Sa/FSa	3.329	2.840	1/135	1/184
SaB/FSaB	3.184	2.388	1/141	1/168

L: span length = 450 mm.

Table 6-18: Effect of textile glass-fabrics on the post-initial-peak strength gain of MPPC concretes/wood composites

Mix	Average strength lost after initial peak (%)	Average mid-span displacement (mm)		δ_2/δ_1
		δ_1*	δ_2**	
FS5	68	0.831	2.578	3.1
FS10	26	1.900	3.802	2.0
FSS5	12	1.586	2.462	1.6
FSS10	26	0.867	2.279	2.6
FSa	38	2.840	13.604	4.8
FSaB	30	2.388	-	-

δ_1: average mid-span displacement at initial peak

**δ_2: average mid-span displacement when the load reached the corresponding initial peak again*

Table 6-19 compares the flexural strengths obtained from the tests and predictions by Eqn. 5-8 and Eqn. 5-9 for the six mixtures considered. The ratios of Test/Prediction values for flexural strength can be found in Table 6-20. It can be seen that the Tassew and Lubell model (Eqn. 5-9) gave the best prediction for mix FS5. Other predictions by either the ACI 213 model (Eqn. 5-8) or the Tassew and Lubell model (Eqn. 5-9) showed a significant difference with the test results.

Table 6-19: Average flexural strength of MPPC concretes/wood composites reinforced with textile glass-fibers from the panel tests and predictions

Mix	Average cylinder compressive strength, f'_c (MPa)	Average flexural strength, $f_{b\text{-}pa}$ (MPa)		
		From test	Predicted by Eqn. 5-8	Predicted by Eqn. 5-9
FS5	35.4	1.9	2.7	2.0
FS10	35.3	3.5	2.7	2.0
FSS5	37.4	5.5	2.8	2.0
FSS10	35.9	6.9	2.7	2.0
FSa	12.7	5.8	1.6	1.2
FSaB	14.3	4.9	1.7	1.2

Table 6-20: Test/Prediction ratio for flexural strength of MPPC concretes/wood composites reinforced with textile glass-fibers

Mix	Test/Predicted by Eqn. 5-8	Test/Predicted by Eqn. 5-9
FS5	0.70	0.95
FS10	1.29	1.75
FSS5	1.96	2.75
FSS10	2.55	3.45
FSa	3.62	4.83
FSaB	2.88	4.08

6.4 Summary

The following conclusions can be drawn from this chapter:

- Fresh mixtures of MPPC concretes containing chopped glass-fibers exhibited good slump flow property. The increase in SF content decreased the slump flow for these mixes. The addition of chopped glass-fibers decreased the slump flow of sand mortars containing SF. Fresh mixtures of MPPC wood composites containing glass-fibers did not exhibit flow property but they were still workable.
- The addition of chopped glass-fibers had negligible effect on the densities of all mixes.
- The addition of chopped glass-fibers increased the compressive strength for all mixes. The highest improvement occurred for mix FSS5 at 19% compared to similar mix without fibers.
- The strains at peak stress of MPPC binders containing SF and MPPC wood composites were higher when chopped glass-fibers were added. The increase in SF content decreased the strains at peak stress for MPPC binders containing SF and MPPC wood composites.
- The modulus of elasticity of all mixes except FSa increased by 13% to 31% when chopped glass-fibers were added. An increase in SF content increased the modulus of elasticity of MPPC binders containing SF but

decreased those of sand mortars containing SF. The addition of baking soda increased the modulus of elasticity of MPPC wood composites. The model of Tassew and Lubell (2011) gave good predictions for modulus of elasticity of MPPC concretes.

- The flexural strengths of MPPC concretes/wood composites from the prism tests significantly increased as the chopped glass-fibers were added. The flexural strengths were about 9% to 29% of the corresponding cylinder compressive strengths. The increase in SF content decreased the flexural strengths of prisms for MPPC binders containing SF but increased those for sand mortars containing SF. The addition of baking soda increased the flexural strengths of MPPC wood composites. The model of ACI 213 (2009) gave good predictions for flexural strengths of MPPC binders containing SF.
- The flexural strengths from the panel tests of all mixes, except for FS5 and FSaB, increased as the textile glass-fibers were added. The flexural strengths of the panels were much higher than those of the prisms and were about 5% to 46% of the corresponding cylinder compressive strengths. An increase in SF content increased the flexural strengths of both MPPC binders containing SF and sand mortars containing SF. Meanwhile, the addition of baking soda decreased the flexural strengths of MPPC wood composites. The equation by Tassew and Lubell (2011) gave good prediction for mix FS5.

Chapter 7 CONCLUSIONS

The main objective of this research program was to develop and then characterize the basic mechanical properties of MPPC concretes/wood composites. An understanding of these properties will allow future investigation of potential commercial application of these materials as part of structural systems.

In this research, a comprehensive laboratory program was conducted at the University of Alberta which included: 1) Trial mix development to find candidate mixtures for MPPC concretes/wood composites; 2) Characterization of the fresh and hardened properties of MPPC concretes/wood composites; 3) Characterization of the fresh and hardened properties of MPPC concretes/wood composites reinforced with chopped glass fibers or textile glass fibers. A total of 456 cube, 36 cylinder, 36 prism and 36 panel specimens were cast and tested in this laboratory program.

This chapter summarizes the results obtained from this research program.

7.1 Conclusions from the trial mix program

The trial mixes of MPPC concretes/wood composites were developed and evaluated for compression strength and workability. Based on the results obtained from these trial mixes, six mixtures were chosen for further study. The following conclusions can be drawn from this trial mix program:

- The increase in *w/b* ratio increased the workability but reduced both the density and the compressive strength of MPPC concretes/wood composites. MPPC concretes and MPPC wood composites with *w/b* ratios of 0.20 and 0.36, respectively, were found to exhibit good workability and compressive strength.

- Delvo Stabilizer at 2% by total mass of the binder was found to effectively retard the setting times and allow enough working time for MPPC concretes/wood composites.
- MPPC concretes/wood composites had a rapid strength gain at early ages up to 28 days after casting. After 28 days, the compressive strength development was insignificant.
- Addition of bentonite at up to 1% by total mass of the binder increased the compressive strength of MPPC binders. Changes in bentonite content had negligible influence on the workability of fresh mixtures and the density of hardened MPPC concretes.
- Addition of SF in MPPC concretes increased the compressive strength gain at early ages and gave higher compressive strengths than mixes without SF. An increase in SF content increased the compressive strength of MPPC concretes containing SF but the effect was negligible when the SF content exceeded 10% by total mass of the binder. The addition of SF visibly increased the viscosity and decreased the setting time of MPPC concretes containing SF.
- MPPC sand mortars containing SF had lower strength than MPPC binders containing SF. Changes in sand type had negligible influence on the compressive strength of MPPC sand mortars containing SF.
- The addition of baking soda decreased the compressive strength and the density of MPPC sand mortars. Baking soda improved the flowability and workability of the fresh mixtures; however, it caused swelling after the mixing and shrinkage after the setting of the fresh mixtures. When baking soda was used at 1% by total mass of the dry mix, adding 10% more sand by mass of the binder resulted in a reduction of the compressive strength of MPPC sand mortars by 5-6.5%.
- The increase in FA content from 20 to 40% by total mass of the binder plus FA decreased the compressive strength of MPPC wood composites. The highest compressive strength was obtained with 20% FA by total mass of the binder and FA.

- When baking soda was used in MPPC wood composite mixtures, an increase in baking soda content from 1 to 3% by total mass of the dry mix resulted in increases in both the compressive strength and density. There was some shrinkage observed for mixes that used 3% baking soda by total mass of the dry mix.

7.2 Conclusions for the expanded study of MPPC concretes/wood composite properties

Based on the results from the trial mix program, six mixtures of MPPC concretes/wood composites were further studied. Workability, setting time, compression and flexural properties were evaluated. The conclusions for this study program are as follows:

- Fresh MPPC concretes exhibited good slump flow property. The increase in SF content from 5% to 10% by total mass of the binder decreased the slump flow for these mixtures. Fresh MPPC wood composites exhibited a reasonable workability though they did not flow.
- Delvo Stabilizer at 2% by total mass of the binder was found to be a better retarder for MPPC concretes/wood composites compared with Borax or Lignosulphonate if the application requires an extended finishing time.
- The increase in SF content from 5% to 10% by total mass of the binder increased the setting time of sand mortars containing SF but decreased that of MPPC binders containing SF. The addition of baking soda decreased the setting time of MPPC wood composites.
- The compressive strength of MPPC concretes/wood composites increased as their density increased. The increase in SF content had negligible influence on the densities of MPPC concretes. Meanwhile, the addition of 2% baking soda by total mass of the dry mix slightly increased the densities of MPPC wood composites.
- The increase in SF content had negligible influence on the compressive strengths of MPPC concretes. The addition of baking soda increased the

cube compressive strengths but decreased the cylinder compressive strengths of MPPC wood composites.

- The increase in SF content increased the modulus of elasticity of MPPC binders containing SF and the modulus of rupture of prisms for all mixes. Meanwhile, that increase in SF content decreased the strain at peak stress of MPPC binders containing SF, the modulus of elasticity of sand mortars containing SF and the modulus of rupture of panels for all mixes.
- The addition of baking soda increased the strain at peak stress and the modulus of rupture of MPPC wood composites. However, it decreased the modulus of elasticity of MPPC wood composites.

7.3 Conclusions for the expanded study of MPPC concretes/wood composites reinforced with glass-fibers and textile glass-fibers

The six of MPPC concretes/wood composite mixtures used in chapter 5 were reinforced with glass-fibers and textile glass-fabrics for further study. Workability, setting time, compression and flexural properties were evaluated. The conclusions for this study program are as follows:

- Fresh MPPC concretes containing chopped glass-fibers exhibited good slump flow property. The addition of 1% glass-fibers by total mass of the mix decreased the slump flow of sand mortars containing SF. The increase in SF content from 5% to 10% by mass of the binder also decreased the slump flow for MPPC concretes containing glass-fibers. Fresh MPPC wood composites containing glass-fibers had reasonable workability though they do not flow.
- The addition of 1% glass-fibers by total mass of the mix had negligible effect on densities of all mixes.
- The addition of 1% glass-fibers by total mass of the mix increased the strains at peak stress, the modulus of elasticity, the compressive strength, and the flexural strength of the MPPC binders containing SF and MPPC wood composites.

- When glass-fibers were added at 1% by mass, the increase in SF content increased the modulus of elasticity of MPPC binders containing SF, the flexural strength of prisms for sand mortars containing SF, and the flexural strength of panels for all mixes containing SF. However, it decreased the modulus of elasticity of sand mortars containing SF and the flexural strength of prisms for MPPC binders containing SF.
- The addition of 2% baking soda by total mass of the dry mix increased the modulus of elasticity and the flexural strengths of prisms for MPPC wood composites containing fibers. Meanwhile, it decreased the strain at peak stress and the flexural strength of panels for MPPC concretes containing fibers.

7.4 Future research

Based on the findings of the basic characteristics of MPPC concretes/wood composites, it is recommended that future research should investigate the following:

- Other properties of hardened MPPC concretes/wood composites should be evaluated including the water absorption, shrinkage and coefficient of thermal expansion.
- The potential use of MPPC concretes/wood composites in severe environmental conditions should be evaluated through durability tests. Examples include freeze and thaw resistance, chloride penetration resistance, abrasion resistance and fracture toughness under impact loading.
- Other aggregates (e.g. gravel, light weight aggregates) should be trialed with MPPC concretes/wood composites in order to reduce the unit cost and the density of the products.
- The bond strength between MPPC concretes/wood composites with Portland cement concretes should be evaluated for application in the repair or strengthening of existing concrete structures.

- The bond characteristic between MPPC concretes/wood composites with steel reinforcement should be evaluated to examine the viability of use of steel reinforcement in MPPC concretes/wood composites
- Chopped glass-fibers of different lengths and other types of textile glass-fabrics should be examined to optimize the performance of MPPC concretes/wood composites reinforced with fibers.
- Alternative fabric materials of higher stiffness should be trialed with panels using MPPC concretes/wood composites.

REFERENCES

BS 1881:Part 115:1986, Testing concrete. Specification for compression testing machines for concrete. (1986). British Standards Institution.

ASTM C469-02, Standard Test Method for Static Modulus of Elasticity and Poisson's Ratio of Concrete in Compression. (2002). ASTM International.

ASTM C136-06, Standard Test Method for Sieve Analysis of Fine and Coarse Aggregate. (2006). ASTM International.

ASTM C1437-07, Standard Test Method for Flow of Hydraulic Cement Mortar. (2007). ASTM International.

ASTM C191-08, Standard Test Methods for Time of Setting of Hydraulic Cement by Vicat Needle. (2008). ASTM International.

ASTM C230/C230M-08, Standard Specification for Flow Table for Use In Test of Hydraulic Cement. (2008). ASTM International.

ASTM C29/C29M-09 Standard test method for bulk density ("unit weight") and voids in aggregate. (2009). ASTM International.

ASTM C39/C39M-09, Standard Test Method for Compressive Strength of Cylindrical Concrete Specimens. (2009). ASTM International.

ASTM C617-10, Standard Practice for Capping Cylindrical Concrete Specimens. (2010). ASTM International.

ASTM C78/C78M-10, Standard test method for flexural strength of concrete (using simple beam with third point loading). (2010). ASTM International.

ASTM C109/C109M-12, Standard test method for compressive strength of hydraulic cement mortars (using 2-in. or [50mm] cube specimens). (2012). ASTM International.

ACI Committe 213. (n.d.). Guide for Structural Lightweight-Aggregate Concrete (ACI 213R-03). In *ACI Manual of Concrete Practice (2009 Part 1)* (pp. 1-20). American Concrete Institute, Farmington Hills, MI 2009.

ACI Committee 116. (1990). *ACI 116R-90, Cement and Concrete Terminology.* American Concrete Institue.

ACI Committee 234. (2006). *ACI 234R-06. Guide for the use of Silica Fume in concrete.* American Concrete Institue.

Ando, J., Shinada, T., & Hiraoka, G. (1974). Reactions of Monoaluminum Phosphate with Alumina and Magnesia. *Yogyo-Kyokai-Shi*, 644-649.

ASTM International. (2003). ASTM Manual of aggregate and concrete testing. In *Annual Book of ASTM Standards* (Vol. 4.02). ASTM International.

Banthia, N., & Sheng, J. (1996). Fracture toughness of micro-fiber reinforced cement composites. *Cement and Concr. Compo., 18*(4), pp. 251-269.

Bentur, A., & Mindess, S. (1990). *Fiber reinforced cementitious composites.* London: Elsevier Applied Science.

Borger, J., Carrasquillo, R. L., & Fowler, D. W. (1994, Nov). Use of Recycled Wash Water and Returned Plastic Concrete in the Production of Fresh Concrete. *Advance Cement Based Materials, 1*(6), pp. 267-274.

Carpinteri, A., & Chiaia, B. (2002, August). Embrittlement and Decrease of Apparent Strength in Large-Sized Concrete Structure. *Academy Proceedings in Engineering Sciences, 27* (4), pp. 425-448.

Chen, W. F., & Lui, E. M. (2005). High Performance Concrete. In W. F. Chen, & E. M. Lui, *Handbook of Structural Engineering* (pp. 23-24). CRC Press.

Collins, M. P., & Mitchell, D. (1997). Material Properties. In M. P. Collins, & D. Mitchell, *Prestressed Concrete Structures* (p. 61). Toronto and Montreal: Response Publication.

Dattel, C. D. (2002, Nov 26). *Patent No. US 6485561 B1.* United States.

Demotakis, E. D., Klemperer, W. G., & Young, J. F. (1992). Polyphosphate Chain Stability in Magnesia Polyphosphate Cements. *Mater. Res. Symp. Proc.*, 205-210.

Ding, Z., & Li, Z. (2005). Effect of aggregate and water content on the properties of magnesium phospho-silicate cement. *Cement and Concrete Composites, 27*, pp. 11-18.

Ding, Z., & Li, Z. (2005, 11). High-Early-Strength Magnesium Phosphate Cement with Fly Ash. *ACI Materials Journal, 102*(6), 375-381.

Dolen, T. P., & Benavidez, A. A. (1998). Properties of Low-Strength Concrete for Meeks Cabin Dam Modification Project, Wyoming. (A. K. Howard, & J. L. Hitch, Eds.) *The Design and Application of Controlled Low-Strength Materials (Flowable Fill), ASTM STP 1331*.

Donahue, P., & Aro, M. (2009). Durable phosphate-bonded natural fiber composite products. *Construction and Building Materials*.

Earnshaw, R. (1960). Investments for Casting Cobalt-Chromium Alloys, Part I. *108*, 389-396.

Earnshaw, R. (1960). Investments for Casting Cobalt-Chromium Alloys, Part II. *108*, 429-440.

El-Jazairi, B. (1982). Rapid Repair of Concrete Pavings. *Concrete*, 12-15.

Eubank, W. R. (1951). Calcination Studies of Mg Oxide. *J. Am. Ceram. Soc.*, 225-229.

Finch, T., & Sharp, J. H. (1989). Chemical Reactions Between Magnesia and Aluminum Orthophosphate to Form Magnesia-Phosphate Cements. *J. Matter. Sci.*, 4379-4386.

Giri, M., Rochefort, W., & Simonsen, J. (1998). The Novel Technique of Extrusion of Pulp using Carboxy-methyl-cellulose (CMC): Effect of CMC Characteristic on Pulp Rheology. *70th Annual Meeting of The Society of Rheology*, p. Paper IR4.

Glasser, F. (1990). Cements from micro to macrostructures. *Ceramic Trans*, 195-202.

Glauberman, N. (2011, Nov 1). *BASF celebrates 25 years of sustainable construction leadership with DELVO Stabilizer hydration-controlling admixture technology.* Retrieved Feb 22, 2013, from BASF-The Chemical Company: http://www.basf.com/group/corporate/en/news-and-media-relations/news-releases/news-releases-usa/P-10-0113

Grutzeck, M. W., Roy, D. M., & Wolfe-Confer, D. (1982). Mechanism of Hydration of Porland Cement Composites Containing Ferrosilicon Dust. *4th International Conference on Cement Microscopy* (pp. 193-202). Duncanville, Tex. : International Cement Microscopy Association.

IMA-NA. (2009). *Bentonite*. Retrieved Feb 25, 2013, from Industrial Minerals Association - North America: http://www.ima-na.org/bentonite

Jahren, P. (1983). Use of Silica Fume in Concrete. In V. M. Malhotra (Ed.), *Fly Ash, Silica Fume, Slag, and Other Mineral By-Products in Concrete, Proceedings of the First CANMET/ACI International Conference* (pp. 625-642). American Concrete Institue.

Jeong, S., & Wagh, A. (2003). Cementing the gap between ceramics, cements, and polymers. *Mater. Technol., 18*(3), 162-168.

Kosmatka, S. H., Kerkhoff, B., Panarese, W. C., MacLeod, N. F., & McGrath, R. J. (2002). *Design and Control of Concrete Mixtures.* Cement Association of Canada and the Porland Cement Association.

Li, Z., Ding, Z., & Zhang, Y. (2004). Development of sustainable cementitious materials. *International Workshop on Sustainable Development and Concrete Technology*, (pp. 55-76).

Neville, A. M. (2012). *Properties of Concrete, 5th edition.* Prentice Hall.

Poole, G. J. (Mar. 6, 1990). *Evaluating Stabilized/Activated PCC.* Minor Research Report, Office of Transportation Materials and Research, California Department of Transportation .

Prosen, E. (1939). *Patent No. 2,152,152.* US.

Prosen, E. (1941). *Patent No. 2,209,404.* US.

Quiao, F., Chau, C. K., & Li, Z. (2009). Property assessment of magnesium phosphate cement. *Key Eng Mat, 400-402*, pp. 115-120.

Quiao, F., Chau, C., & Li, Z. (2009). Setting and compressive strength characteristics of magnesium phosphate cement paste. *Adv Cem Res, 21*(4), pp. 175-80.

Quiao, F., Chau, C., & Li, Z. (2010). Properties evaluation of magnesium phosphate cement mortars as patch repair material. *Constr Build Mater, 24*(5), pp. 695-700.

Roy, D. (1987). New strong cement materials: chemically bonded ceramics. *Science, 235*, 651-658.

Roy, R., Agarwal, D., & Srikanth, V. (1991). Accoustic wave stimulation of low temperature ceramic reactions: the system Al2O3-P2Ọ-H2O. *J. Mater. Res., 6*(11), 2412-2416.

Sarkar, A. K. (1991). Hydration/dehydration characteristics of struvite dittmarite pertaining to magnesium ammonium phosphate cement system. *J. Mater. Sci.* , 2514-2518.

Scali, M. J., Chin, D., & Berke, N. S. (1987). Effect of Microsilica and Fly Ash upon the Microstructure and Permeability of Concrete. *Ninth International*

Conference on Cement Microscopy (pp. 375-387). Duncanville, Tex.: International Cement Microscopy Association.

Seehra, S. S., Gupta, S., & Kumar, S. (1994). Rapid setting magnesium phosphate cement for quick repair of concrete pavements: characterization and durability aspects. *Cement and Concrete Research, 24*, 595-596.

Sharp, J. W. (1946). *Patent No. 2410954.* United States Patent Office.

Sigvaldason, O. T. (1966, Dec). The Influence of Testing Machine Characteristics Upon the Cube and Cylinder Strength of Concrete. *Magazine of Concrete Research, 18*(57), pp. 197-206.

Sugama, T., & Kukacka, L. E. (1983). Characteristics of Magnesium Polyphosphate Cements Derived from Ammonium Polyphosphate Solutions. *Cem. Con. Res.*, 499-506.

Sugama, T., & Kukacka, L. E. (1983). Magnesium Monophosphate Cement Derived from Diammonium Phosphate Solutions. *Cem. Con. Res.*, 407-416.

Tassew, S. T., & Lubell, A. S. (2010). Textile Reinforced Ceramic Composites for Structural Infill Slab Applications. *34th IABSE Symposium*, (p. 8). Venice, Italy.

Tassew, S. T., & Lubell, A. S. (2013). Properties of phosphate-based cements with hight fly ash content. In *ACI Special Publication on Green Cement.* ACI Committee 236.

Tassew, S. T., & Lubell, A. S. (Submitted 2012). Mechanical Properties of Lightweight Ceramic Concrete. *Material and Structure Journal, 45*(4), 561-574.

Tassew, S. T., Mutsuddy, R., Bindiganavile, V. S., & Lubell, A. S. (Submitted 2010). Drop-weight impact response of glass-fiber reinforced ceramic concretes. *High performance fiber reinforced cementitious composites.* Michigan.

Tucker, J. (1941). Statistical theory of the effect of dimensions and of method of loading upon the modulus of rupture of beams. *ASTM Proc.*, *41*, pp. 1072-1094.

U.S. Geological Survey. (2010, Jan). *Mineral Commodity Summaries.* Retrieved Mar 08, 2013, from U.S. Geological Survey: http://minerals.usgs.gov/minerals/pubs/mcs

Wagh, A. J., Singh, D., & Jeong, S. Y. (1998). *Patent No. 5830815.* US.

Wagh, A. S. (2004). *Chemically Bond Phosphate Ceramics: Twenty-first century material with diverse applications.* Elsevier Ltd.

Wagh, A. S., & Jeong, S. Y. (2003). *Patent No. 6518212.* US.

Wagh, A. S., & Jeong, S. Y. (2003). Chemically bonded phosphate ceramics: I. A dissolution model of formation. *J. Ceram. Soc.* , 1838-1844.

Wagh, A. S., Jeong, S. Y., & Singh, D. (July 1997). High-strength phosphate ceramic (cement) using industrial by-product ash and slag. *Proc. of Int. Conf. on High-Strength Concrete.* Kona, HI.

Wagh, A., Singh, D., & Jeong, S. (2001). Chemically Bonded Phosphate Ceramics. In *Handbook of Mixed Wasted Management Techonology.* Boca Raton: CRC Press.

Yamato, T., Emoto, Y., & Soeda, M. (1986). Strength and Freezing and Thawing Resistance of Concrete Incorporating Condensed Silica Fume. In V. M. Malhotra (Ed.), *Fly Ash, Silica Fume, Slag and Natural Pozzolans in Concrete. 2*, pp. 1095-1117. Farmington Hills, Mich.: Proceedings of the Second CANMET/ACI International Conference, American Concrete Institue.

Yang, Quangbing, Zhang, Shuqing, & Xueli, W. (2002). Deicer-scaling resistance of phosphate cement-based binder for rapid repair of concrete. *Cement and concrete research, 32*, 165-168.

Yeong, S., & Wagh, A. (2002). *Chemically bonded phosphate ceramics: cementing the gap between ceramics and cements.* Argonne National Laboratory.

Yoshizake, Y., Ikeda, K., Yoshida, S., & Yoshizumi, A. (1989). Phisicochemical study of magnesium-phosphate cement. *MRS Int'l. Mtg. On Adv., 13*, 27-38.

APPENDIX A

TRIAL MIXES

Table A-1: Compressive strength development of MPPC binders using cube specimens (w/b=0.2)

Mix ID	Age (days)	Compressive strength (MPa)	Average compressive strength, f_{cu} (MPa)	COV	Density (kg/m^3)	Average density, γ (kg/m^3)	COV
T(1)-1		12.9			1925		
T(1)-2	1	13.1	13.5	0.068	1930	1916	0.010
T(1)-3		14.6			1894		
T(3)-1		19.7			1920		
T(3)-2	3	21.5	20.1	0.064	1908	1912	0.003
T(3)-3		19.0			1907		
T(7)-1		27.4			1906		
T(7)-2	7	23.8	24.7	0.097	1888	1883	0.013
T(7)-3		22.8			1856		
T(14)-1		28.1			1910		
T(14)-2	14	24.0	25.4	0.091	1884	1884	0.013
T(14)-3		24.2			1856		
T(28)-1		29.1			1854		
T(28)-2	28	34.7	32.7	0.095	1871	1868	0.006
T(28)-3		34.3			1879		
T(56)-1		36.6			1837		
T(56)-2	56	33.3	34.3	0.057	1856	1851	0.006
T(56)-3		33.1			1859		

Table A-2: Compressive strength of MPPC concretes containing bentonite from cube tests at 7 days

Mix ID	Bentonite (%)	w/b mass ratio	Compressive strength (MPa)	Average compressive strength, f_{cu} (MPa)	COV	Density (kg/m^3)	Average density, γ (kg/m^3)	COV
TB1(7)(0.16)-1	1.0	0.16	44.9	41.2	0.128	1947	1948	0.001
TB1(7)(0.16)-2			37.4			1950		
TB1(7)(0.18)-1	1.0	0.18	50.9	53.0	0.056	1944	1923	0.011
TB1(7)(0.18)-2			55.1			1903		
TB1(7)(0.20)-1	1.0	0.20	42.4	43.7	0.042	1924	1911	0.008
TB1(7)(0.20)-2			45.0			1893		
TB1(7)(0.22)-1	1.0	0.22	32.2	36.0	0.105	1883	1871	0.008
TB1(7)(0.22)-2			39.8			1854		
TB1(7)(0.22)-3			35.9			1879		
TB1(7)(0.24)-1	1.0	0.24	27.2	26.1	0.063	1824	1837	0.006
TB1(7)(0.24)-2			24.2			1845		
TB1(7)(0.24)-3			26.9			1843		
TB1(7)(0.26)-1	1.0	0.26	11.8	12.4	0.062	1756	1747	0.008
TB1(7)(0.26)-2			12.9			1736		
TB1(7)(0.28)-1	1.0	0.28	18.2	19.6	0.074	1710	1705	0.005
TB1(7)(0.28)-2			21.1			1710		
TB1(7)(0.28)-3			19.5			1695		
TB1.5(7)(0.16)-1	1.5	0.16	44.5	42.2	0.078	1948	1934	0.009
TB1.5(7)(0.16)-2			39.8			1921		
TB1.5(7)(0.18)-1	1.5	0.18	41.4	42.4	0.031	1920	1921	0.001
TB1.5(7)(0.18)-2			43.3			1922		
TB1.5(7)(0.20)-1	1.5	0.20	44.0	45.7	0.051	1921	1912	0.007
TB1.5(7)(0.20)-2			47.3			1902		

Table A-2: Compressive strength of MPPC concretes containing bentonite from cube tests at 7 days (continued)

Mix ID	Bentonite (%)	w/b mass ratio	Compressive strength (MPa)	Average compressive strength, f_{cu} (MPa)	COV	Density (kg/m^3)	Average density, γ (kg/m^3)	COV
TB1.5(7)(0.22)-1			39.4			1872		
TB1.5(7)(0.22)-2	1.5	0.22	40.0	38.8	0.042	1840	1859	0.009
TB1.5(7)(0.22)-3			36.9			1868		
TB1.5(7)(0.24)-1			29.2			1842		
TB1.5(7)(0.24)-2	1.5	0.24	31.8	30.9	0.048	1855	1833	0.021
TB1.5(7)(0.24)-3			31.8			1804		
TB1.5(7)(0.26)-1	1.5	0.26	18.1	18.6	0.034	1804	1791	0.009
TB1.5(7)(0.26)-2			19.0			1779		
TB3(7)(0.18)-1			50.0			1924		
TB3(7)(0.18)-2	3.0	0.18	49.7	49.6	0.009	1887	1909	0.010
TB3(7)(0.18)-3			49.1			1916		
TB3(7)(0.20)-1	3.0	0.20	36.0	35.8	0.008	1920	1924	0.003
TB3(7)(0.20)-2			35.6			1929		
TB3(7)(0.22)-1			38.4			1888		
TB3(7)(0.22)-2	3.0	0.22	41.9	39.4	0.056	1862	1876	0.006
TB3(7)(0.22)-3			37.8			1878		
TB3(7)(0.24)-1			36.9			1873		
TB3(7)(0.24)-2	3.0	0.24	33.7	36.5	0.073	1852	1857	0.007
TB3(7)(0.24)-3			39.0			1845		
TB3(7)(0.26)-1			11.3			1796		
TB3(7)(0.26)-2	3.0	0.26	11.9	11.2	0.062	1761	1781	0.001
TB3(7)(0.26)-3			10.5			1786		
TB3(7)(0.28)-1			15.4			1720		
TB3(7)(0.28)-2	3.0	0.28	16.2	16.4	0.067	1756	1746	0.011
TB3(7)(0.28)-3			17.6			1748		

Bentonite content is by mass percent of the binder

Table A-3: Compressive strength of MPPC concretes containing bentonite from cube tests at 28 days

Mix ID	Bentonite (%)	w/b mass ratio	Compressive strength (MPa)	Average compressive strength, f_{cu} (MPa)	COV	Density (kg/m^3)	Average density, γ (kg/m^3)	COV
TB1(28)(0.16)-1	1.0	0.16	57.6	59.9	0.054	1952	1935	0.012
TB1(28)(0.16)-2			62.2			1919		
TB1(28)(0.18)-1	1.0	0.18	48.8	54.9	0.157	1950	1933	0.012
TB1(28)(0.18)-2			61.0			1915		
TB1(28)(0.20)-1	1.0	0.20	52.6	54.2	0.040	1896	1899	0.002
TB1(28)(0.20)-2			55.7			1903		
TB1(28)(0.22)-1	1.0	0.22	44.0	47.2	0.094	1875	1858	0.012
TB1(28)(0.22)-2			50.3			1841		
TB1(28)(0.24)-1	1.0	0.24	34.4	32.9	0.066	1816	1814	0.002
TB1(28)(0.24)-2			31.3			1812		
TB1(28)(0.26)-1	1.0	0.26	29.8	29.9	0.097	1718	1713	0.003
TB1(28)(0.26)-2			27.1			1717		
TB1(28)(0.26)-3			32.9			1706		
TB1(28)(0.28)-1	1.0	0.28	22.8	21.3	0.062	1671	1655	0.008
TB1(28)(0.28)-2			20.4			1654		
TB1(28)(0.28)-3			20.6			1643		
TB1.5(28)(0.16)-1	1.5	0.16	56.8	57.9	0.018	1938	1935	0.008
TB1.5(28)(0.16)-2			58.1			1918		
TB1.5(28)(0.16)-3			58.9			1949		
TB1.5(28)(0.18)-1	1.5	0.18	49.3	45.9	0.106	1941	1936	0.003
TB1.5(28)(0.18)-2			42.4			1932		
TB1.5(28)(0.20)-1	1.5	0.20	58.6	56.9	0.041	1884	1893	0.006
TB1.5(28)(0.20)-2			55.3			1902		

Table A-3: Compressive strength of MPPC concretes containing bentonite from cube tests at 28 days (continued)

Mix ID	Bentonite (%)	w/b mass ratio	Compressive strength (MPa)	Average compressive strength, f_{cu} (MPa)	COV	Density (kg/m^3)	Average density, γ (kg/m^3)	COV
TB1.5(28)(0.22)-1			48.7			1857		
TB1.5(28)(0.22)-2	1.5	0.22	49.6	49.2	0.009	1862	1852	0.007
TB1.5(28)(0.22)-3			49.2			1835		
TB1.5(28)(0.24)-1	1.5	0.24	38.3	41.5	0.107	1804	1800	0.003
TB1.5(28)(0.24)-2			44.6			1796		
TB1.5(28)(0.26)-1			28.4			1748		
TB1.5(28)(0.26)-2	1.5	0.26	27.6	27.3	0.044	1748	1741	0.006
TB1.5(28)(0.26)-3			26.0			1727		
TB3(28)(0.18)-1	3.0	0.18	56.9	53.1	0.099	1904	1910	0.003
TB3(28)(0.18)-2			49.4			1915		
TB3(28)(0.20)-1	3.0	0.20	59.9	59.4	0.011	1884	1901	0.012
TB3(28)(0.20)-2			58.9			1918		
TB3(28)(0.22)-1	3.0	0.22	47.0	45.4	0.049	1868	1864	0.003
TB3(28)(0.22)-2			43.8			1860		
TB3(28)(0.24)-1			46.6			1842		
TB3(28)(0.24)-2	3.0	0.24	48.0	46.7	0.026	1823	1835	0.006
TB3(28)(0.24)-3			45.5			1841		
TB3(28)(0.26)-1			15.3			1759		
TB3(28)(0.26)-2	3.0	0.26	14.5	16.1	0.127	1780	1761	0.010
TB3(28)(0.26)-3			18.4			1744		
TB3(28)(0.28)-1			16.7			1724		
TB3(28)(0.28)-2	3.0	0.28	16.8	17.6	0.008	1732	1724	0.005
TB3(28)(0.28)-3			19.2			1715		

Bentonite content is by mass percent of the binder

Table A-4: Compressive strength of MPPC binders containing SF from cube tests (w/b = 0.20)

Mix ID	SF (%)	Age (days)	Compressive strength (MPa)	Average compressive strength, f_{cu} (MPa)	COV	Density (kg/m^3)	Average density, γ (kg/m^3)	COV
TS5(1)-1			15.8			1943		
TS5(1)-2	5	1	13.5	14.8	0.078	1963	1956	0.005
TS5(1)-3			15.0			1961		
TS5(3)-1	5	3	46.7	44.8	0.061	1909	1918	0.006
TS5(3)-2			42.8			1927		
TS5(7)-1	5	7	46.4	46.4	0.000	1914	1899	0.010
TS5(7)-2			46.4			1886		
TS5(14)-1			52.7			1895		
TS5(14)-2	5	14	49.4	49.0	0.078	1909	1905	0.004
TS5(14)-3			45.0			1909		
TS5(28)-1	5	28	38.6	42.7	0.135	1908	1901	0.005
TS5(28)-2			46.8			1893		
TS5(56)-1	5	56	44.6	49.2	0.132	1904	1910	0.003
TS5(56)-2			53.8			1915		
TS10(1)-1			16.5			1948		
TS10(1)-2	10	1	16.4	15.8	0.075	1929	1944	0.007
TS10(1)-3			14.4			1956		
TS10(3)-1			50.8			1926		
TS10(3)-2	10	3	42.7	47.1	0.086	1935	1930	0.002
TS10(3)-3			47.8			1928		
TS10(7)-1			48.4			1918		
TS10(7)-2	10	7	54.8	53.5	0.085	1897	1907	0.005
TS10(7)-3			57.3			1907		

Table A-4: Compressive strength of MPPC binders containing SF from cube tests (w/b = 0.20) (continued)

Mix ID	SF (%)	Age (days)	Compressive strength (MPa)	Average compressive strength, f_{cu} (MPa)	COV	Density (kg/m^3)	Average density, γ (kg/m^3)	COV
TS10(14)-1	10	14	56.6	54.5	0.055	1911	1920	0.007
TS10(14)-2			52.3			1931		
TS10(28)-1	10	28	54.9	57.9	0.072	1916	1919	0.003
TS10(28)-2			60.8			1924		
TS10(56)-1	10	56	67.9	65.6	0.048	1899	1913	0.011
TS10(56)-2			63.4			1928		
TS15(1)-1	15	1	16.3	17.7	0.085	1924	1921	0.004
TS15(1)-2			19.3			1911		
TS15(1)-3			17.4			1928		
TS15(3)-1	15	3	45.1	48.2	0.087	1949	1940	0.009
TS15(3)-2			53.0			1918		
TS15(3)-3			46.6			1953		
TS15(7)-1	15	7	52.8	53.1	0.007	1923	1916	0.004
TS15(7)-2			53.3			1909		
TS15(14)-1	15	14	47.6	48.4	0.021	1924	1930	0.003
TS15(14)-2			49.1			1935		
TS15(28)-1	15	28	59.2	63.4	0.058	1941	1923	0.008
TS15(28)-2			65.1			1911		
TS15(28)-3			66.0			1918		
TS15(56)-1	15	56	68.3	64.6	0.058	1922	1907	0.007
TS15(56)-2			60.8			1906		
TS15(56)-3			64.8			1892		

Silica fume content is by mass percent of the binder

Table A-5: Compressive strength of sand-1 mortars from cube tests (w/b = 0.20)

Mix ID	SF (%)	Age (days)	Compressive strength (MPa)	Average compressive strength, f_{cu} (MPa)	COV	Density (kg/m^3)	Average density, γ (kg/m^3)	COV
TS5S1(1)-1			25.3			2132		
TS5S1(1)-2	5	1	29.8	27.7	0.081	2175	2151	0.010
TS5S1(1)-3			27.9			2146		
TS5S1(3)-1			29.7			2171		
TS5S1(3)-2	5	3	30.7	30.4	0.019	2140	2153	0.007
TS5S1(3)-3			30.7			2147		
TS5S1(7)-1			34.9			2110		
TS5S1(7)-2	5	7	35.2	35.6	0.025	2114	2125	0.010
TS5S1(7)-3			36.6			2150		
TS5S1(14)-1			39.5			2109		
TS5S1(14)-2	5	14	37.6	36.8	0.087	2140	2126	0.007
TS5S1(14)-3			33.2			2130		
TS5S1(28)-1			42.4			2105		
TS5S1(28)-2	5	28	47.6	44.0	0.071	2128	2124	0.008
TS5S1(28)-3			42.0			2138		
TS10S1(1)-1			30.4			2192		
TS10S1(1)-2	10	1	30.5	30.7	0.016	2182	2178	0.008
TS10S1(1)-3			31.3			2160		
TS10S1(3)-1			33.2			2185		
TS10S1(3)-2	10	3	34.9	34.5	0.032	2170	2180	0.004
TS10S1(3)-3			35.3			2187		
TS10S1(7)-1			36.3			2141		
TS10S1(7)-2	10	7	33.3	35.0	0.044	2110	2136	0.011
TS10S1(7)-3			35.5			2157		

Table A-5: Compressive strength of sand-1 mortars from cube tests (w/b = 0.20) (continued)

Mix ID	SF (%)	Age (days)	Compressive strength (MPa)	Average compressive strength, f_{cu} (MPa)	COV	Density (kg/m^3)	Average density, γ (kg/m^3)	COV
TS10S1(14)-1			42.9			2172		
TS10S1(14)-2	10	14	42.0	43.1	0.029	2134	2154	0.008
TS10S1(14)-3			44.5			2156		
TS10S1(28)-1			36.0			2128		
TS10S1(28)-2	10	28	36.6	39.1	0.122	2132	2127	0.003
TS10S1(28)-3			44.6			2120		
TS15S1(1)-1			33.8			2181		
TS15S1(1)-2	15	1	31.0	33.5	0.069	2199	2197	0.006
TS15S1(1)-3			35.6			2209		
TS15S1(3)-1			36.4			2194		
TS15S1(3)-2	15	3	37.6	37.8	0.038	2194	2204	0.007
TS15S1(3)-3			39.3			2223		
TS15S1(7)-1			34.9			2188		
TS15S1(7)-2	15	7	37.6	37.7	0.076	2170	2180	0.004
TS15S1(7)-3			40.7			2183		
TS15S1(14)-1			43.4			2184		
TS15S1(14)-2	15	14	41.8	40.8	0.080	2146	2174	0.011
TS15S1(14)-3			37.1			2192		
TS15S1(28)-1			42.9			2166		
TS15S1(28)-2	15	28	46.3	46.0	0.065	2149	2168	0.009
TS15S1(28)-3			48.9			2188		

Silica fume content is by mass percent of the binder

Table A-6: Compressive strength of sand-2 mortars from cube tests (w/b = 0.2)

Mix ID	SF (%)	Age (days)	Compressive strength (MPa)	Average compressive strength, f_{cu} (MPa)	COV	Density (kg/m^3)	Average density, γ (kg/m^3)	COV
TS5S2(1)-1			21.8			2116		
TS5S2(1)-2	5	1	22.3	21.8	0.022	2070	2101	0.013
TS5S2(1)-3			21.3			2119		
TS5S2(3)-1			26.0			2102		
TS5S2(3)-2	5	3	25.2	25.7	0.016	2101	2098	0.003
TS5S2(3)-3			25.8			2091		
TS5S2(7)-1			24.7			2085		
TS5S2(7)-2	5	7	29.4	25.9	0.118	2072	2088	0.008
TS5S2(7)-3			23.6			2108		
TS5S2(14)-1			31.0			2068		
TS5S2(14)-2	5	14	28.7	31.4	0.093	2117	2097	0.012
TS5S2(14)-3			34.5			2106		
TS5S2(28)-1			33.1			2086		
TS5S2(28)-2	5	28	39.9	36.7	0.093	2047	2077	0.012
TS5S2(28)-3			37.1			2098		
TS5S2(56)-1	5	56	45.9	44.8	0.036	2100	2099	0.001
TS5S2(56)-2			43.6			2099		
TS10S2(1)-1			28.1			2231		
TS10S2(1)-2	10	1	27.7	27.9	0.007	2190	2212	0.009
TS10S2(1)-3			27.9			2216		
TS10S2(3)-1			31.1			2197		
TS10S2(3)-2	10	3	35.9	34.3	0.080	2176	2199	0.011
TS10S2(3)-3			35.9			2223		
TS10S2(7)-1			31.2			2168		
TS10S2(7)-2	10	7	36.4	34.6	0.085	2153	2174	0.011
TS10S2(7)-3			36.3			2220		

Table A-6: Compressive strength of sand-2 mortars from cube tests (w/b = 0.2) (continued)

Mix ID	SF (%)	Age (days)	Compressive strength (MPa)	Average compressive strength, f_{cu} (MPa)	COV	Density (kg/m^3)	Average density, γ (kg/m^3)	COV
TS10S2(14)-1			36.0			2164		
TS10S2(14)-2	10	14	36.6	37.1	0.039	2180	2180	0.007
TS10S2(14)-3			38.8			2198		
TS10S2(28)-1			46.7			2200		
TS10S2(28)-2	10	28	39.7	44.2	0.088	2184	2184	0.007
TS10S2(28)-3			46.2			2168		
TS10S2(56)-1			45.8			2218		
TS10S2(56)-2	10	56	49.9	49.4	0.069	2159	2183	0.014
TS10S2(56)-3			52.6			2173		
TS15S2(1)-1			31.1			2218		
TS15S2(1)-2	15	1	37.6	34.3	0.094	2236	2227	0.004
TS15S2(1)-3			34.3			2228		
TS15S2(3)-1			40.9			2204		
TS15S2(3)-2	15	3	40.5	40.9	0.009	2210	2216	0.007
TS15S2(3)-3			41.3			2236		
TS15S2(7)-1			34.5			2227		
TS15S2(7)-2	15	7	35.7	35.5	0.025	2208	2214	0.005
TS15S2(7)-3			36.3			2208		
TS15S2(14)-1			41.3			2167		
TS15S2(14)-2	15	14	38.7	41.5	0.068	2178	2178	0.007
TS15S2(14)-3			44.4			2189		
TS15S2(28)-1			49.8			2219		
TS15S2(28)-2	15	28	49.2	47.9	0.057	2186	2199	0.007
TS15S2(28)-3			44.8			2192		
TS15S2(56)-1			50.5			2176		
TS15S2(56)-2	15	56	53.4	50.7	0.052	2170	2185	0.009
TS15S2(56)-3			48.1			2211		

Table A-7: Compressive strength of sand-3 mortars from cube tests (w/b = 0.20)

Mix ID	SF (%)	Age (days)	Compressive strength (MPa)	Average compressive strength, f_{cu} (MPa)	COV	Density (kg/m^3)	Average density, γ (kg/m^3)	COV
TS5S3(1)-1			23.5			2248		
TS5S3(1)-2	5	1	21.6	22.7	0.044	2202	2223	0.011
TS5S3(1)-3			23.1			2211		
TS5S3(3)-1	5	3	27.5	27.4	0.008	2187	2181	0.007
TS5S3(3)-2			27.2			2164		
TS5S3(7)-1			28.3			2173		
TS5S3(7)-2	5	7	31.2	30.2	0.054	2167	2161	0.007
TS5S3(7)-3			31.1			2144		
TS5S3(14)-1	5	14	30.6	29.7	0.042	2176	2151	0.008
TS5S3(14)-2			28.8			2151		
TS5S3(28)-1			38.4			2150		
TS5S3(28)-2	5	28	38.7	38.4	0.006	2170	2147	0.011
TS5S3(28)-3			38.2			2121		
TS5S3(56)-1			44.5			2170		
TS5S3(56)-2	5	56	37.8	40.3	0.090	2149	2157	0.005
TS5S3(56)-3			38.6			2152		
TS10S3(1)-1			26.7			2228		
TS10S3(1)-2	10	1	25.3	26.8	0.056	2208	2229	0.009
TS10S3(1)-3			28.3			2250		
TS10S3(3)-1			28.2			2233		
TS10S3(3)-2	10	3	32.1	31.3	0.087	2210	2209	0.011
TS10S3(3)-3			33.5			2186		
TS10S3(7)-1			36.8			2214		
TS10S3(7)-2	10	7	33.1	35.1	0.053	2188	2207	0.008
TS10S3(7)-3			35.3			2220		

Table A-7: Compressive strength of sand-3 mortars from cube tests (w/b = 0.20) (continued)

Mix ID	SF (%)	Age (days)	Compressive strength (MPa)	Average compressive strength, f_{cu} (MPa)	COV	Density (kg/m^3)	Average density, γ (kg/m^3)	COV
TS10S3(14)-1			41.0			2221		
TS10S3(14)-2	10	14	37.7	38.0	0.074	2191	2196	0.011
TS10S3(14)-3			35.4			2175		
TS10S3(28)-1			41.1			2208		
TS10S3(28)-2	10	28	44.4	43.1	0.041	2256	2225	0.012
TS10S3(28)-3			43.9			2211		
TS10S3(56)-1			47.6			2220		
TS10S3(56)-2	10	56	43.9	46.5	0.047	2160	2190	0.013
TS10S3(56)-3			47.9			2192		
TS15S3(1)-1			30.9			2213		
TS15S3(1)-2	15	1	29.2	29.6	0.037	2240	2234	0.008
TS15S3(1)-3			28.8			2249		
TS15S3(3)-1			35.9			2202		
TS15S3(3)-2	15	3	37.0	35.7	0.038	2221	2220	0.007
TS15S3(3)-3			34.3			2235		
TS15S3(7)-1			39.3			2228		
TS15S3(7)-2	15	7	41.4	39.8	0.034	2188	2214	0.011
TS15S3(7)-3			38.8			2228		
TS15S3(14)-1			39.3			2187		
TS15S3(14)-2	15	14	42.4	41.1	0.038	2156	2162	0.009
TS15S3(14)-3			41.5			2145		
TS15S3(28)-1			46.6			2220		
TS15S3(28)-2	15	28	48.3	46.8	0.029	2215	2207	0.008
TS15S3(28)-3			45.6			2186		
TS15S3(56)-1			49.7			2160		
TS15S3(56)-2	15	56	55.3	52.4	0.053	2176	2178	0.008
TS15S3(56)-3			52.2			2198		

Table A-8: Compressive strength and density of sand-4 mortars containing baking soda from cube tests at 3 days (w/b = 0.20; b/s = 1:0.5)

Mix ID	Baking soda (%)	Compressive strength (MPa)	Average compressive strength, f_{cu} (MPa)	COV	Density (kg/m^3)	Average density, γ (kg/m^3)	COV
TBa01S45(3)(0.20)-1		37.3			2150		
TBa01S45(3)(0.20)-2	0.1	37.5	38.8	0.062	2118	2146	0.012
TBa01S45(3)(0.20)-3		41.6			2171		
TBa03S45(3)(0.20)-1		40.7			2168		
TBa03S45(3)(0.20)-2	0.3	37.7	38.5	0.050	2132	2142	0.010
TBa03S45(3)(0.20)-3		37.1			2128		
TBa05S45(3)(0.20)-1		34.3			2048		
TBa05S45(3)(0.20)-2	0.5	36.3	34.7	0.042	2067	2073	0.013
TBa05S45(3)(0.20)-3		33.4			2104		
TBa1S45(3)(0.20)-1		35.5			2088		
TBa1S45(3)(0.20)-2	1.0	32.3	34.3	0.051	2113	2107	0.008
TBa1S45(3)(0.20)-3		35.3			2120		
TBa2S45(3)(0.20)-1		19.0			1896		
TBa2S45(3)(0.20)-2	2.0	18.3	19.1	0.042	1987	1934	0.024
TBa2S45(3)(0.20)-3		19.9			1917		

Baking soda content is by mass percent of the dry mix

Table A-9: Compressive strength and density of sand-4 mortars containing baking soda from cube tests at 3 days (w/b = 0.20; baking soda = 1% by mass)

Mix ID	*b/s* mass ratio	Compressive strength (MPa)	Average compressive strength, f_{cu} (MPa)	COV	Density (kg/m^3)	Average density, γ (kg/m^3)	COV
TBa1S45(3)(0.20)-1		35.5			2088		
TBa1S45(3)(0.20)-2	1:0.5	32.3	34.3	0.051	2113	2107	0.008
TBa1S45(3)(0.20)-3		35.2			2120		
TBa1S46(3)(0.20)-1		36.5			2152		
TBa1S46(3)(0.20)-2	1:0.6	33.2	32.6	0.129	1992	2062	0.039
TBa1S46(3)(0.20)-3		28.1			2043		
TBa1S47(3)(0.20)-1		29.9			2054		
TBa1S47(3)(0.20)-2	1:0.7	24.7	26.7	0.104	2014	2042	0.012
TBa1S47(3)(0.20)-3		25.5			2057		
TBa1S48(3)(0.20)-1		26.9			2095		
TBa1S48(3)(0.20)-2	1:0.8	30.7	28.4	0.071	2180	2125	0.022
TBa1S48(3)(0.20)-3		27.6			2098		

Table A-10: Compressive strength and density of sand-3 mortars containing baking soda from cube tests at 7 days (baking soda = 1% by mass; b/s = 1:1)

Mix ID	*w/b* mass ratio	Compressive strength (MPa)	Average compressive strength, f_{cu} (MPa)	COV	Density (kg/m^3)	Average density, γ (kg/m^3)	COV
TBa1S31(7)(0.20)-1		32.5			2187		
TBa1S31(7)(0.20)-2	0.20	27.6	29.8	0.083	2252	2226	0.015
TBa1S31(7)(0.20)-3		29.3			2239		
TBa1S31(7)(0.22)-1		29.2			2234		
TBa1S31(7)(0.22)-2	0.22	27.2	28.0	0.037	2198	2225	0.010
TBa1S31(7)(0.22)-3		27.7			2243		
TBa1S31(7)(0.24)-1		26.9			2218		
TBa1S31(7)(0.24)-2	0.24	24.4	26.9	0.094	2221	2216	0.003
TBa1S31(7)(0.24)-3		29.5			2210		
TBa1S31(7)(0.26)-1		29.6			2184		
TBa1S31(7)(0.26)-2	0.26	27.8	27.6	0.078	2186	2192	0.005
TBa1S31(7)(0.26)-3		25.3			2207		

Table A-11: Compressive strength and density of MPPC wood composites from cube tests at 3 days (b/sdt = 1:0.20)

Mix ID	*w/b* mass ratio	Compressive strength (MPa)	Average compressive strength, f_{cu} (MPa)	COV	Density (kg/m^3)	Average density, γ (kg/m^3)	COV
TSa5(3)(0.32)-1		5.4			1435		
TSa5(3)(0.32)-2	0.32	5.9	5.8	0.062	1423	1431	0.004
TSa5(3)(0.32)-3		6.1			1434		
TSa5(3)(0.36)-1		6.1			1478		
TSa5(3)(0.36)-2	0.36	6.3	6.4	0.056	1484	1468	0.015
TSa5(3)(0.36)-3		6.8			1442		
TSa5(3)(0.40)-1		6.1			1501		
TSa5(3)(0.40)-2	0.40	6.3	6.4	0.047	1473	1481	0.012
TSa5(3)(0.40)-3		6.7			1468		
TSa5(3)(0.46)-1		3.2			1416		
TSa5(3)(0.46)-2	0.46	3.4	3.4	0.058	1402	1393	0.020
TSa5(3)(0.46)-3		3.6			1360		
TSa5(3)(0.50)-1		3.5			1512		
TSa5(3)(0.50)-2	0.50	3.0	3.2	0.082	1490	1504	0.008
TSa5(3)(0.50)-3		3.1			1510		

Table A-12: Compressive strength and density of MPPC wood composites from cube tests at 7 days (b/sdt = 1:0.2; w/b = 0.36; sand 4; b/s = 1:0.5)

Mix ID	Age (days)	MgO:MKP:FA mass ratio	Compressive strength (MPa)	Average compressive strength, f_{cu} (MPa)	COV	Density (kg/m^3)	Average density, γ (kg/m^3)	COV
TSa2S4(7)(0.36)-1			15.9			1709		
TSa2S4(7)(0.36)-2	7	1:3:1.00	17.7	17.6	0.091	1702	1691	0.015
TSa2S4(7)(0.36)-3			19.1			1663		
TSa3S4(7)(0.36)-1			12.8			1619		
TSa3S4(7)(0.36)-2	7	1:3:1.71	10.6	12.3	0.123	1621	1624	0.004
TSa3S4(7)(0.36)-3			13.5			1632		
TSa4S4(7)(0.36)-1			11.9			1574		
TSa4S4(7)(0.36)-2	7	1:3:2.67	12.5	11.7	0.078	1623	1586	0.021
TSa4S4(7)(0.36)-3			10.7			1560		

Table A-12: Compressive strength and density of MPPC wood composites containing baking soda from cube tests at 7 days (b/sdt = 1:0.2; w/b = 0.36; sand 3; b/s = 1:0.5)

Mix ID	Baking soda (%)	Compressive strength (MPa)	Average compressive strength, f_{cu} (MPa)	COV	Density (kg/m^3)	Average density, γ (kg/m^3)	COV
TSa2Ba1S3(7)(0.36)-1		4.6			1506		
TSa2Ba1S3(7)(0.36)-2	1	4.7	4.7	0.015	1504	1494	0.014
TSa2Ba1S3(7)(0.36)-3		4.7			1470		
TSa2Ba2S3(7)(0.36)-1		5.1			1557		
TSa2Ba2S3(7)(0.36)-2	2	4.8	4.9	0.035	1548	1543	0.011
TSa2Ba2S3(7)(0.36)-3		4.8			1524		
TSa2Ba3S3(7)(0.36)-1		6.8			1664		
TSa2Ba3S3(7)(0.36)-2	3	7.2	7.1	0.037	1693	1662	0.020
TSa2Ba3S3(7)(0.36)-3		7.3			1626		

Table A-13: Compressive strength and density of MPPC wood composites containing baking soda from cube tests at 28 days (b/sdt = 1:0.2; w/b = 0.36; sand 3; b/s = 1:0.5)

Mix ID	Baking soda (%)	Compressive strength (MPa)	Average compressive strength, f_{cu} (MPa)	COV	Density (kg/m^3)	Average density, γ (kg/m^3)	COV
TSa2Ba1S3(28)(0.36)-1		6.2			1494		
TSa2Ba1S3(28)(0.36)-2	1	6.1	6.5	0.102	1434	1479	0.026
TSa2Ba1S3(28)(0.36)-3		7.3			1507		
TSa2Ba2S3(28)(0.36)-1		8.2			1532		
TSa2Ba2S3(28)(0.36)-2	2	8.2	8.1	0.021	1562	1540	0.012
TSa2Ba2S3(28)(0.36)-3		7.9			1525		
TSa2Ba3S3(28)(0.36)-1		10.3			1624		
TSa2Ba3S3(28)(0.36)-2	3	12.6	11.0	0.129	1654	1621	0.022
TSa2Ba3S3(28)(0.36)-3		10.0			1583		

APPENDIX B MPPC CONCRETES AND WOOD COMPOSITES

Table B-1: Compressive strength and density of MPPC concretes/wood composites from cube tests (at 90 days; w/b = 0.20 for MPPC concretes; w/b = 0.36 for MPPC wood composites)

Mix ID	Compressive strength (MPa)	Average compressive strength, f_{cu} (MPa)	COV	Density (kg/m^3)	Average density, γ (kg/m^3)	COV
S5-1	33.5			1754		
S5-2	35.8	34.0	0.048	1750	1751	0.001
S5-3	32.6			1750		
S10-1	33.9			1761		
S10-2	33.8	33.9	0.006	1764	1763	0.001
S10-3	34.1			1764		
SS5-1	45.2			2150		
SS5-2	38.1	41.1	0.089	2138	2150	0.006
SS5-3	40.1			2162		
SS10-1	51.6			2173		
SS10-2	46.2	46.8	0.095	2157	2173	0.008
SS10-3	42.7			2190		
Sa-1	6.3			1314		
Sa-2	7.5	7.0	0.089	1354	1315	0.029
Sa-3	7.2			1353		
SaB-1	14.7			1437		
SaB-2	13.8	14.5	0.043	1430	1438	0.006
SaB-3	15.0			1448		

Table B-2: Compressive strength of MPPC concretes/wood composites from cylinder tests (at 90 days; w/b = 0.20 for MPPC concretes; w/b = 0.36 for MPPC wood composites)

Mix ID	**Compressive strength (MPa)**	**Average compressive strength, f'_c (MPa)**	**COV**
S5-1	30.2	31.4	0.039
S5-2	32.7		
S5-3	31.3		
S10-1	31.5	32.6	0.049
S10-2	33.8		
SS5-1	30.7	31.5	0.038
SS5-2	32.4		
SS10-1	32.0	33.2	0.051
SS10-2	34.4		
Sa-1	12.1	13.3	0.083
Sa-2	13.5		
Sa-3	14.3		
SaB-1	13.3	12.7	0.047
SaB-2	12.1		
SaB-3	12.6		

Table B-3: Strain at peak stress and modulus of elasticity of MPPC concretes/wood composites from cylinder tests (at 90 days; w/b = 0.20 for MPPC concretes; w/b = 0.36 for MPPC wood composites)

Mix ID	Strain at peak stress (mm/mm)	Average strain at peak stress, ε_c' (mm/mm)	COV	Modulus of elasticity (GPa)	Average modulus of elasticity, E (GPa)	COV
S5-1	3.44×10^{-3}			8.87		
S5-2	3.93×10^{-3}	3.72×10^{-3}	0.067	8.36	8.47	0.041
S5-3	3.78×10^{-3}			8.19		
S10-1	3.67×10^{-3}	3.47×10^{-3}	0.079	8.77	9.28	0.076
S10-2	3.28×10^{-3}			9.78		
SS5-1	3.43×10^{-3}	3.24×10^{-3}	0.082	11.73	12.23	0.057
SS5-2	3.05×10^{-3}			12.73		
SS10-1	3.36×10^{-3}	3.28×10^{-3}	0.034	11.86	12.16	0.034
SS10-2	3.20×10^{-3}			12.45		
Sa-1	1.10×10^{-2}			1.81		
Sa-2	9.10×10^{-3}	9.72×10^{-3}	0.114	2.80	2.51	0.241
Sa-3	9.03×10^{-3}			2.91		
SaB-1	1.03×10^{-2}			2.38		
SaB-2	9.68×10^{-3}	10.0×10^{-3}	0.038	1.74	2.13	0.159
SaB-3	1.01×10^{-2}			2.26		

Table B-4: Modulus of rupture of MPPC concretes/wood composites from prism tests (at 90 days; w/b = 0.20 for MPPC concretes; w/b = 0.36 for MPPC wood composites)

Mix ID	Modulus of rupture (MPa)	Average modulus of rupture, f_{r-pr} (MPa)	COV	Mid-span deflection (mm)	Average mid-span deflection, δ (mm)	COV
S5-1	0.68			0.081		
S5-2	0.81	0.8	0.087	0.126	0.101	0.226
S5-3	0.76			0.096		
S10-1	1.23	1.3	0.076	0.073	0.088	0.241
S10-2	1.37			0.103		
SS5-1	1.58			0.056		
SS5-2	1.59	1.6	0.004	0.081	0.078	0.264
SS5-3	1.59			0.097		
SS10-1	1.99	1.8	0.123	0.085	0.077	0.156
SS10-2	1.67			0.068		
Sa-1	1.56	1.5	0.076	0.526	0.503	0.064
Sa-2	1.40			0.480		
SaB-1	2.65			0.458		
SaB-2	2.88	2.7	0.044	0.319	0.383	0.183
SaB-3	2.70			0.372		

Table B-5: Modulus of rupture of MPPC concretes/wood composites from panel tests (at 90 days; w/b = 0.20 for MPPC concretes; w/b = 0.36 for MPPC wood composites)

Mix ID	Modulus of rupture (MPa)	Average modulus of rupture, f_{r-pa} (MPa)	COV	Mid-span deflection (mm)	Average mid-span deflection, δ (mm)	COV
S5-1	3.14	3.5	0.154	1.261	1.129	0.165
S5-2	3.91			0.997		
S10-1	3.51			0.989		
S10-2	2.87	3.3	0.104	0.991	0.993	0.007
S10-3	3.38			1.001		
SS5-1	5.17			0.914		
SS5-2	5.36	5.3	0.023	0.954	0.998	0.114
SS5-3	5.41			1.128		
SS10-1	5.40			0.731		
SS10-2	5.32	5.2	0.051	0.851	0.808	0.083
SS10-3	4.90			0.842		
Sa-1	4.10			3.440		
Sa-2	3.93	4.1	0.036	3.275	3.329	0.028
Sa-3	4.23			3.273		
SaB-1	6.07	5.9	0.035	3.193	3.184	0.004
SaB-2	5.77			3.176		

Table B-6: Slopes of MPPC concretes/wood composites from prism and panel tests (at 90 days; w/b = 0.20 for MPPC concretes; w/b = 0.36 for MPPC wood composites)

Mix ID	Prism			Panel		
	Slopes (MPa/mm)	Average slopes (MPa/mm)	COV	Slopes (MPa/mm)	Average slopes (MPa/mm)	COV
S5-1	8.9			-		
S5-2	9.3	8.7	0.089	3.0	3.7	0.287
S5-3	7.8			4.5		
S10-1	18.5			4.3		
S10-2	10.9	14.7	0.365	3.3	3.8	0.131
S10-3	-			3.8		
SS5-1	27.3			6.4		
SS5-2	18.8	19.9	0.345	7.3	6.5	0.123
SS5-3	13.7			5.7		
SS10-1	25.9			8.5		
SS10-2	24.9	25.4	0.027	7.0	7.3	0.148
SS10-3	-			6.4		
Sa-1	2.5			1.4		
Sa-2	3.1	2.8	0.151	1.7	1.6	0.108
Sa-3	-			1.7		
SaB-1	4.9			2.5		
SaB-2	9.2	6.9	0.315	2.5	2.5	0.000
SaB-3	6.5			-		

APPENDIX C MPPC CONCRETES/WOOD COMPOSITES REINFORCED WITH GLASS-FIBERS AND TEXTILE GLASS-FABRICS

Table C-1: Compressive strength and density of MPPC concretes/wood composites reinforced with glass-fibers from cube tests (at 90 days; w/b = 0.20 for MPPC concretes; w/b = 0.36 for MPPC wood composites)

Mix ID	Compressive strength (MPa)	Average compressive strength, f_{cu} (MPa)	COV	Density (kg/m^3)	Average density, γ (kg/m^3)	COV
FS5-1	36.5			1742		
FS5-2	37.6	35.8	0.062	1734	1736	0.003
FS5-3	33.2			1731		
FS10-1	35.1			1738		
FS10-2	38.4	37.5	0.055	1750	1745	0.003
FS10-3	38.9			1745		
FSS5-1	50.1			2030		
FSS5-2	51.8	50.7	0.018	2020	2026	0.003
FSS5-3	50.2			2029		
FSS10-1	53.1			2040		
FSS10-2	50.7	52.3	0.025	2047	2040	0.003
FSS10-3	53.0			2034		
FSa-1	12.1			1380		
FSa-2	10.8	12.0	0.100	1330	1339	0.033
FSa-3	13.2			1386		
FSaB-1	18.3			1493		
FSaB-2	19.7	19.4	0.048	1518	1509	0.009
FSaB-3	20.1			1518		

Table C-2: Compressive strength of MPPC concretes/wood composites reinforced with glass-fibers from cylinder tests (at 90 days; w/b = 0.20 for MPPC concretes; w/b = 0.36 for MPPC wood composites)

Mix ID	Compressive strength (MPa)	Average compressive strength, f'_c (MPa)	COV
FS5-1	35.9		
FS5-2	33.1	35.4	0.060
FS5-3	37.3		
FS10-1	37.6		
FS10-2	33.4	35.3	0.060
FS10-3	34.8		
FSS5-1	36.4		
FSS5-2	40.4	37.4	0.071
FSS5-3	35.3		
FSS10-1	34.1		
FSS10-2	38.0	35.9	0.054
FSS10-3	35.7		
FSa-1	13.6		
FSa-2	12.9	12.7	0.075
FSa-3	11.7		
FSaB-1	14.0		
FSaB-2	15.2	14.3	0.055
FSaB-3	13.7		

Table C-3: Strain at peak stress and modulus of elasticity of MPPC concretes/wood composites reinforced with glass-fibers from cylinder tests (at 90 days; w/b = 0.20 for MPPC concretes; w/b = 0.36 for MPPC wood composites)

Mix ID	Strain at peak stress (mm/mm)	Average strain at peak stress, ε_c' (mm/mm)	COV	Modulus of elasticity (GPa)	Average modulus of elasticity, E (GPa)	COV
FS5-1	4.40×10^{-3}			9.50		
FS5-2	3.69×10^{-3}	3.96×10^{-3}	0.098	9.67	9.93	0.061
FS5-3	3.77×10^{-3}			10.64		
FS10-1	3.77×10^{-3}			11.92		
FS10-2	3.81×10^{-3}	3.80×10^{-3}	0.009	10.36	11.16	0.069
FS10-3	3.84×10^{-3}			11.20		
FSS5-1	3.09×10^{-3}			15.61		
FSS5-2	2.94×10^{-3}	2.99×10^{-3}	0.030	16.43	15.48	0.065
FSS5-3	2.93×10^{-3}			14.41		
FSS10-1	3.10×10^{-3}			13.74		
FSS10-2	3.13×10^{-3}	3.08×10^{-3}	0.018	14.98	14.92	0.077
FSS10-3	3.02×10^{-3}			16.05		
FSa-1	1.59×10^{-2}			1.56		
FSa-2	1.42×10^{-2}	1.57×10^{-2}	0.092	2.00	1.63	0.206
FSa-3	1.71×10^{-2}			1.34		
FSaB-1	1.34×10^{-2}	1.20×10^{-2}	0.164	2.42	2.69	0.144
FSaB-2	1.06×10^{-2}			2.97		

Table C-4: Flexural stress at first cracking of MPPC concretes/wood composites reinforced with glass-fibers from prism tests (at 90 days; w/b = 0.20 for MPPC concretes; w/b = 0.36 for MPPC wood composites)

Mix ID	Flexural stress (MPa)	Average flexural stress, f_{b-pr} (MPa)	COV	Mid-span deflection at peak load (mm)	Average mid-span deflection, δ (mm)	COV
FS5-2	3.03	3.4	0.153	0.190	0.245	0.317
FS5-2	3.77			0.300		
FS10-1	3.18	3.0	0.067	0.283	0.271	0.213
FS10-2	2.79			0.209		
FS10-3	2.92			0.323		
FSS5-1	4.52	4.8	0.056	0.213	0.227	0.199
FSS5-2	5.01			0.191		
FSS5-3	4.97			0.278		
FSS10-1	4.43	5.1	0.114	0.237	0.271	0.168
FSS10-2	5.38			0.253		
FSS10-3	5.50			0.323		
FSa-2	2.92	2.7	0.120	0.295	0.342	0.196
FSa-3	2.46			0.390		
FSaB-1	4.39	4.1	0.074	0.326	0.392	0.202
FSaB-2	3.78			0.369		
FSaB-3	4.09			0.480		

Table C-5: Flexural stress at first cracking of MPPC concretes/wood composites reinforced with glass-fibers from panel tests (at 90 days; w/b = 0.20 for MPPC concretes; w/b = 0.36 for MPPC wood composites)

Mix ID	Flexural stress (MPa)	Average flexural stress, f_{b-pa} (MPa)	COV	Mid-span deflection at initial peak load (mm)	Average mid-span deflection, δ (mm)	COV
FS5-1	1.90	1.9	0.005	0.615	0.831	0.367
FS5-2	1.91			1.047		
FS10-1	3.37	3.5	0.041	1.378	1.900	0.240
FS10-2	3.38			2.622		
FS10-3	3.62			1.700		
FSS5-1	6.09	5.5	0.103	1.956	1.586	0.148
FSS5-2	4.95			1.309		
FSS5-3	5.59			1.494		
FSS10-1	7.12	6.9	0.076	0.912	0.867	0.079
FSS10-2	7.31			0.934		
FSS10-3	6.32			0.756		
FSa-2	5.29	5.8	0.111	2.466	2.840	0.201
FSa-3	6.20			2.406		
FSaB-1	4.59	4.9	0.075	2.529	2.388	0.194
FSaB-2	5.11			2.831		

Table C-6: Slopes of MPPC concretes/wood composites reinforced with textile glass-fibers from prism and panel tests (at 90 days; w/b = 0.20 for MPPC concretes; w/b = 0.36 for MPPC wood composites)

Mix ID	Prism			Panel		
	Slope of load-deflection curve (MPa/mm)	Average slope (MPa/mm)	COV	Slope of load-deflection curve (MPa/mm)	Average slope (MPa/mm)	COV
FS5-1	-	19.0	0.219	3.2	2.7	0.260
FS5-2	22.0			2.2		
FS5-3	16.1			-		
FS10-1	10.4	14.5	0.615	1.7	1.5	0.141
FS10-2	24.7			1.3		
FS10-3	8.3			1.6		
FSS5-1	22.1	25.9	0.129	2.3	2.2	0.106
FSS5-2	27.1			2.3		
FSS5-3	28.5			1.9		
FSS10-1	17.2	18.9	0.280	3.5	4.3	0.186
FSS10-2	24.8			5.1		
FSS10-3	14.6			4.3		
FSa-2	11.2	9.2	0.307	2.2	2.6	0.246
FSa-3	7.2			3.1		
FSaB-1	22.6	14.9	0.445	1.9	1.8	0.124
FSaB-2	12.1			1.6		
FSaB-3	10.3			-		